Finanziato dall'Unione europea NextGenerationEU | Ministero dell'Università e della Ricerca | Italiadomani PIANO NAZIONALE DI RIPRESA E RESILIENZA

multi-Risk sciEnce for resilienT commUnities undeR a changiNg climate Codice progetto MUR: **PE00000005** – D43C22003030002

Deliverable title: Dynamic risk maps for multi-objective strategies

Deliverable ID: 3.7.2

Due date:31/03/2026

Submission date: 31/03/2026

AUTHORS

Mattia Anghileri (POLIMI), Fabio Biondini (POLIMI), Elena Candigliota (ENEA), Eugenio Chioccarelli (UNINA), Daniela De Gregorio (UNINA), Claudio Di Prisco (POLIMI), Teresa Girardi (UNINA), Iunio Iervolino (UNINA), Arsal Jourshari (POLIMI), Mattia Federico Leone (UNINA), Pietro Marveggio (POLIMI), Anna Marzo (ENEA), Lorenzo Moretti (ENEA), Stefano Nardone (UNINA), Maria Giovanni Nocerino (UNINA), Alice Pallotta (UNINA), Roberto Paolucci (POLIMI), Lorenza Petrini (POLIMI), Francesca Linda Perelli (UNINA), Salvatore Sessa (UNINA), Chiara Smerzini (POLIMI),

Manuela Vanini (POLIMI), Matteo Zerbi (POLIMI), Aldo Zollo (UNINA), Giulio Zuccaro (UNINA)

Technical references

Project Acronym	RETURN
Project Title	multi-Risk sciEnce for resilienT commUnities undeR a changiNg climate
Project Coordinator	Domenico Calcaterra UNIVERSITA DEGLI STUDI DI NAPOLI FEDERICO II domcalca@unina.it
Project Duration	December 2022 – November 2025 (36 months)

Deliverable No.	DV3.7.2
Dissemination level*	PU
Work Package	WP7 - Strategies for loss reduction based on a systemic approach
Task	T7.2 - Dynamic risk maps for multi-objective strategies
Lead beneficiary	POLIMI, M. Anghileri,R. F. Biondini, C. Di Prisco, A. Jourshari, P. Marveggio, R. Paolucci, L. Petrini, C. Smerzini, M. Vanini, M. Zerbi
Contributing beneficiary/ies	ENEA E. Candigliota, L. Moretti, A. Marzo UNINA, E. Chioccarelli, D. Degregorio, M. T. Girardi, I. Iervolino, M. Leone, A. Pallotta, L. Perelli, S. Sessa, A. Zollo, G. Zuccaro UNIGE, S. Alfano, S. Cattari, S. Lagomarsino, M.G.B. Merani, D. Sivori

* PU = Public

PP = Restricted to other programme participants (including the Ministry Services)

RE = Restricted to a group specified by the consortium (including the Ministry Services)

CO = Confidential, only for members of the consortium (including the Ministry Services)

Document history

Version	Date	Lead contributor	Description
0.1	xx.xx.xxxx	First name Last name (Partner short name)	First draft
0.2			Critical review and proofreading
0.3			Edits for approval
1.0			Final version

ABSTRACT

In this task, methodologies were developed based on the integration of advanced hazard and vulnerability models to estimate multi-risk dynamic maps, aimed at supporting multi-objective intervention strategies in complex urban and infrastructure systems. The proposed approach combines advanced modelling techniques across seismology, geotechnical engineering, structural analysis, and urban planning to capture the dynamic and interconnected nature of risk under multiple hazards and changing environmental conditions.

First, innovative physics-based seismic risk assessment tools are developed and applied to the Campi Flegrei area, integrating fault-to-city numerical simulations with simplified structural models of the built environment. This approach enables the generation of realistic damage scenarios based on high-resolution ground motion simulations, improving the representation of local seismic effects in volcanic environments.

Second, an integrated multi-risk modelling framework is proposed to address cascading hazard processes, specifically focusing on earthquake-induced landslides and their interaction with aging infrastructure. The methodology combines seismic wave propagation, landslide initiation and propagation, impact modelling, and structural performance assessment within a unified computational workflow, allowing for a physically consistent representation of multi-hazard interactions.

Third, a Multi-Hazard Resilient Urban Development framework is developed to support urban-scale decision-making by integrating climatic and geophysical risks within a GIS-based analytical environment. The framework enables the construction of dynamic risk maps and the evaluation of design strategies for buildings and open spaces through ex-ante and ex-post scenarios. The application to the Bagnoli district in Naples demonstrates how coordinated interventions can significantly reduce multi-risk conditions while enhancing urban functionality and environmental performance.

In addition, a Markov-chain-based model is introduced to describe damage accumulation and recovery processes during seismic sequences, highlighting the importance of temporal dynamics in resilience assessment. This approach allows the probabilistic representation of both loss evolution and recovery processes under repeated hazard events.

Finally, a methodology for mapping environmental, natural, and anthropic risks is developed through the integration of open geospatial datasets within GIS platforms, supporting location-based decision-making and enabling the visualization of complex risk patterns at the municipal scale.

Overall, the deliverable demonstrates how the integration of dynamic modelling, multi-hazard assessment, and spatial analysis can support the development of advanced decision-support tools for resilience-oriented planning.

3. Table of contents

List of Tables

List of Figures

4 Innovative physics-based tools for seismic risk assessment

4.1 Introduction

This research represents an advanced effort to implement a holistic fault-to-city numerical simulation framework for seismic risk assessment in the Campi Flegrei area. This integrated approach aims at putting the basis for bridging the gap between regional earthquake ground motion modeling and damage scenarios at urban scale by coupling physics-based simulations (PBS) of the fault rupture and of the seismic wave propagation with a simplified structural characterization of the built environment. The study area includes the highly urbanized municipalities of Pozzuoli and Bacoli, as well as several districts within the city of Naples, such as Bagnoli, Fuorigrotta, Soccavo, and Pianura. This study area is notably affected by bradyseism, a distinctive seismogenic process in which volcanic-related ground uplift and subsidence drive the local seismicity, characterized by ground shaking records with distinctive features, in terms of shallow hypocentral depth and of high-frequency spectral content. These conditions are hardly represented by the vast majority of strong-motion records from tectonic earthquakes, so that they need a specialized approach to urban risk modeling.

The work takes advantage of many of the research activities represented by the different Work Packages of the VS3. Indeed, it has involved both seismological experts, as regards the fault characterization of the Campi Flegrei area and the analysis of the accelerometric data used for the validations (WP4 and WP5), as well as the engineering experts of the spoke, as regards the vulnerability assessment and the strategies for risk assessment and loss reduction (WP6 and WP7).

In such a multi-disciplinary framework, the research has the following objectives:

- devise a physics-based framework to integrate seismological and engineering concepts within an innovative holistic approach to seismic risk assessment;
- exploit high-performance computational tools providing multi-scale simulations of the earthquake chain from the seismic source to the wave propagation path up to the building response;
- simulate various realistic damage scenarios, including predictive analyses for potential events of magnitudes not yet experienced. Comparing the estimated response of the SDOF oscillators in terms of roof drifts with conventional damage thresholds allows to quantify the potential impact at the urban scale in terms of structural damage severity, extent and impact on the population.

4.2 Methodology

4.2.1 The seismic hazard

The work is based on the use of numerical tools for the earthquake ground motion simulation, by suitable models of the seismic source, of the seismic wave propagation path and of the shallow crustal models. The main computational tool for this purpose is the spectral element code SPEED (https://speed.mox.polimi.it/), developed at Politecnico di Milano within a continuing cooperation of the Department of Civil and Environmental Engineering with the Department of Mathematics. SPEED is suited to solve multi-scale elastodynamic problems by taking advantage of the flexibility derived by the discontinous Galerkin approach, as well as by its optimization within a high-performance parallel computing domain.

For the purpose of the RETURN Project a "site-city interaction" tool was developed in SPEED to model explictly the interaction between the earthquake and the built environment by associating, with each residential building, a nonlinear single (or multi-) -degree-of-freedom (SDOF) oscillator whose constitutive parameters in the linear and nonlinear ranges are calibrated based on the available structural information. For the model development, the available geological and geophysical information was collected to construct a 3D numerical model of the Campi Flegrei area, including a 30km x 30km in-plan portion, with a thickness of about 8 km (Figure 1).

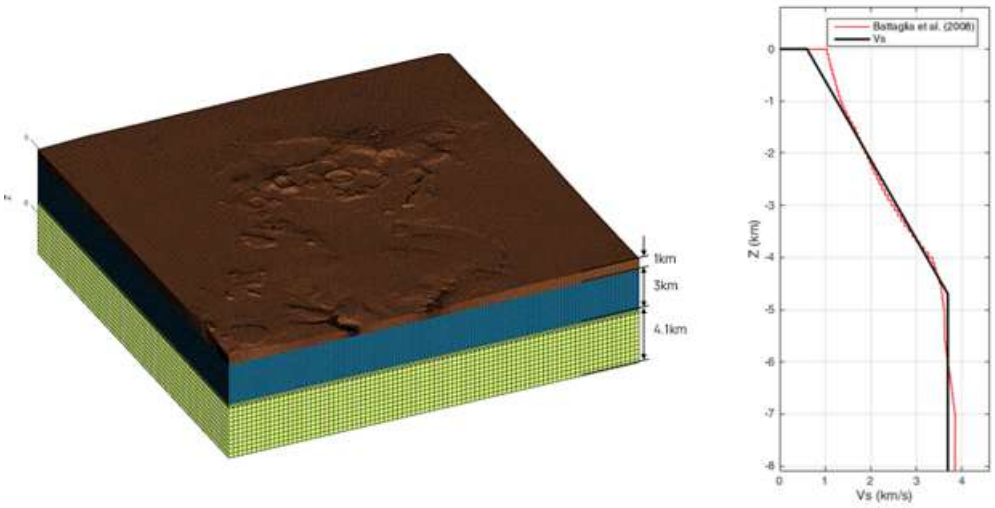

Figure 1: Sketch of the spectral element numerical model, designed to propagate accurately seismic waves up to a frequency of 10 Hz, together with a Vs wave velocity profile.

The accelerometric records of the recent bradyseismic sequence in the area were organized in a specific dataset and processed, with specific reference to the largest ones, usable for validation purposes. Some of the recorded earthquakes were considered for validation, typically consisting of comparison of simulated shake maps with the distribution of recorded peak values of ground motion (Figure 2).

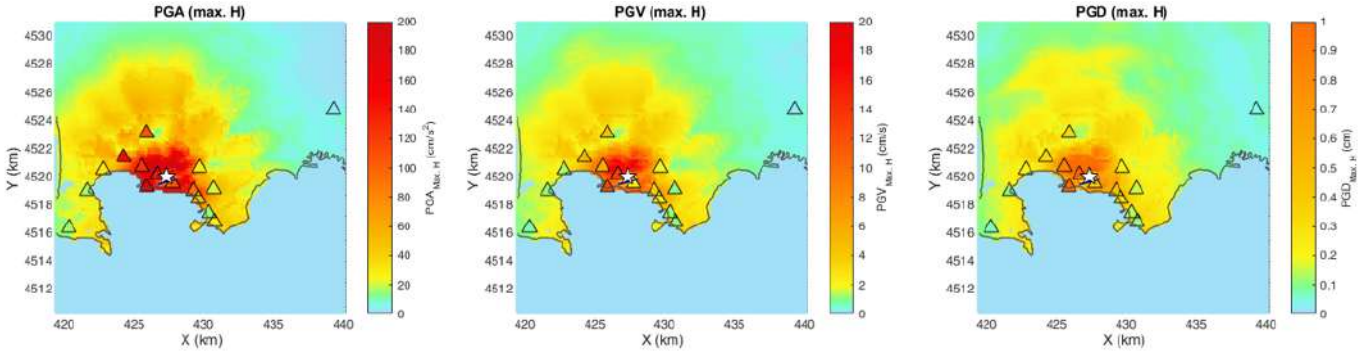

Figure 2: Maps of simulated peak values of Peak Ground Acceleration (left), Peak Ground Velocity (center) and Peak ground Displacement (right) of the May 20, 2024, earthquake, with estimated moment magnitude Mw3.8. Triangles show the recorded values.

The validations included three earthquakes (Sep 27, 2023; May 20, 2024; Feb 16, 2025) for which an extensive comparison in terms of amplitude and attenuation with distance was carried out, showing an overall good agreement. This validation activity proved the accuracy of the 3D numerical model, on the one side, and the possibility to obtain realistic results also for larger magnitude earthquakes, up to Mw5, on the other side. Indeed, the empirical models based on recorded ground motions within the area are hardly applicable because of the limits in extrapolating the empirical results on ground motion levels not recorded yet, while such predictions can be obtained via numerical simulations. For this purpose, twelve Mw5 scenarios were devised, with the support of the seismological experts of the University Federico II di Napoli, accounting for different potential faults and different kinematic rupture mechanisms. The resulting ground motions were used as input for the vulnerability models described in the sequel, to produce damage scenarios.

4.2.2 The vulnerability models

Two different approaches were taken for the vulnerability definition. In one case, denoted in the following by UniGE, a detailed modeling of the city environment was obtained, transforming raw exposure data into mechanical parameters of single-degree-of-freedom (SDOF) oscillators, representative of the seismic buildings response. Available open data sources on buildings were first collected to mechanically characterize the residential building stock. In particular, the study exploits ISTAT census data, which provides information regarding building typologies at the census tract scale. These datasets detail the number of buildings classified according to a three-attribute taxonomy: construction material (masonry, reinforced concrete, other), construction period (<1919, 1919-45, 1946-60, 1961-70, 1971-80, 1981-90, 1991-2000, 2001-05, >2005), and number of stories (1, 2, 3, 4+). This information is provided, for each census tract, by independent statistical distributions of the three taxonomic attributes. Thus, an ad-hoc disaggregation algorithm was employed to estimate, for example, how many three-story masonry structures built before 1919 are present in the census tract. To define the position and orientation of each buildings on the 3D ground model, the Regional Technical Map (CTR) of the Campania Region was utilized. The spatial distribution of the generated SDOF oscillators, categorized by material typology (masonry and reinforced concrete) across the study area, is shown in Figure 3. In most cases, a single node of the ground model corresponds to a single building belonging to a specific typology; in densely urbanized areas, the SDOF oscillator connected in one node of the SPEED model may represent a cluster of several buildings belonging to different ISTAT typologies. To this end, a proper formulation has been developed to derive the dynamic features (period, strength and displacement capacity).

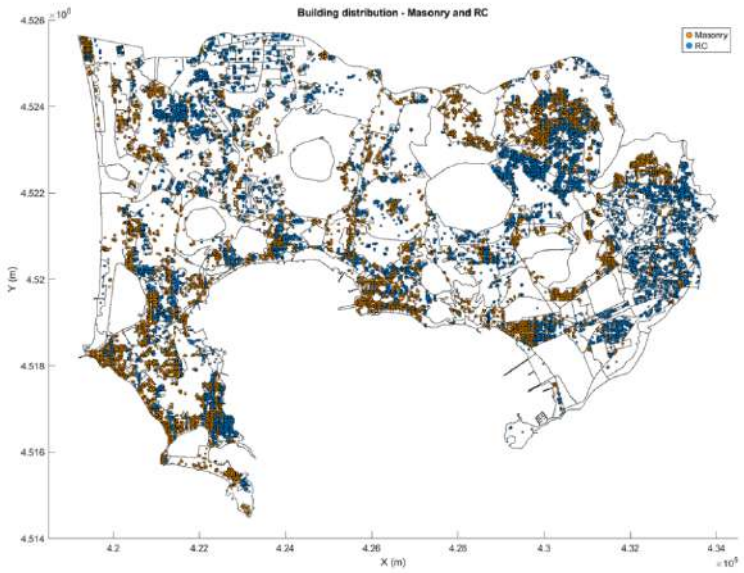

Figure 3: Distribution of the generated SDOF oscillators, categorized by material typology (masonry and reinforced concrete)

The heuristic-macroseismic method (Lagomarsino et al., 2021) has been used to describe the seismic vulnerability buildings, according to the above-mentioned ISTAT taxonomy. The method defines fragility curves for each building type, by two parameters: 1) the vulnerability index V, a number between 0 and 1 that identifies the intensity measure (PGA - peak ground acceleration) corresponding to 50% of probability of moderate damage (DL2); 2) the ductility index Q, which defines the how much the PGA must increase to attain the substantial to heavy damage (DL3). The calibration of these parameters is supported by empirical damage data from the Da.D.O. database, specifically focusing on L'Aquila (2009) and Irpinia (1980) earthquakes. For masonry structures in the Campi Flegrei region, which are predominantly built with tuff stone, specific modifiers were derived from observed data to account for material properties,

structural regularity, floor typology, and construction details, resulting in a regionalized exposure model tailored to the local context.

A crucial methodological step involves defining the mechanical capacity curves of each building class. The capacity curves (mechanical parameters of the SDOF oscillator) have been obtained from the heuristic-macroseismic model through an inverse application of the Capacity Spectrum Method (CSM). The CSM is a non-linear static procedure that calculates the seismic displacement demand by intersecting the capacity curve and the seismic response spectrum (in acceleration-displacement form). In particular, this approach has been used for reinforced concrete buildings, while for masonry buildings, the DBV-Masonry (Displacement-Based Vulnerability) mechanical-analytical model (Lagomarsino and Cattari, 2013) was utilized to directly derive capacity curves.

The resulting capacity curves were idealized as trilinear, identifying specific thresholds for three damage levels: slight (DL1), moderate (DL2), and near-collapse (DL5) (Figure 4). In instances where a single simulation node represented multiple buildings of varying sub-typologies, derivation rules were established to define a representative oscillator by making informed assumptions on equivalent stiffness, accelerations, and ultimate displacement.

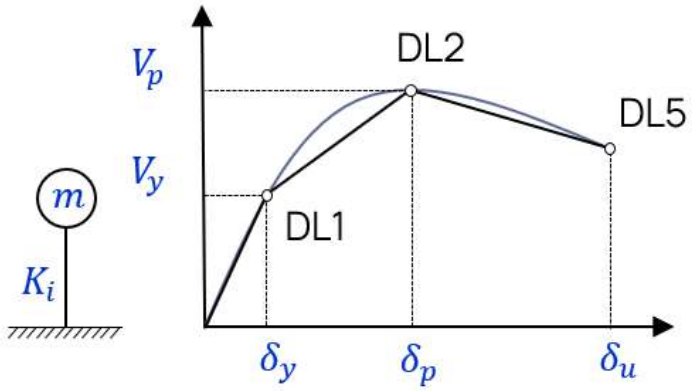

Figure 4: Representative trilinear capacity curve derived for an equivalent SDOF system

In the second case, denoted by UniNA, the dataset considered consisted of the detailed building population in the Campi Flegrei area, the characteristics of which were constrained by the post-earthquake surveying activity, for which a statistical evaluation of the dynamic and non-linear properties of the buildings was provided, in terms of average (and std) values of natural period of vibration, initial stiffness, shear capacity, yield and ultimate displacements. The buildings were later assigned to each node of the numerical grid based on a nearest neighbour criterion, implying that each building was displaced in the position of the closest numerical node. If the adjacent nodes to the building were already occupied within a given distance, than the building was removed. This implied a slight reduction of the total number of studied buildings (from about 9000 to about 7500) but the variations in terms of total statistics are irrelevant.

As shown in Figure 5, the overall number of buildings and their spatial distribution for the UniNA and UniGE criteria are in good agreement, as well as the distribution between masonry and reinforced concrete materials.

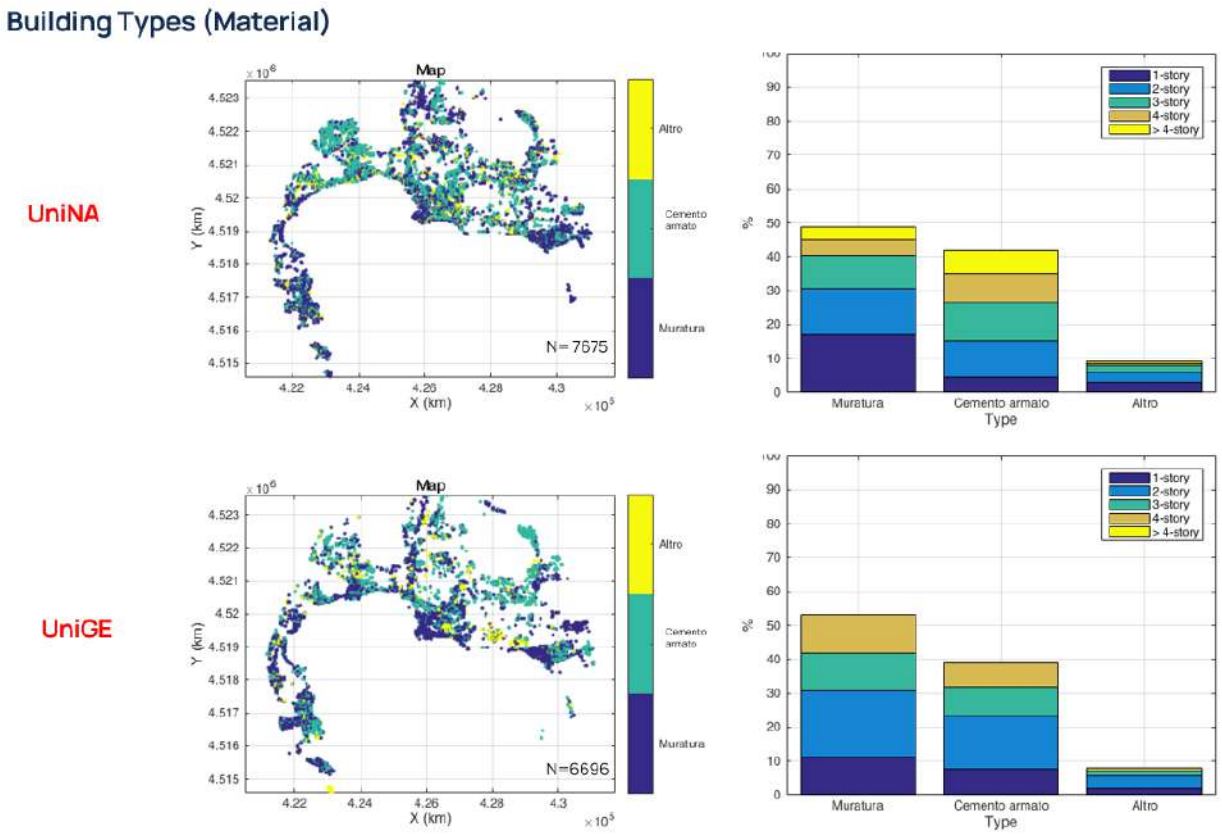

Figure 5: Spatial and material distribution of buildings within the two numerical meshes of the Campi Flegrei area, including a population of nonlinear SDOF buildings coupled within the numerical model.

In Figure 6, the statistical distributions of natural period of vibration (Tn) and of the normalized shear strength of the building (PGAy) are also shown. While UniGE buildings are sampled within a relatively narrow interval of Tn values (typically within 0.2 and 0.4 s), the Tn distribution for UniNA is more spread, although with similar mean values. The differences of the two building populations lie especially in terms of shear strength. While for UniNA this is mostly within the range of 7 to 15% of the weight, the values from UniGE are more spread and cover substantially larger values with mean around 45%.

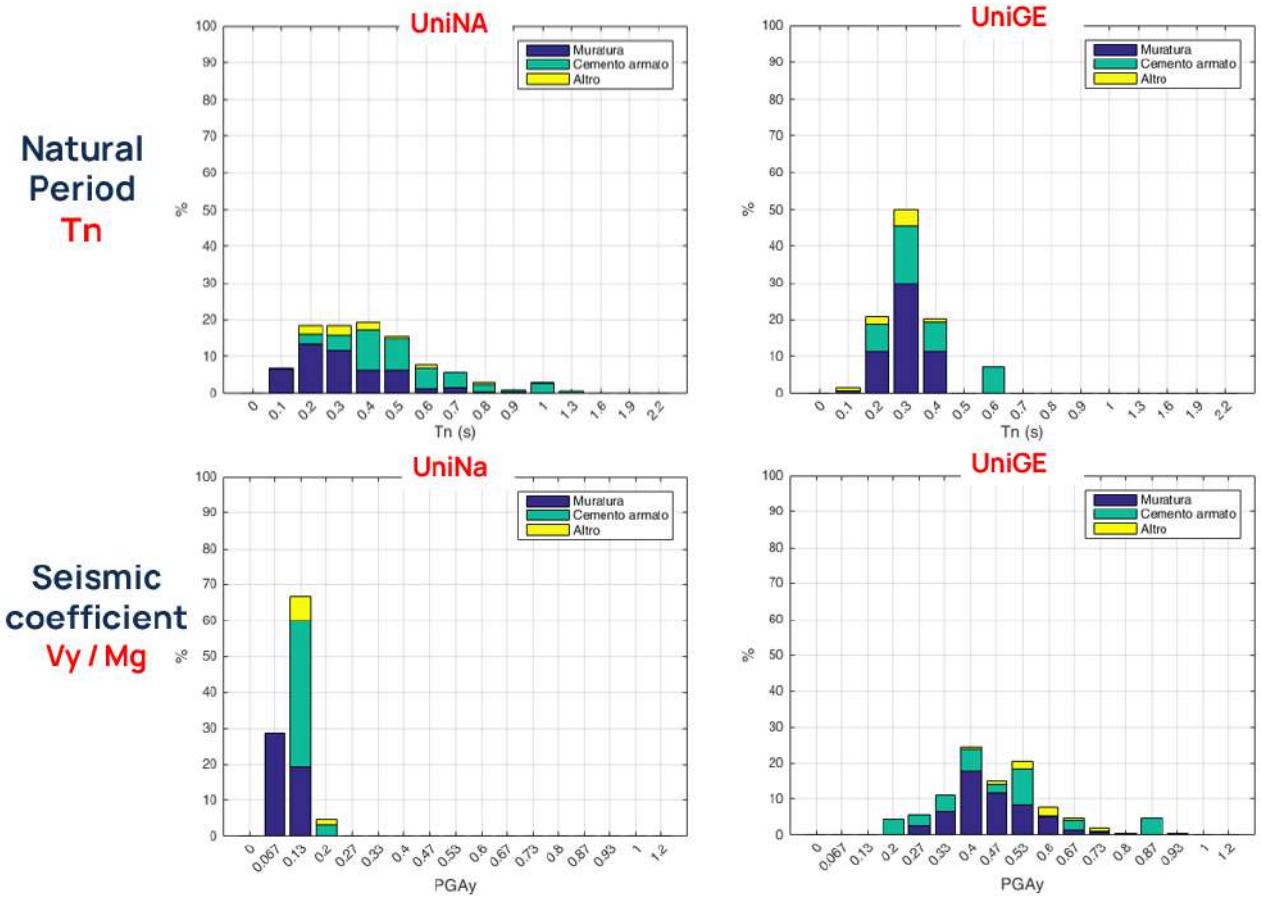

Figure 6: Statistical distributions of the natural vibration periods (Tn) and of the normalized shear strength (Vy/Mg) according to the UniGE and UniNA buildings populations.

4.3 Results

The finalized dataset of SDOF oscillator properties was integrated into the PBS framework to simulate urban damage for both the May 2024 M_w 3.9 Pozzuoli earthquake and a hypothetical, higher-intensity M_w 5.0 event, selected among those considered as scenario events for the area.

Results for these two case studies were first considered in terms of drift values, for both the UniNA and UniGE building populations, and are shown in Figure 7 and Figure 8 for the M_w3.9 and M_w5.0 earthquakes, respectively. While for the Mw3.9 validation case study (May 20, 2024) the drift values are in substantially good agreement and overall consistent with the limited observed damage during such event, for the Mw5.0 earthquake the UniNA drift values are larger, with about 32% buildings exceeding 1.2% compared to about 10 % for UniGE, as a consequence of the different shear strength values considered within both building populations.

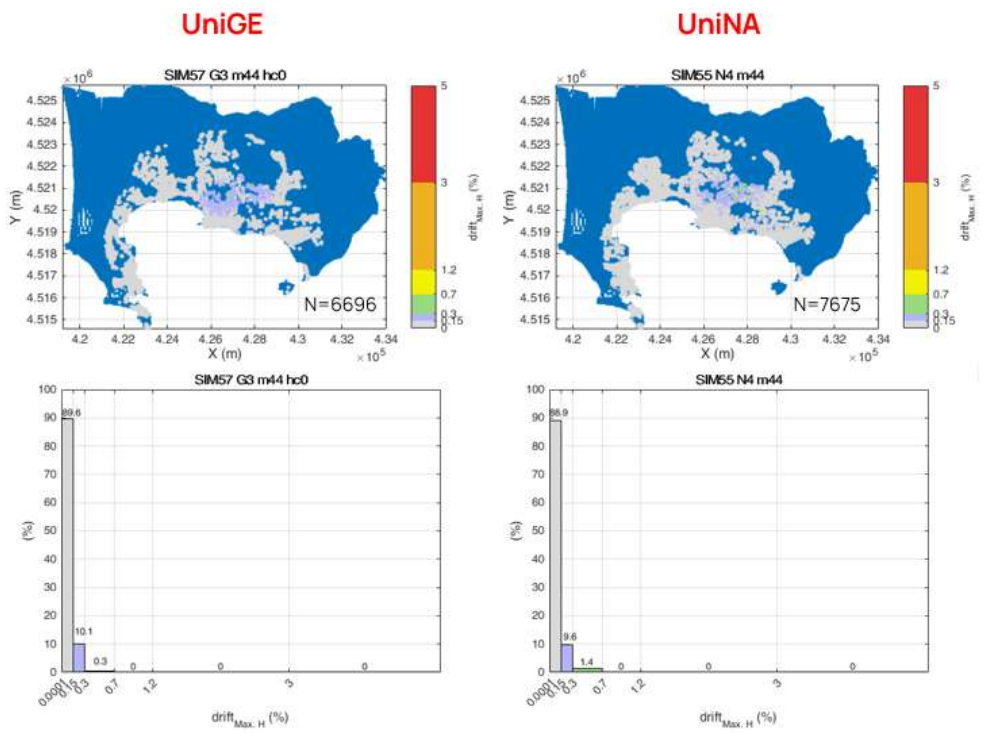

Figure 7: Spatial distributions of drift values according to the UniGE and UniNA buildings populations, for the validation case study of the Mw3.9 earthquake of May 20, 2024.

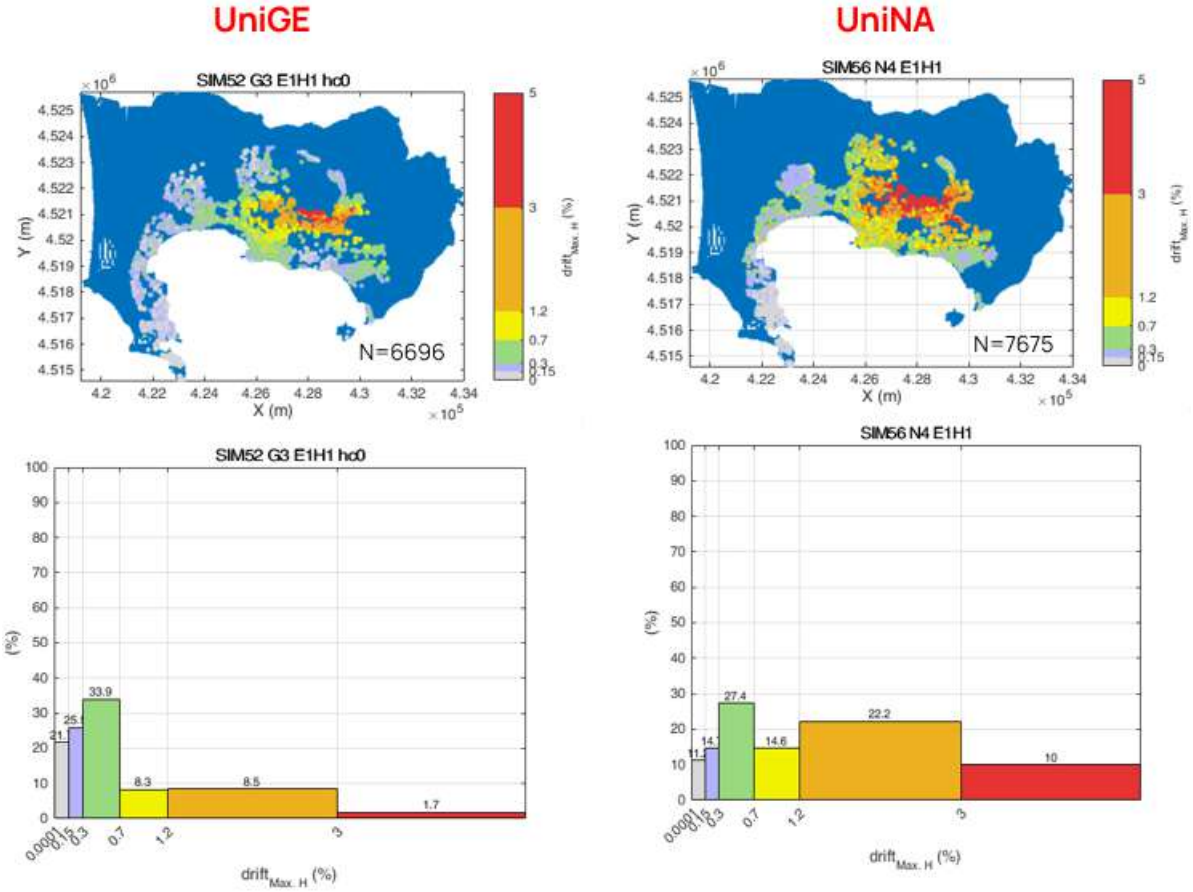

Figure 8: Same as Figure 7, for a Mw5.0 scenario event.

For the UniGE case, the drift limits were also associated to damage levels defined according to the EMS98 scale. Results for the M_w 3.9 scenario (shown in Figure 9a) indicate a high level of overall structural resilience, as 92.8% of the building stock remains undamaged (DL0) and only 6.7% experiences slight damage (DL1). Despite this general stability, a typology-specific analysis reveals the early susceptibility of masonry structures, which represent nearly 60% of all slight damage and 100% of the moderate damage cases recorded at this magnitude. In contrast, reinforced concrete buildings demonstrate remarkable robustness, staying almost exclusively within the undamaged or slight damage categories without transitioning to more severe states. These results are closely compatible with the patterns and intensity levels observed in the field.

The hypothetical M_w 5.0 scenario (Figure 9b) marks a drastic escalation in seismic impact, with the proportion of undamaged buildings (DL0) decreasing to just 26.6%. In this case, moderate damage (DL2) emerges as the most prevalent outcome at 27%, while more critical states—including heavy damage and collapse—collectively affect over a quarter of the total building stock. The performance gap between construction materials becomes even more pronounced at this intensity, with masonry buildings dominating every damage category from moderate to near-collapse. While reinforced concrete structures also sustain increased damage, they consistently maintain a significantly higher proportion of buildings in lower damage states compared to their masonry counterparts.

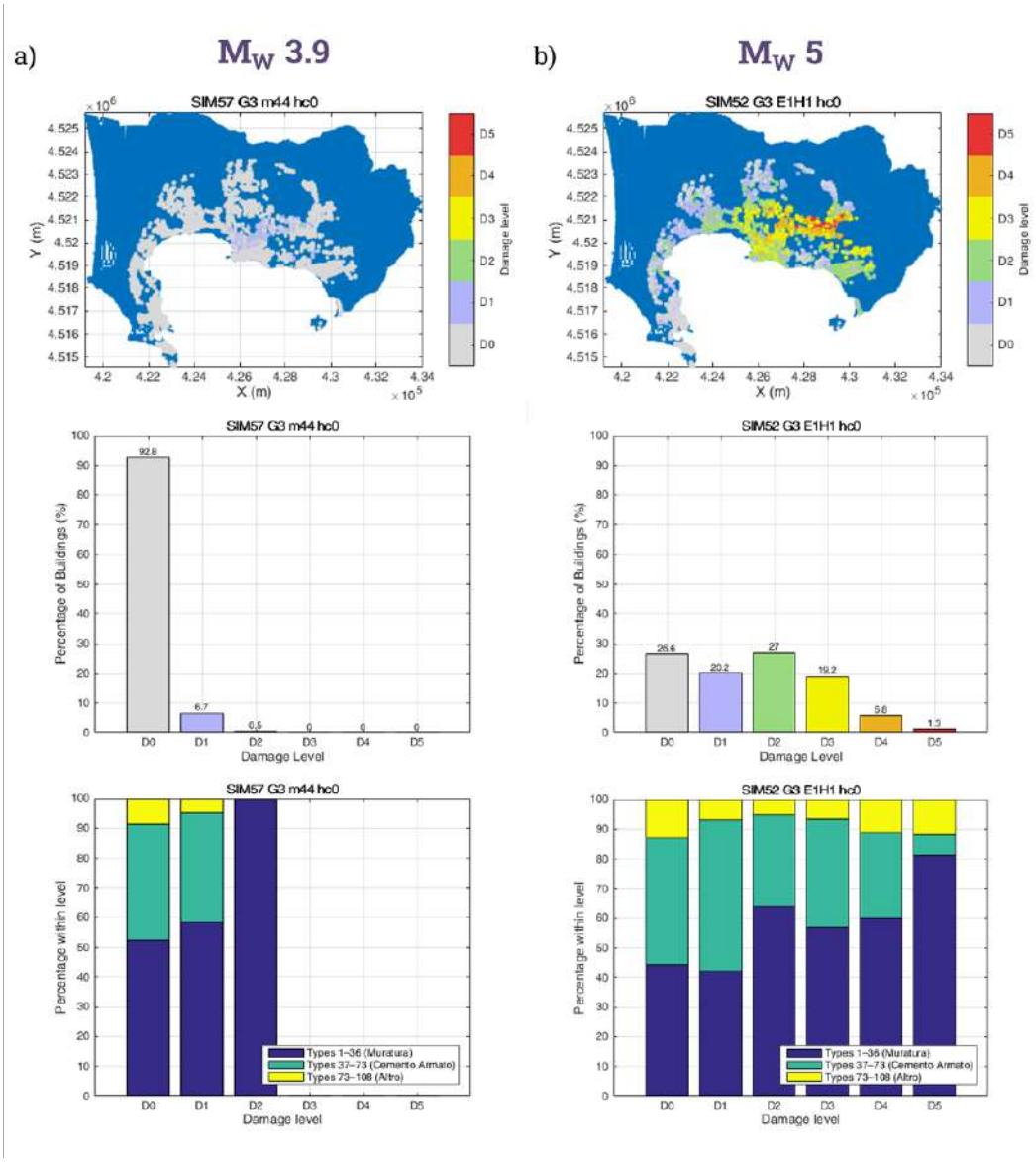

Figure 9: Comparative seismic damage analysis for (a) M_w 3.9 and (b) M_w 5.0 earthquake scenarios

4.4 Conclusions

A holistic fault-to-city numerical simulation framework for seismic risk assessment in the Campi Flegrei area was implemented in the framework of the RETURN Project. This framework is founded on physical and mechanical grounds, by considering kinematic models of the fault rupture, seismic wave propagation within arbitrarily heterogeneous media modeled by spectral elements, at the top of which nonlinear SDOF (or MDOF) models are introduced, fully coupled with the rest of the numerical model.

The relatively small-size of the seismic faults of the volcanic earthquakes (maximum Mw=5 considered for Campi Flegrei) as well as of the modeled area (up to 30 km width in the horizontal direction and 8 km in the vertical direction), together with extensive use of High-Performance Computing facilities, allowed to treat the problem within reasonable computer times, and to obtain one of the first examples of fully coupled seismic scenarios, from the fault to the response of a large urban area.

The ground motion simulation results were successfully validated with available records for earthquakes of Magnitude up to Mw4, occurred within the bradyseismic crisis still in progress. Results of the Mw5 hypothetical scenarios were found to be in good agreement with empirical models of other volcanic areas, such as Etna, where earthquake magnitudes up to Mw5 were measured and may actually constrain ground motions also for the Campi Flegrei.

Two distribution of buildings were considered, obtained with different levels of available information. Results were compared in terms of drift values, that were found in very good agreement, on a statistical basis, for the Mw3.9 validation case. For the Mw5 scenario, the seismic impact, quantified in terms of drift values, tends to increase dramatically, because of the increasing effect of the non-linear response of buildings. The different assumptions behind the construction of the two considered building populations and of the corresponding capacity parameters also imply a major difference in terms of damage extent. In one case, the drift values were used to define damage intervals according to the EMS98 scale. While a good agreement with the observed damage during the validation event was found, a significant damage extent was obtained for the selected Mw5 scenario, with about 7% of the whole building population in the considered area suffering either extensive structural damage or collapse.

The research will continue by exploring in detail the different earthquake scenarios produced within this work with the objective of studying in detail the correlation of damage with different ground motion intensity measures and of producing updated fragility curves for the Campi Flegrei volcanic area.

5 Development of an integrated tool for multi-risk analysis considering cascading events

5.1. Introduction

In recent decades, critical infrastructures such as bridges, viaducts, and transportation networks have become increasingly exposed to complex multi-hazard environments. In these contexts, different natural processes do not act independently but interact in ways that can significantly amplify their combined effects. Among these, earthquake-induced landslides represent a particularly critical scenario, especially in regions characterized by high seismicity and complex geological conditions, such as Southern Italy.

Despite the growing recognition of these interactions, traditional risk assessment approaches remain largely fragmented. Seismology, geotechnical engineering, and structural engineering have typically evolved as separate disciplines, each focusing on a specific aspect of the problem. As a result, seismic hazard is often evaluated independently from slope stability, and structural performance is assessed without fully accounting for secondary effects such as landslide impact or long-term deterioration. This separation limits the ability to capture the real behavior of infrastructure systems under multi-hazard conditions.

The present work addresses this gap by proposing an integrated multi-risk assessment framework that explicitly considers the causal relationships between different hazards. In this perspective, risk is not interpreted as the simple coexistence of multiple threats, but rather as the outcome of a chain of interconnected processes. An earthquake may trigger slope instability, generating a landslide that propagates and impacts infrastructure elements that may already be weakened by aging and deterioration. Accordingly, the proposed methodology couples advanced numerical and analytical tools across geophysics, geotechnics, and structural engineering domains, with specific focus on the Irpinia area in Southern Italy, a seismically active region with steep terrain and aging infrastructure. It allows to show demonstrates how a physically based, modular, and computationally tractable workflow can support risk-informed decision making for infrastructure resilience and can be integrated into operational multi-risk platforms for effective mitigation strategies.

5.2 Methodology

5.2.1 Conceptual Approach

The methodology is based on a conceptual interpretation of multi-risk as a dynamic and sequential process. Instead of treating hazards as independent events, the framework represents them as stages of a cascading chain, where each process influences the next. This approach allows for a more realistic representation of the physical mechanisms involved and highlights the importance of interactions between different domains.

To operationalize this concept, the framework is structured into five interconnected stages (“rings”), each corresponding to a specific phase of the hazard evolution. These stages are not isolated components but are linked through the exchange of input and output variables, ensuring consistency across the entire analysis (Figure 10)

Figure 10: Schematic representation of the developed physics-based cascading multi-risk methodology for seismic assessment of aging bridge under seismic induced landslides. It is structured into five sequential computational modules ("rings"), each representing a distinct physical process and exchanging physically meaningful state variables.

5.2.2 Ring 1 - Seismic Wave Propagation

The first stage of the methodology focuses on the simulation of seismic ground motion. Unlike traditional approaches that rely on empirical relationships, this framework adopts a physics-based numerical model capable of reproducing three-dimensional wave propagation. This allows for a more accurate representation of local site effects, including soil stratigraphy, basin amplification, and topographic influences.

The output of this phase consists of acceleration time histories that describe the ground motion at specific locations. These signals are essential for driving the subsequent analyses, particularly the evaluation of slope stability. However, the accuracy of this stage depends on the characterization of seismic sources and subsurface conditions, which introduces a degree of uncertainty that propagates through the entire framework.

5.2.3 Ring 2 - Landslide Inception

The second stage represents the transition from seismic loading to slope failure. In this phase, the framework evaluates whether the ground motion generated by the earthquake is sufficient to trigger instability in the soil. This is achieved through a constitutive modeling approach that captures the nonlinear and cyclic behavior of soils, including stiffness degradation and pore pressure accumulation in undrained conditions (Castro 1969, Casagrande 1976).

The analysis is conducted under simplified assumptions, such as one-dimensional conditions, in order to maintain computational efficiency while preserving the essential physical mechanisms (Been and Jefferies, 1985, Ishihara, 1993). The results provide key information on the onset of liquefaction, including eventually the thickness of the liquefied layer needed to estimate the volume of mobilized material. These outputs define the initial conditions for the subsequent propagation phase and represent a critical interface within the multi-risk chain.

5.2.4 Ring 3 - Landslide Propagation

Once instability has been triggered, the third stage models the movement of the mobilized mass along the slope. This phase is crucial because it determines the kinematic characteristics of the landslide, such as its velocity, runout distance, and flow depth. These parameters directly influence the intensity of the impact on downstream structures.

To address this problem, the framework adopts a dual modeling strategy. On one hand, advanced numerical simulations based on Smoothed Particle Hydrodynamics (Pastor et al, 2004, Pastor et al., 2009, Pastor et al., 2015) are used to capture complex flow dynamics and interactions with topography. On the other hand, a simplified analytical formulation based on a Bingham viscoplastic model is introduced to provide rapid

estimates for scenario-based analyses (Gioffre et al., 2017). This combination ensures a balance between physical accuracy and computational efficiency.

The results of this phase are expressed in terms of key propagation metrics, which are subsequently used to define the loading conditions for the interaction with structural elements.

5.2.5 Ring 4 - Landslide–Structure Interaction

The fourth stage focuses on the interaction between the propagating landslide and infrastructure components, such as bridge piers. This interaction is inherently complex and involves dynamic processes that evolve over time. Initially, the impact is characterized by a rapid transfer of momentum, leading to a peak force. This is followed by a transition phase, during which the flow reorganizes around the obstacle, and a quasi-steady phase in which the force stabilizes due to viscous effects. Finally, the interaction diminishes as the mass moves downstream.

To model this behavior, the framework combines numerical simulations based on the Material Point Method (Bandara 2013, Sulsky at al., 1995, Fern et al., 2019) with analytical formulations that allow for the reconstruction of the force–time history. This approach provides a detailed description of the loads acting on the structure (Ceccato et al., 2018, Cuomo et al., 2021), which is essential for the subsequent structural analysis.

5.2.6 Ring 5 - Structural Performance of Aging Infrastructure

The final stage of the methodology evaluates the response of infrastructure subjected to the combined effects of landslide impact and long-term deterioration. Unlike conventional approaches that consider structures in their original condition, this framework explicitly accounts for aging processes, such as corrosion and material degradation, which can significantly reduce structural capacity over time.

The analysis is performed using nonlinear finite element models that incorporate time-dependent changes in material properties and structural behavior. This allows for a life-cycle assessment of infrastructure performance under realistic conditions.

5.3 Case study

The methodology is applied to a case study in Southern Italy, focusing on an existing viaduct. In particular, real seismic and geotechnical conditions were adopted, while for the viaduct is was preferred not to study the specific case, but to consider an archetype able to represent the most common types of structures built in Italy in the past. In Figure 11, the location of the case study is indicated.

Figure 11: Location selected for the study (Salerno, Italy)

In the following, a schematic summary of the conducted activities and obtained results is reported.

Ring 1 – Seismic Wave Propagation.

A physics-based ground-motion simulation was adopted to reproduce spatially variable earthquake excitation at the site. In particular, the opensource SPEED spectral element solver was adopted as three-dimensional

numerical wave-propagation engine. The Irpinia region was selected as representative testbed due to its high seismicity, steep geomorphology, and presence of aging strategic viaducts. A preliminary activity of information acquisition about historical seismicity and geologic context, including reference to major past events (e.g., 1980 Irpinia earthquake) was performed to set up and validate the model. Finally a physics-based seismic wave propagation analysis using a 3D regional velocity model was conducted, including filtering, de-trending, and compatibility checks.

- Inputs: seismic source scenario (Mw ≈ 6.5–6.8), detailed fault geometry, velocity model, and topography.
- Outputs: acceleration time histories at slope location, Vs-dependent amplification patterns, Arias intensity, and cumulative strain-compatible parameters. These outputs define the input motion for the geotechnical analyses.

In Figure 12 a sketch where the Irpinia region is represented and the computational domain considered f to build the Speed model is plotted. In Figure 13, as an example, the predicted time histories

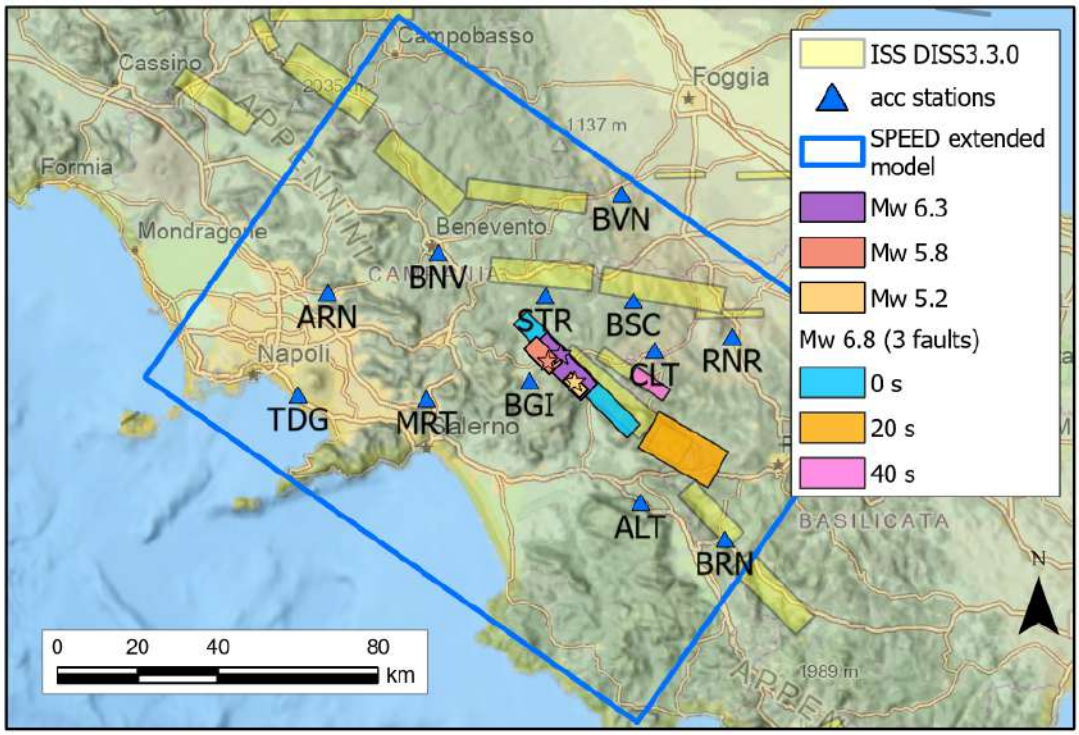

Figure 12: Irpinia region, highlighting the domain considered for the Speed model.

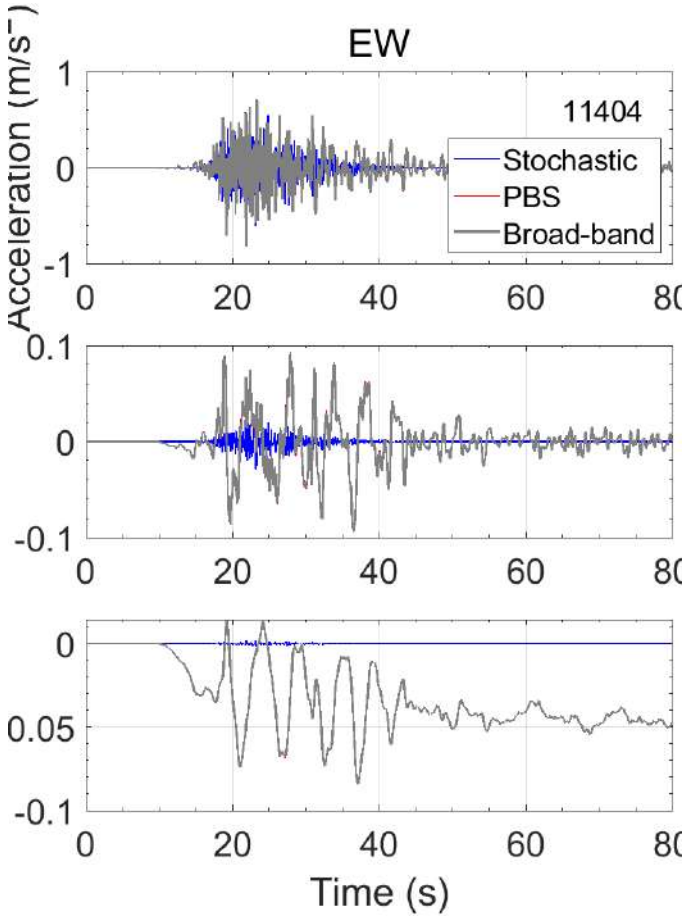

Figure 13: Example of outputs obtained from Speed analysis at a given reference node.

Ring 2 – Landslide Inception

Landslide inception was modelled through one-dimensional cyclic elastoplastic analysis with pore-pressure generation, implemented as a 1D finite element shear column assuming an infinite-slope representation. A strain-hardening multi-surface elastoplastic model was adopted with non-associative flow and kinematic hardening (di Prisco et al., 2010). Once selected the location of the analysis (Irinia region), a preliminary activity of collection of geological and geotechnical data (stratigraphy, soil state index, shear stiffness, drainage conditions) was conducted. Several parametric analyses were conducted.

- Inputs: soil relative density (Dr), state index, constitutive parameters, slope geometry (slope angle α) and seismic input from Ring 1.
- Outputs: liquefied layer thickness (0.25–3 m) and corresponding mobilized volumes, which fed directly into the propagation phase, as well as indicators of cyclic degradation such as shear strain accumulation and pore-pressure ratio. In particular, it was found that: i) loose soils (Dr ≈ 10-15%) developed rapid cyclic mobility and liquefaction within 8-12 strong-motion cycles; ii) medium-dense soils (Dr ≈ 40%) exhibited partial pore-pressure rise and strain accumulation, still capable of partial loss of stiffness and strength under long-duration shaking; iii) slope inclination significantly affected stress build-up, with $\alpha \geq 10°$ accelerating instability. These results confirm the importance of site-specific geotechnical and seismic conditions, often oversimplified in deterministic screening approaches.

The constitutive model implemented has been calibrated on a set of simple shear cyclic tests available in the literature (Porcino et al., 2010). An example of the calibration outcome is given in where for different relative densities in Figure 14 and Figure 15.

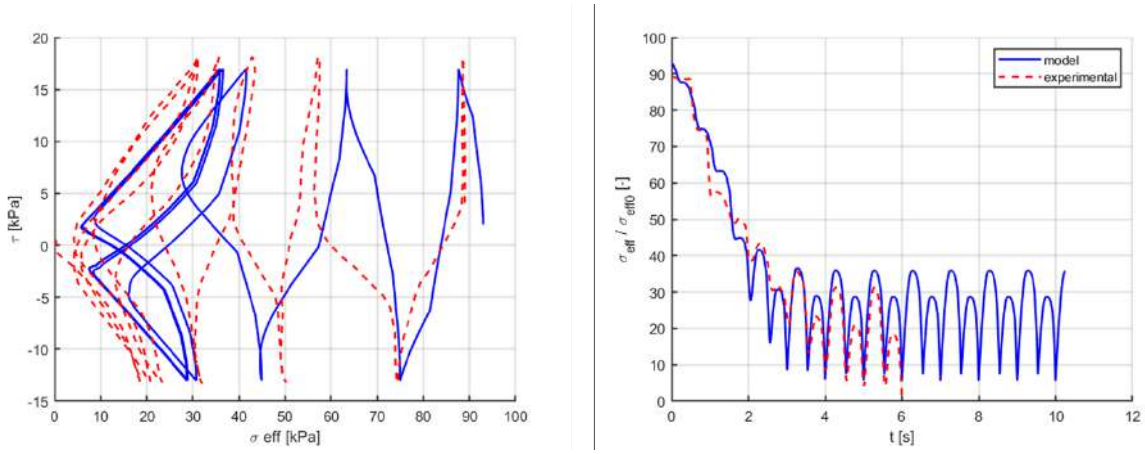

Figure 14: Calibration procedure Dr=40%: τ-σ' and σ'/τ planes.

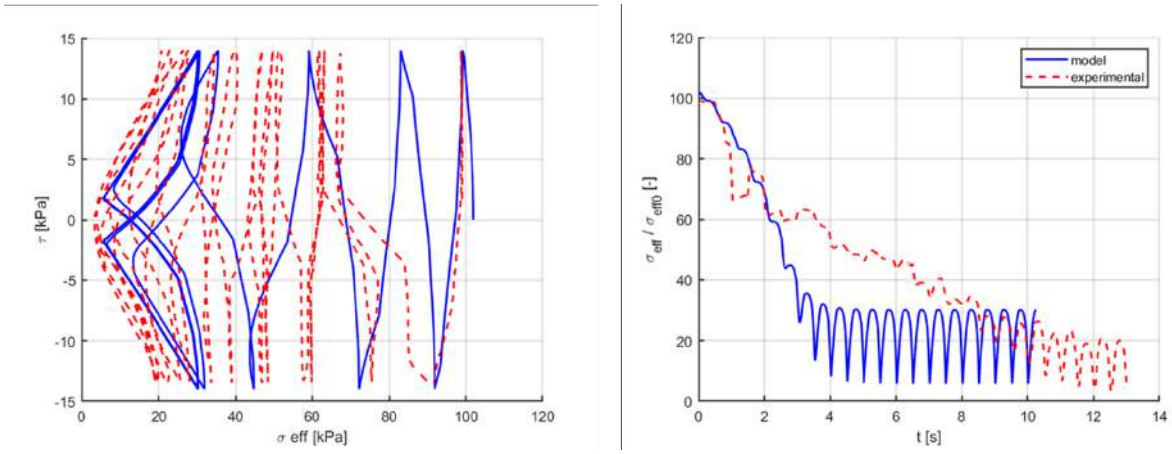

Figure 15: Calibration procedure Dr=20%: τ-σ' and σ'/τ planes.

In Figure 16, a parametric study is reported to show the effect of the initial slope induced anisotropy on the liquefaction potential of the material for a given shear controlled cyclic test. Higher stress level, due to the dilatancy, may be beneficial concerning excess pore pressure accumulation.

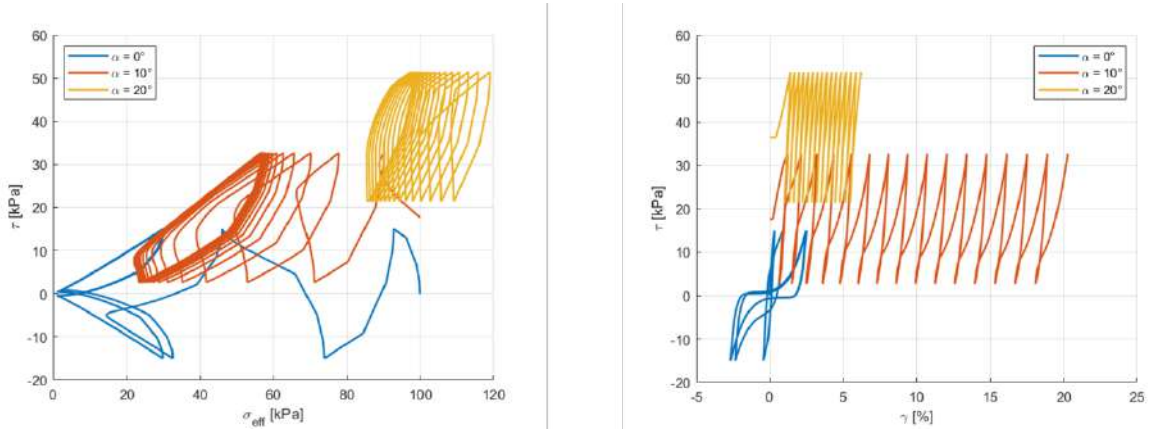

Figure 16: Parametric study to highlight the effect of the initial anisotropic state of the material: τ-σ' and τ-γ planes.

In Figure 17 and Figure 18, the outcomes of the analysis are reported, highlighting for different depths, the stress path, the accumulated displacement with time , the accumulated excess pore water pressure, as well as the final displacement profile. In case of a medium dense material, only a very shallow layer experience

inception, while in case of loose material, the volume undergoing liquefaction is higher and involves material at a greater depth.

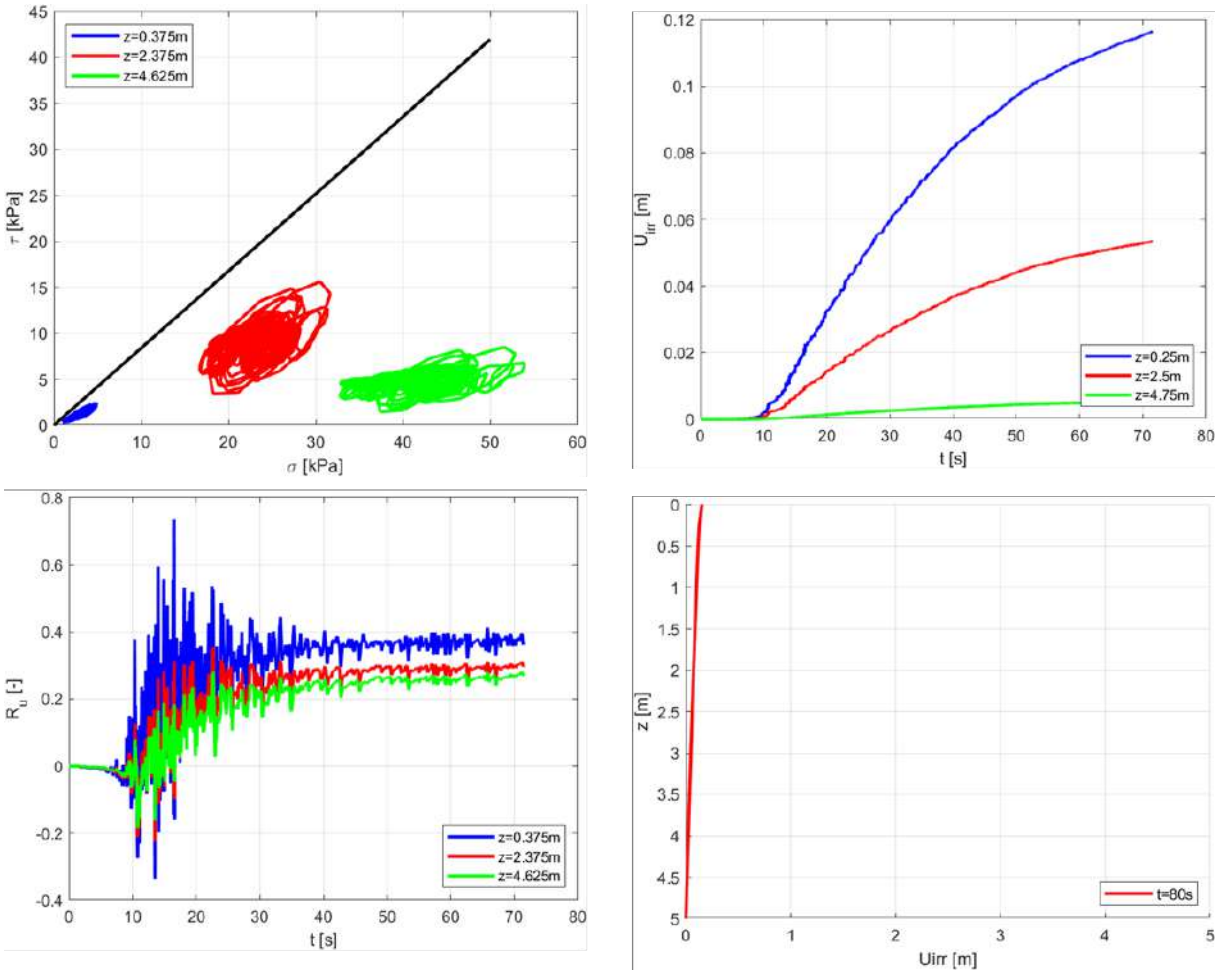

Figure 17: Outcomes of the inception phase, for Dr=40% and $\alpha = 10°$

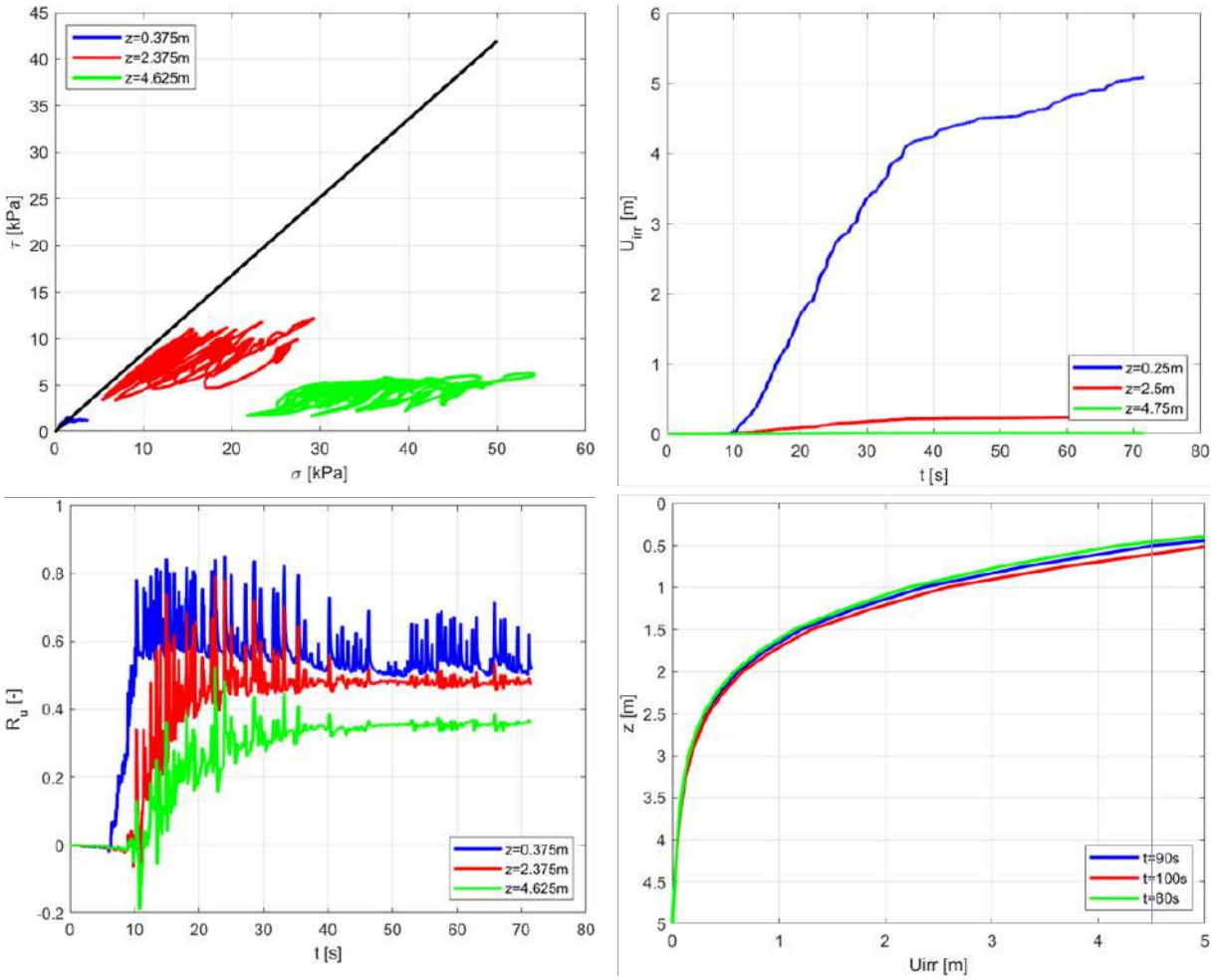

Figure 18: Outcomes of the inception phase, for Dr=10% and $\alpha = 10°$

Ring 3 – Landslide Propagation

The third ring is dedicated to modelling the propagation of the mobilized volume downslope. This is achieved through a combination of analytical and numerical approaches. In particular, analytical Bingham viscoplastic acceleration-phase modelling was adopted to rapidly estimate front velocity evolution, run-out distance, flow height during impact-critical stage; at the same time, Smoothed-Particle Hydrodynamics (SPH) depth-averaged simulations using GEOFLOW framework was adopted for selected cases to capture geometry-dependent effects. Cross-comparison of analytical and SPH outputs was performed for consistency checks.

- Inputs: mobilized mass, rheological parameters (τ_0, η), slope inclination
- Outputs: the Analytical Bingham model allowed to capture the acceleration-dominant regime governing peak velocity and dynamic impact potential, predict front velocities up to 24 m/s, depending on rheology (governed by relative density) and slope geometry, provide closed-form laws for run-out and velocity decay, enabling rapid scenario exploration; depth-averaged SPH simulation confirmed analytical trends, with deviations linked to topographic curvature and later-stage spreading, resolved flow thickness evolution for complex geometries. The combined use of analytical and SPH models provides a scalable and physically consistent benchmark approach for return-period–dependent debris-flow hazard modelling.

In Figure 19 the geometry of the propagation area, located under the zone where inception takes place is reported, as well as the position of the bridge.

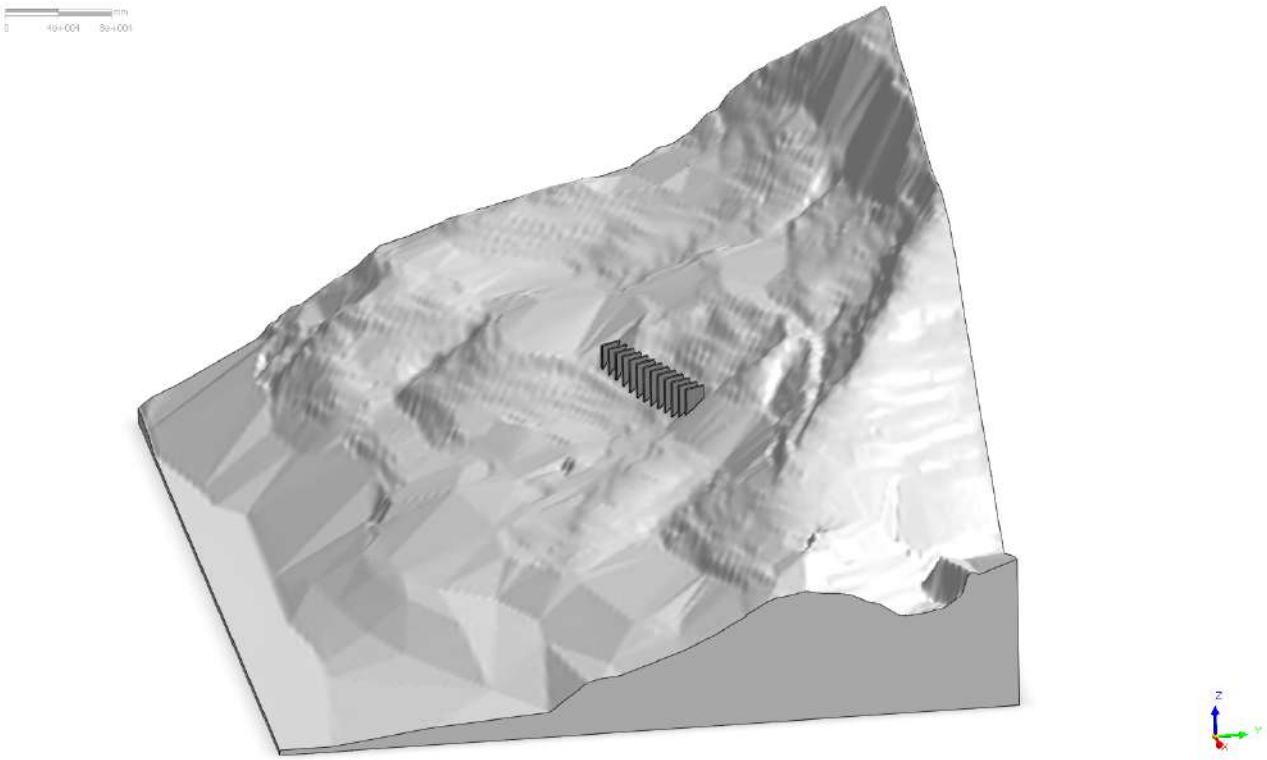

Figure 19: Landslide propagation geometry

The real geometry has been simplified, as sketched in Figure 20 such that the proposed tool could be used to estimate the runout and mass height and velocity in case of impact with the structure.

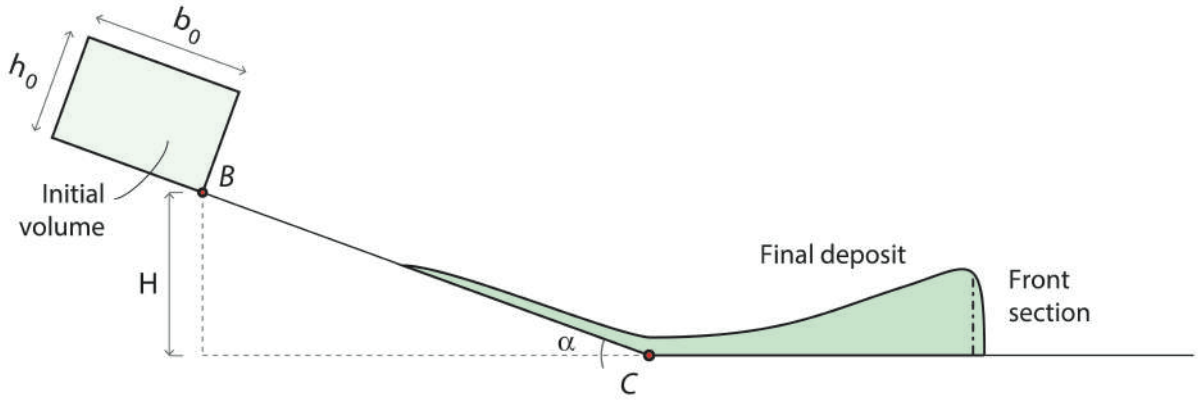

Figure 20: Simplified 2D geometry profile adopted in GEOFLOW-SPH to study the landslide runout

Ring 4 – Landslide - Structure Interaction

This stage evaluates the interaction between the debris flow and structural elements. Impact forces on bridge piers are evaluated via dynamic momentum-transfer formulation accounting for flow height, velocity and front inclination.

- Inputs: velocity, height, and density from Ring 3
- Outputs: time-dependent impact force, equivalent lateral pressure distribution, impulsive demand envelopes acting on bridge piers.

The result of this analyses have been used to calibrate an analytical formula for the impact force transmitted by the granular flow to the bridge pier is proposed. The time history of the impact force to be used for dynamic analyses is constructed following the procedure below (Figure 21):

- Initial phase (dynamic impact):
  The initial part of the force–time curve is assumed to be linear until $F_{peak} - t_{peak}$, that can be estimated taking advantage of two-dimensional numerical simulations.

- Transition phase:
  The force is assumed to decrease until the plateau value associated with the dragging phase. The time t_{drag} can be estimated as $t_{drag} = 3\, t_{peak}$.

- Viscous dragging phase:
  After the peak, the impact force decreases until it reaches a quasi-steady plateau, corresponding to the dragging phase. The value of this dragging force can be estimated using available experimental test results (cit.). In particular, many authors proposed to assume

$$F_{drag} = \frac{1}{2} c_d \rho u_0^2 H$$

  where c_d is a drag coefficient function of the obstacle geometry, ρ is the mixture density, u_0 is the average flow velocity and H is the average flow height. This expression is based on the analogy with the resistance calculation method of flow around column. For circular/square columns, $c_d \cong 1$ can be assumed (cit.).

  The end time of the force plateau (and so of the dragging phase) may be defined as a function of the length of the body of the impacting mass L_{body} L and the impact velocity u_0:

$$t_{tail} = t_{drag} + \frac{L_{body}}{u_0}$$

- Deposition phase:
  After the dragging phase, the impact force is assumed to decrease linearly until it vanishes. The time corresponding to zero force can be expressed as a function of the tail length of the granular mass, as obtained from SPH simulations:

$$t_{fin} = t_{tail} + \frac{L_{tail}}{u_0}$$

  This approach provides a physically consistent and computationally efficient framework to reconstruct the complete temporal evolution of the impact force from two-dimensional MPM results, allowing its subsequent use in dynamic structural analyses of the bridge pier.

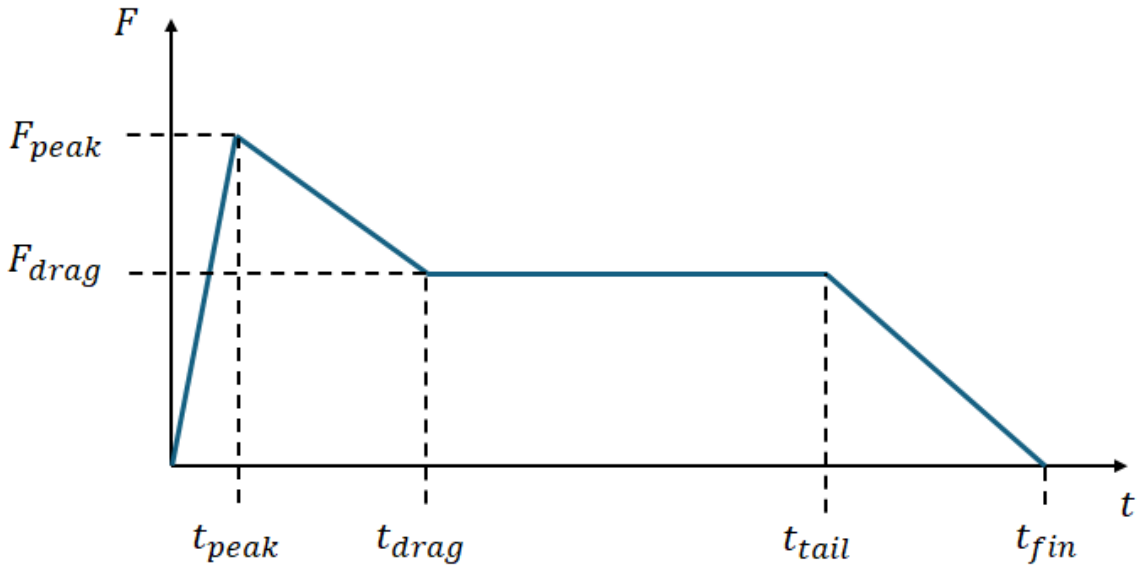

Figure 21: Structure of the landslide impact interaction force expression proposed

For the case study considered, assuming a Dr=20% for the material in the inception area, the impact force time evolution obtained is reported in Figure 22. The peak value is characterized by an impulsive nature, followed by a constant value, which is approximately six time smaller than the peak one. The totalduration of the interaction is mainly governed by the volume of the landslide, which is associate with its length.

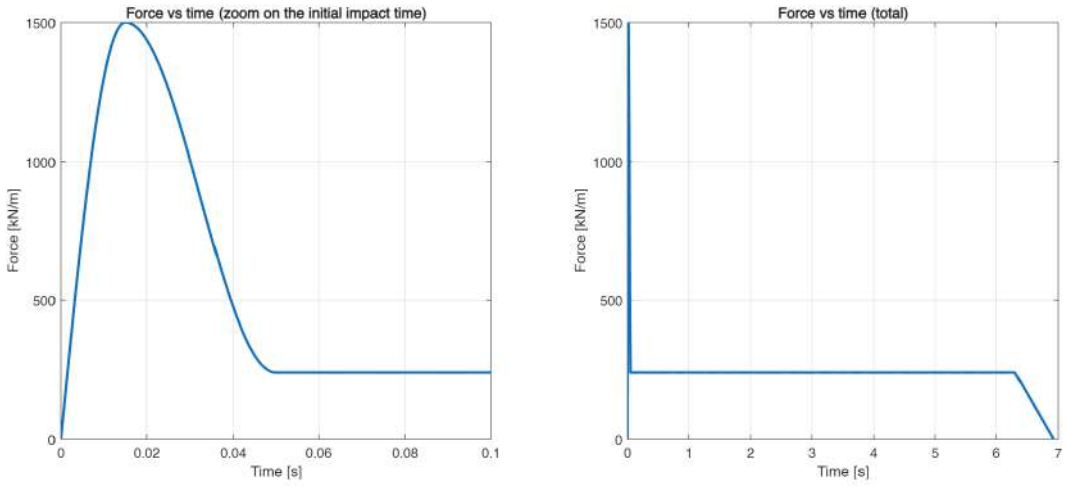

Figure 22: Impact force vs time for the considered case study

Ring 5 – Structural Performance of Aging Viaduct

The final ring is devoted to the assessment of the structural performance of aging reinforced concrete viaducts under cascading hazard loading incorporating deterioration mechanisms. This activity is still ongoing. At the moment, an accurate model of a RC viaduct archetype able to reflect the most common types of structures built in Italy in the past has been developed and a life-cycle seismic assessment procedure, including corrosion-related section loss and bond degradation model, has been finalized, as described in the following. In the next step, the impact forces calculated in the previous ring will be integrated to obtain demand-to-capacity ratios, residual performance classification and failure mode interpretation. When completely developed, the procedure will allow the evaluation of time-dependent fragility under multi-hazard interaction.

The case study selected to illustrate the life-cycle seismic assessment of a RC viaduct based on a time-variant pushover analysis is briefly presented The case study is inspired to the geometrical and structural

characteristics of the Cesi viaduct built in the early '70s. The viaduct is included in the OSS inventory of the Department of Civil Protection. The viaduct has a single carriageway with two lanes, for a total of 11 straight spans with length of 32 m each. The bridge deck is simply supported on each span and made of five PC longitudinal beams with a top RC slab and 4 transversal RC cross-beams, as shown in Figure 23. The bridge piers are characterized by a frame configuration with height ranging from 8 to 31 m. Each frame is composed by two RC columns having a two-cellular cross-section and a top connecting RC beam. Figure 24 shows the steel reinforcement of each column, that includes 138 steel bars with diameter Ø16mm constant over the pier height. The stirrups have a diameter of 12 mm with 250 mm spacing, constant along the pier column. The longitudinal reinforcement of the top connecting beam is based on 13Ø24 and 13Ø20 steel bars at top and bottom, respectively. The shear reinforcement is made by Ø12/100 constant along the beam. The bridge deck is supported by the piers through neoprene pads, which allow the relative displacement between deck and pier. The material properties of the structures are obtained from the acceptance tests performed during the construction phase. The steel yield strength is f_{sy} = 497.30 MPa and the concrete compression strength is f_c = 36.30 MPa.

The bi-dimensional structural model of the bridge piers has been developed using OpenSees for the non-linear analysis. Fiber displacement-based elements are adopted for the finite elements associated with both bridge pier and top connecting beam. Sensitivities analyses on the finite element discretization were performed in order to identify the optimal solution between the accuracy of the results and the computational cost. To better capture the deformation response of the most stressed sections, the model is built with a higher node density near the extremities of the vertical elements. The columns have been assumed clamped at the base. The material properties have been selected based on laboratory test results. Steel is modelled in OpenSees through the Steel01 uniaxial material with ultimate strain equals to 0.01, while concrete constitutive law has been associated with Concrete01 uniaxial material with ultimate strain in compression equals to 0.0035.

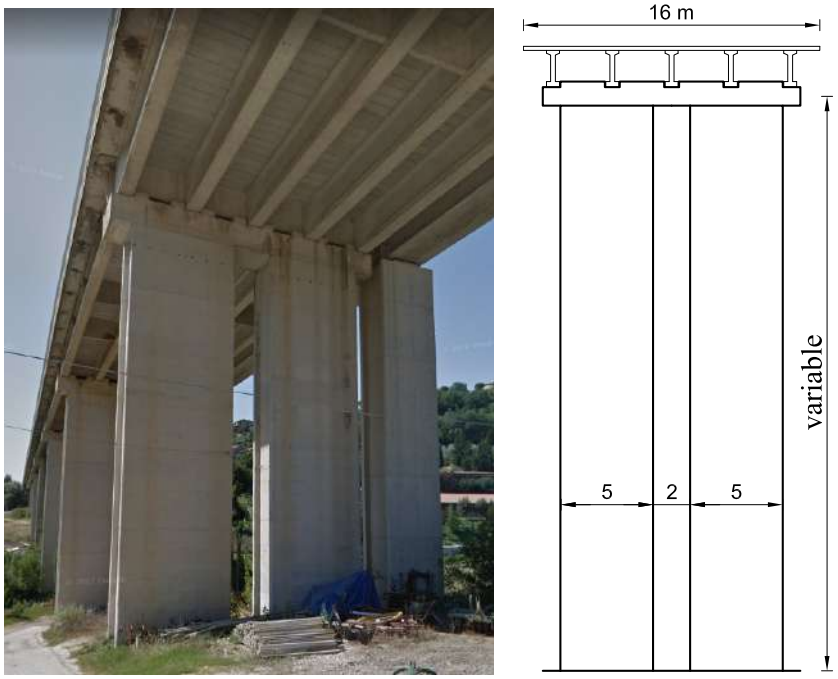

Figure 23. Cesi Viaduct: (a) View of the bridge; (b) Geometry and side view of bridge pier

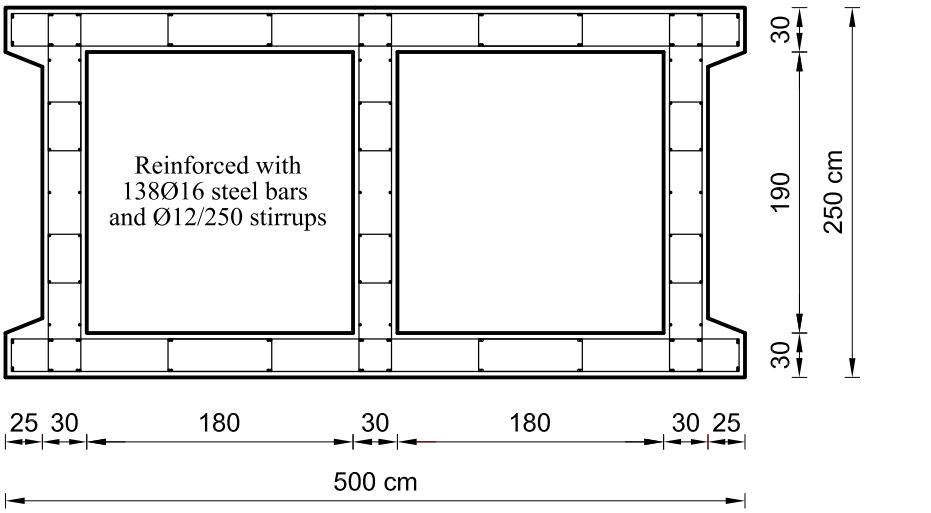

Figure 24. RC bridge pier: cross section and reinforcement layout of a single column bent

Carbonation-induced corrosion in RC structures is the result of a chemical reaction between carbon dioxide (CO_2) present in the atmosphere and calcium hydroxide in the concrete leading to a reduction of alkalinity in the pore solution, altering the passivity and causing the corrosion of reinforcing steel bars. The effects of concrete carbonation are generally evaluated by mean of the Fick's law of diffusion of CO_2 in concrete through the time-variant carbonation depth $x_c(t)$ based on concrete properties and environmental conditions. To explore the role and effects of steel corrosion, the bridge is considered subjected to carbonation-induced corrosion. The analysis timeframe ranges from the year of construction (1970) to the year 2100. Figure 25 shows the time-variant carbonation depth of the RC bridge pier in terms of mean μ and standard deviation σ. The corrosion initiation phase corresponds to time at which the carbonation depth reaches the surface of reinforcing steel bars. A concrete cover of 3 cm has been assumed. The propagation process is influenced by the availability of oxygen and moisture and is described by means of corrosion current density.

The effects of steel corrosion on the structural performance of the bridge pier are captured through the reduction of cross-sectional area of corroded bars, the reduction of strength and ductility of steel calibrated based on experimental test results, as well as the deterioration of concrete strength due to splitting cracks, delamination, and spalling of the concrete cover. In carbonated concrete without significant chloride content, corrosion tends to develop uniformly over the steel bar cross-section. The effects of steel corrosion are captured by means of damage-dependent geometric and mechanical properties of concrete and reinforcing steel bars (Biondini & Vergani, 2015). Steel corrosion can also alter the concrete-steel bond. However, the deterioration of steel-concrete bond strength and the effects of the bond-slip of corroded steel bars are not considered since bond-slip does not represent a critical issue for this application. In order to characterize the time-variant bridge pier response, a monotonic non-linear static analysis is performed. The analysis has been carried out considering a load pattern consistent with the first modal vibration period. Considering the axial force under permanent combination (N = 7.1 MN), Figure 26 shows the results of the pushover analysis for the 31.00m tall pier of the Cesi viaduct considering the carbonation-induced corrosion effects. The figure also represents different limit states associated with concrete cracking, steel yielding, and ultimate condition of the pier. The results highlight the effects of steel corrosion on the ultimate capacity of the bridge pier. Moreover, the loss of ductility of the section at the base of the pier, related to the reduction of the ultimate strain of the reinforcing bars, leads to a significant reduction of the drift.

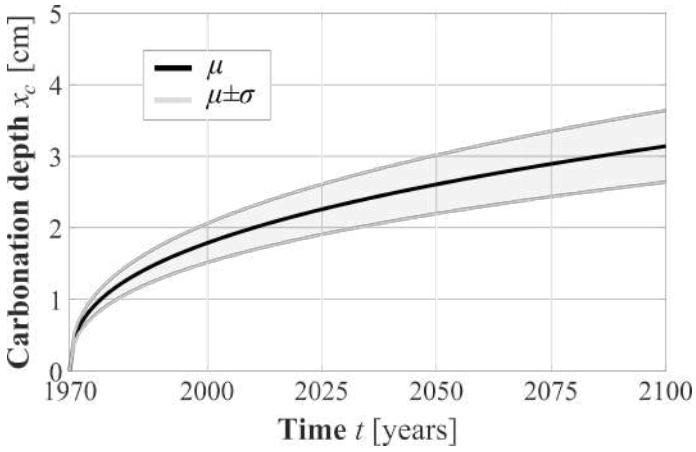

Figure 25. Time-variant carbonation depth on the RC bridge pier

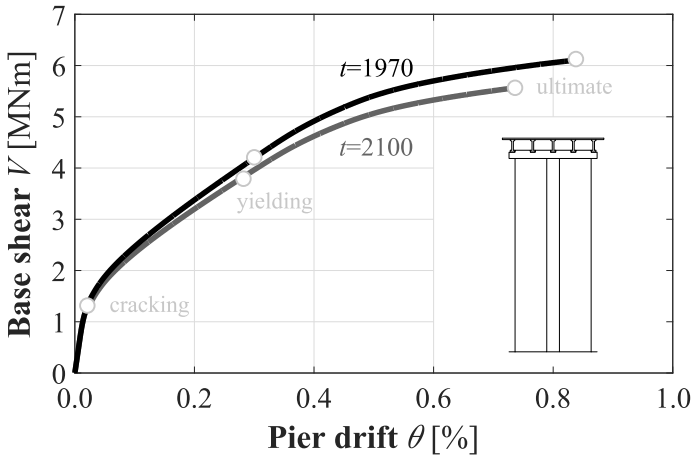

Figure 26. Nominal base shear V vs pier drift θ capacity curves at year 1970 and year 2100

5.4 Conclusions

A fundamental aspect of the proposed framework is the integration of the different methodological components into a coherent analytical pipeline. Each stage produces outputs that serve as inputs for the next, creating a continuous flow of information along the hazard chain. For example, the acceleration time histories generated in the seismic analysis are used to evaluate slope stability, which in turn defines the initial conditions for landslide propagation. The results of the propagation phase are then used to estimate impact forces, to be applied to the structural model.

This sequential structure ensures consistency in the representation of physical processes and allows for the propagation of uncertainties across the entire system. Variations in input parameters at one stage can influence the outcomes of subsequent analyses, highlighting the importance of sensitivity studies and probabilistic approaches, that will be the next steps. At the same time, the framework adopts a hierarchical modeling strategy, introducing simplifications where necessary to maintain computational feasibility while preserving the essential mechanisms of interaction.

Accordingly, the proposed framework represents an advancement in the field of multi-risk assessment. By integrating seismic, geotechnical, and structural analyses into a single methodology, it provides a more comprehensive understanding of how different hazards interact and affect infrastructure systems. One of the main contributions of the work lies in its ability to capture cascading effects, moving beyond traditional approaches that treat hazards independently.

From an engineering perspective, the framework aims to provide a practical tool for assessing the vulnerability of aging infrastructure under realistic conditions. It emphasizes the importance of accounting for both hazard interactions and time-dependent deterioration, which are often overlooked in conventional assessments. Once fully developed, the methodology has the potential to become a valuable tool for supporting infrastructure management and resilience planning.

6 A Multi-Hazard Resilient Urban Development framework

6.1 Introduction

Assessing the observed and future impacts of natural hazards and their cascading effects on interconnected urban infrastructures requires robust, risk-based approaches that provide quantitative indicators to guide resilience policies and integrated DRR-CCA strategies (Leone et al., 2025). Building on the IPCC concept of Climate Resilient Development (IPCC, 2022) – aimed at concurrently achieving GHG emission reduction, adaptation and well-being for people and ecosystems – a Multi-Hazard Resilient Urban Development framework should extend this integration to include both geophysical and climate-related hazard in risk assessments and scenario modelling (Turchi et al., 2023).

The methodology follows a progressive process structured around the definition of integrated parameters, spatial analysis, and the formulation of design measures for buildings and open spaces. Within this perspective, the modelling approach stems from the nature of the measures themselves, focusing on modelling the climatic hazards (heat waves and flood) and geophysical impacts (from volcanic earthquakes and ash fall). In fact, in the case of climatic risks, adaptation measures act primarily on the hazard component - since these phenomena can be mitigated by modifying the environmental and spatial conditions that amplify them - whereas for geophysical risks the measures aim at reducing exposure and vulnerability through structural and functional improvements of the built environment.

Building on these parameters, a GIS-based analytical framework integrates spatial datasets, environmental simulations, and multi-layer overlay techniques to produce ex-ante and ex-post scenarios that allow the quantitative evaluation of combined strategies and the identification of priority interventions.

A harmonized catalogue of adaptation measures for buildings and open spaces, addressing earthquakes, volcanic ashfall, heat waves, and flooding was built to assess their potential to influence hazard, exposure or vulnerability conditions, enabling its integration into Decision Support Systems for multi-risk resilience planning.

The method was tested in the Bagnoli district of Naples, a complex urban area characterized by multiple natural hazards and socio-environmental fragility conditions. The modelling results provided quantitative evidence of the potential effects of the combined measures, supporting comparative evaluation across ex-ante and ex-post scenarios. The application produced thematic maps and hazard/impact distributions that highlight how coordinated interventions – linking structural retrofitting and climate-adaptive spatial transformations – can reduce risk and enhance the overall adaptive capacity of the urban system across multiple scales.

Overall, the research contributes to advancing the integration between multi-risk assessment and urban design practice. Beyond its methodological advancement, the framework offers a transferable operational tool that supports planners and designers in developing context-specific, performance-driven strategies for urban resilience. Its scalability across different hazard configurations and urban morphologies positions it as a replicable approach for translating multi-risk knowledge into adaptive and sustainable design actions.

6.1.1 Multi-hazard approach and design framework

The growing complexity of natural hazards affecting urban systems calls for approaches capable of capturing the interdependent nature of risks and their impacts. Recent studies highlight the need for robust, indicator-based assessment methods to support resilience policies and integrated strategies for Disaster Risk Reduction (DRR) and Climate Change Adaptation (CCA) (Leone et al., 2025). At the international level, the IPCC framework of Climate Resilient Development (IPCC, 2022) provides a key reference by integrating mitigation, adaptation, and ecosystem well-being. However, in multi-risk urban contexts, this framework requires methodological extensions that explicitly address both climatic and geophysical hazards within a unified assessment process (Turchi et al., 2023). This need has led to the concept of Multi-Hazard Resilient Urban Development, which combines the IPCC perspective with DRR principles and an integrated reading of interactions between natural phenomena and urban systems.

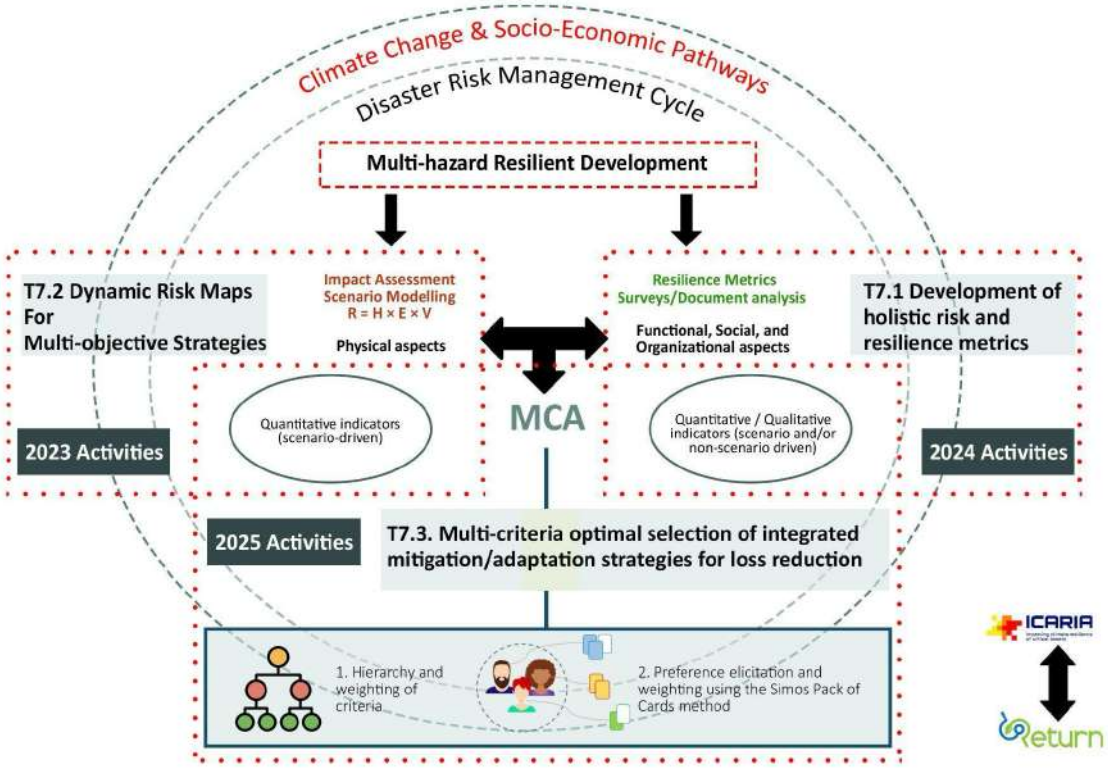

Figure 27: Holistic modelling framework for multi-hazard risk/impact assessment. This approach combines DRR and CCA principles, extending the IPCC framework by jointly addressing climatic and geophysical hazards. The cycle progresses through defining metrics (T7.1), dynamic risk mapping (T7.2), and optimizing mitigation/adaptation strategies (T7.3), all supported by Multi-Criteria Analysis (MCA) for loss reduction (modified after Leone et al., 2025).

In complex urban environments, the outcomes of risk depend on non-linear interactions between hazard, exposure, and vulnerability, influenced by spatial configuration, the quality of open spaces, and the characteristics of the built environment (Leone et al., 2025). The analysis therefore adopts the established risk equation R=H×E×V as a conceptual framework to interpret how different hazards affect exposed elements depending on their vulnerability and context. Within a Climate Resilient Urban Development perspective, this formulation is interpreted dynamically, acknowledging that risk evolves over time as urban conditions and environmental stresses change. A clear distinction is also made between risk and impact: risk represents the cumulative potential losses associated with multiple events over a given time period, while impact describes the spatial distribution of expected damage associated with a specific event scenario (Zuccaro et al., 2018b). This distinction allows the analysis to link long-term probabilistic risk assessments with spatially explicit evaluations useful for planning and design.

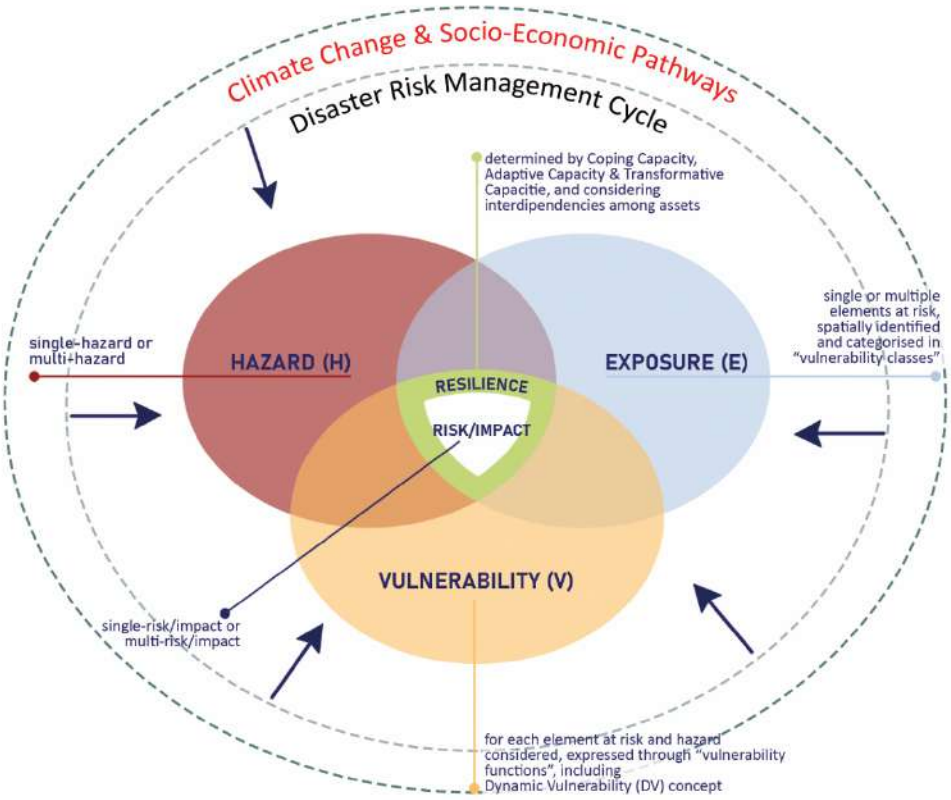

Figure 28: Concept of the holistic asset-level modelling framework for a multi-hazard risk/impact assessment, consolidated in the field of geophysical hazards (updated by the 2017 UNDRR's terminology) and harmonized in the context of climate change introducing resilience components (modified after Leone et al., 2025).

Coherently with these premises, the methodology adopted in this study follows a progressive process articulated in three main steps: definition of integrated parameters, spatial analysis, and formulation of multi-risk design measures. The model builds on the nature of the considered hazards: for climate-related risks—heatwaves and pluvial flooding—interventions primarily act on hazard conditions by modifying environmental and spatial factors that intensify the phenomena; for geophysical risks—earthquakes and volcanic ashfall—measures mainly target exposure and vulnerability through structural improvements and functional upgrades to the built environment. On this basis, a GIS-based analytical framework integrates spatial datasets, environmental simulations and multilayer overlay techniques, generating ex-ante and ex-post scenarios that allow the quantitative assessment of the effects of combined measures and the identification of priority intervention areas. To support this process, a harmonized catalogue of measures for buildings and open spaces was developed, describing how each intervention can influence hazard, exposure or vulnerability components and therefore contribute to reducing overall multi-risk conditions.

Within the broader project framework, a Multi-Criteria Analysis (MCA) was also conducted at the city scale as part of Tasks 3.7.1 and 3.7.3. In this case, the MCA is intended as a governance-oriented assessment rather than a tool for directly comparing design alternatives. It evaluates enabling conditions for urban resilience strategies, including the presence of risk management plans, the accessibility of risk information, and the inclusion of stakeholders and vulnerable groups in decision-making processes. This step provides an initial understanding of the institutional and planning context from which multi-risk strategies can be developed and prioritized.In addition, the research contributed to TS1 activities through participation in the development of *What-If* scenario sheets. The contribution consisted in compiling the scenario templates with the empirical data and analytical results produced in this study, enabling their integration into the wider scenario-building process developed within the project.

The framework is applied to the case study of Naples, focusing on the Bagnoli district, an urban area characterized by the coexistence of multiple natural hazards and socio-environmental vulnerabilities. The

application allowed the identification of minimum data requirements for multi-hazard assessment, the modelling of impacts on exposed systems, and the evaluation of the effectiveness of integrated interventions. The resulting thematic maps and scenario comparisons show how strategies that combine structural vulnerability reduction with climate-adaptive transformations of public space can simultaneously address climatic and geophysical risks while improving everyday urban performance.

Overall, the research strengthens the link between multi-risk assessment and urban design. The proposed framework provides a transferable operational tool capable of supporting planners and designers in developing context-sensitive, performance-oriented strategies that translate risk knowledge into adaptive and sustainable urban interventions.

6.1.2 Research references for the multi-hazard measures catalogue

The multi-hazard measures catalogue developed within the RETURN Project builds on a broader European research trajectory that increasingly integrates climate change adaptation, disaster risk reduction, and sustainable urban planning.

The CLARITY project developed a structured system of technical factsheets for climate adaptation measures, focusing on microclimatic effects and stormwater management. Through digital tools and spatial simulations, it enabled the quantitative ex-ante evaluation of interventions such as green roofs, permeable pavements, and increased tree canopy coverage, moving beyond purely descriptive approaches (Zuccaro et al., 2019).

The SPeED project addressed the integration of seismic safety and energy efficiency, showing how structural retrofitting can be combined with energy renovation strategies to generate multiple benefits, particularly in urban contexts characterized by aging building stock (Zuccaro et al., 2013).

This perspective was further expanded by the ICARIA project, which developed a decision-support platform for prioritizing multi-risk measures. By introducing Multi-Criteria Analysis tools, ICARIA enabled the comparison of design alternatives according to effectiveness, costs, and environmental co-benefits (Turchi et al., 2023).

Within this context, the contribution of RETURN lies in the systematic integration of these experiences into a single multi-hazard catalogue that jointly considers climate-related and geophysical risks. The innovation does not lie only in the collection of measures, but in their integrated evaluation with respect to hazard, exposure, and vulnerability, allowing the identification of solutions capable of generating cross-cutting effects and multiple benefits across urban systems.

6.1.3 Models and tools for evaluating the effects of measures

The assessment of design measures relies on the use of modelling tools capable of integrating geospatial datasets, building characteristics, and climatic and geophysical parameters. The objective is to quantitatively estimate how adaptation and mitigation strategies modify hazard, exposure, and vulnerability conditions, enabling the construction of decision-support scenarios. In this framework, design interventions are treated as input variables within the models, allowing their effects to be tested on urban risk scenarios and translated into locally tailored planning strategies.

Climate-related models

Climate scenarios are defined in accordance with the framework of the Intergovernmental Panel on Climate Change AR6 report (2022), which recommends the joint modelling of hazard, exposure, and vulnerability. Historical climate datasets are combined with projections up to 2070 under two emission pathways: SSP5-8.5, reflecting current trends, and SSP2-4.5, representing moderate mitigation.

Urban heat risk in open spaces is analyzed using the HWLEM (Heat Wave Local Effect Model), developed by the University of Naples Federico II within the CLARITY and KNOWING projects. The model evaluates urban heat island conditions and thermal comfort through a 2.5D approach that combines land-use data with three-dimensional parameters such as elevation, shading, and Sky View Factor. Bioclimatic indicators include Mean Radiant Temperature (MRT) and the Universal Thermal Climate Index (UTCI), allowing the

estimation of how spatial interventions—such as vegetation or surface modifications—can reduce heat hazard and improve outdoor comfort.

Pluvial flooding scenarios are simulated using SFINCS (Super-Fast INundation of CoastS), developed by Deltares. This model rapidly simulates urban flood events by integrating hydrological and climatic inputs, including precipitation, sea levels, and runoff conditions. It accounts for urban infrastructure and planned measures—such as green areas, drainage systems, and infiltration solutions—allowing the evaluation of their effectiveness and the estimation of potential damages.

Energy performance of the building stock is assessed through a spatialized estimation model that calculates energy consumption per square meter based on building typology. The model correlates building use, morphological characteristics, and envelope properties with energy demand. Consumption is estimated through coefficients associated with key parameters, including building use, internal heat loads, window-to-wall ratio, surface-to-volume ratio, structural typology, and construction period, enabling a consistent urban-scale representation of energy demand.

Geophysical models

The geophysical scenario considers buildings and population exposed to seismic and volcanic hazards based on historically documented events. Recorded intensities provide reference conditions for modelling, enabling the correlation between hazard levels and observed damage. Seismic vulnerability and exposure are evaluated through the S.A.V.E. (Seismic Assessment for Vulnerability Expectation) (Zuccaro et al., 2014) method, an empirical procedure that classifies building behaviour according to typological characteristics, observed damage levels, and seismic intensity. By integrating hazard, exposure, and vulnerability datasets, the model estimates potential impacts in terms of building losses, ashfall-related damage, and the number of residents potentially displaced.

Overall, these modelling tools allow the integration of the multi-hazard catalogue measures into spatial risk assessments, testing how design strategies influence impacts on both open spaces and the built environment. The simulations generate reference scenarios rather than deterministic forecasts: their outputs represent possible evolutions of the urban system under different intervention strategies. In this sense, resilience measures become operative variables within the modelling process, enabling the exploration of alternative territorial configurations and supporting the definition of context-specific design solutions.

6.2 Methodology

6.2.1 Structure of the multi-risk analytical framework

The methodology adopted in this study operationalizes the conceptual framework introduced earlier, addressing the complexity of urban contexts exposed to multiple natural hazards. It is grounded in an integrated perspective that combines climate resilience and Disaster Risk Reduction (DRR), extending the Intergovernmental Panel on Climate Change paradigm of Climate Resilient Development toward an explicitly multi-hazard interpretation.

The approach recognizes that urban risk cannot be adequately interpreted through sectoral or single-risk perspectives, but rather emerges from the interaction between natural phenomena and complex urban systems. Within this framework, the risk equation $R = H \times E \times V$ is adopted as a conceptual reference to describe how different hazards affect exposed elements depending on their vulnerability and spatial context. Consistent with the principles of Climate Resilient Urban Development, risk is interpreted as a dynamic and evolving configuration, influenced by urban transformations, the quality of built and open spaces, and social dynamics.

The analysis therefore focuses on the interaction between hazards and three main urban systems: open spaces, buildings, and people. Open spaces are examined as areas of direct interaction with climatic hazards, where morphology, permeability, vegetation, and spatial continuity influence the intensity and distribution of impacts. Buildings are assessed according to their capacity to absorb or amplify geophysical and climatic effects, considering typological characteristics, conservation conditions, and spatial distribution as key determinants of vulnerability. Population is analyzed as the exposed component, whose vulnerability is

shaped by demographic, socio-economic, and accessibility factors that influence the capacity to respond to risk.

Figure 29: The diagram illustrates the relationship between the considered natural hazards (climate-related and geophysical) and the main urban systems (open spaces, buildings, and people). The overlapping area highlights the interactions between the hazards and the systems which constitute the core domain of analysis and provide the knowledge base for identifying integrated multi-hazard design strategies and measures (source: authors' elaboration).

Understanding these interactions provides the basis for identifying design interventions capable of selectively reducing the components of risk. The objective is not only to characterize urban risk conditions, but also to support the selection of integrated design solutions that act simultaneously on hazard, exposure, and vulnerability according to the spatial context.

From this perspective, the integrated reading of risks and urban systems allows the compatibility of measures across multiple hazards to be assessed, highlighting their multi-hazard potential. Design solutions are therefore interpreted not as isolated responses to individual events, but as interventions capable of generating multiple benefits and co-benefits by acting across different components of risk and improving overall urban performance.

A central element of the framework is the explicit recognition of the triple operational dimension of design measures, evaluated under three reference conditions: the ordinary functioning of the city, seismic and volcanic emergency scenarios, and climate emergency conditions. In ordinary conditions, interventions contribute to improving urban quality, accessibility, and usability of public space. In geophysical emergencies, they support population protection, reduction of exposure, and continuity of urban functions. Under climate stress conditions, they contribute to mitigating thermal stress and reducing the impacts of extreme events.

This perspective allows design measures to be assessed not only for their emergency performance, but also for their contribution to everyday urban functioning, recognizing them as permanent urban devices that integrate safety, adaptation, and spatial quality. The results of the analysis provide the basis for the comparative evaluation of solutions and support the prioritization of interventions through Multi-Criteria Analysis, enabling the development of context-specific multi-risk design strategies.

PROJECT SOLUTIONS	HEATWAVE			FLOODING			EARTHQUAKE			ASHFALL		
	H	E	V	H	E	V	H	E	V	H	E	V
Green & Blue Infrastructure	X			X								
Reflective surfaces	X											
Permeable surfaces	X			X								
Canopies/Shading systems	X											
Energy retrofitting & greening		X				X			X			X
Structural retrofitting									X	X		X
Sloped roof										X		

Figure 30: Matrix linking design strategies to multi-hazard risk components. The matrix illustrates the relationship between selected design strategies and the different natural hazards considered, highlighting for each intervention whether it primarily reduces hazard, exposure, or vulnerability (source: authors' elaboration).

6.2.2 Risk assessment indicators and criteria

The indicators adopted are calibrated according to the specific characteristics of each hazard, while being integrated within a common evaluation framework to enable consistent comparison across risks (Table 1).

For heat waves, indicators consider thermal stress classes and associated estimated health costs. In the case of pluvial flooding, flood probability is combined with estimates of potential economic damage. Seismic risk indicators include the number of severely damaged buildings and the potential population displaced, while volcanic risk is assessed through ash load accumulation and the probability of roof collapse. Vulnerability is represented through vulnerability classes reflecting the structural and socio-spatial characteristics of exposed elements, while exposure is defined in terms of building and population density. The integration of these indicators enables a systemic interpretation of urban risk, allowing different hazards to be assessed within a unified analytical structure.

Table 1 – The table summarizes the metrics used to characterize the various hazards, consistent with the methodological framework adopted for the case study

Hazard	Indicator	Max/Min	Expected impacts
Heat wave	Mean radiant temperature of urban areas [Tmrt °C]	Min	Hospitalization costs related to heat-related illnesses [€]
Heat wave	Heat stress levels in vulnerable population groups [UTCI °C]	Min	Hospitalization costs related to heat-related illnesses [€]
Pluvial flooding	Probability of flooding in case of extreme precipitation events [m]	Min	1. Economic impact of road cleaning and restoration 2. Impact of flooding on buildings
Pluvial flooding	Infiltration capacity of urban soils [%]	Max	1. Economic impact of road cleaning and restoration 2. Impact of flooding on buildings

Earthquake	Macroseismic intensities [MCS]	Min	1. Number of buildings lost 2. Number of displaced persons
Ashfall	Ash fall load [kPa]	Min	Number of collapsed roofs

6.3 Application to the urban context of Naples: the case of Bagnoli

6.3.1 Risk assessment framework for the city of Naples

The construction of the knowledge base for the city of Naples builds upon the methodological framework previously described, enabling an integrated representation of how the urban system responds to natural hazards of different nature and intensity, and supporting the identification of priority areas for intervention.

The multi-hazard knowledge framework for Naples integrates climatic, geological, morphological, and socio-economic datasets, providing a comprehensive overview of urban risk conditions. Climatic hazards are analyzed through indicators related to thermal stress and flood probability. Heat waves are assessed using Mean Radiant Temperature (MRT) and the Universal Thermal Climate Index (UTCI), which capture the influence of urban morphology, surface characteristics, and vegetation on outdoor thermal comfort and potential health impacts, particularly for vulnerable groups such as children and the elderly. Pluvial flooding is evaluated through parameters related to surface permeability, runoff coefficients, and watershed morphology, allowing the estimation of flood-prone areas during extreme precipitation events.

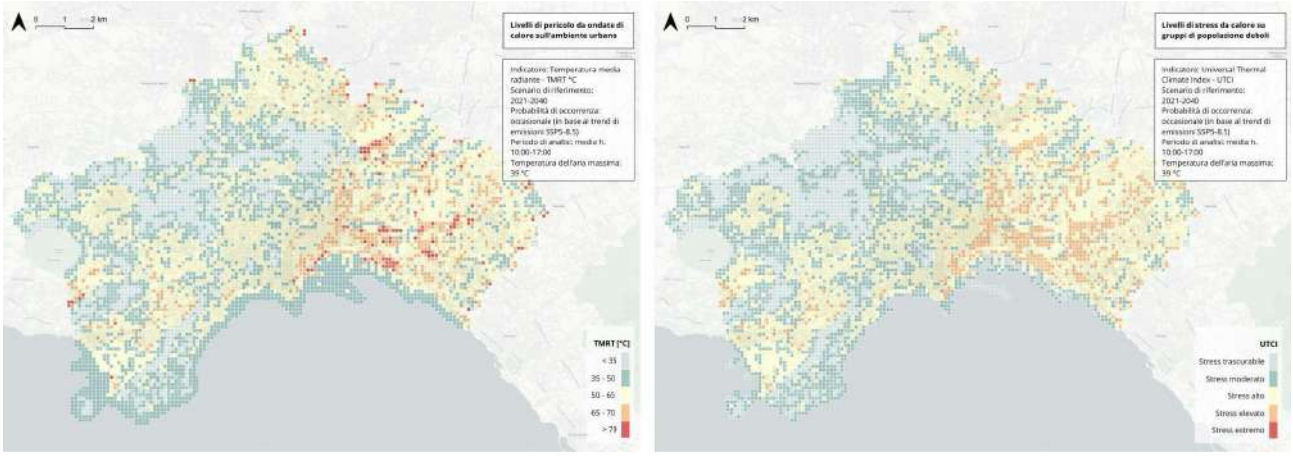

Figure 31: Maps of the Mean Radiant Temperature (TMRT) and the Universal Thermal Climate Index (UTCI) for a heat wave event with a peak air temperature of 39°C, with a probability of occurrence of “occasional” in the period 2021-2040 and “frequent” in the period 2041-2070, based on the SSP5-8.5 emissions trend. The map represents the average of the TMRT values during daytime hours (10:00-17:00) in the scenario referring to the current situation in November 2024 (Source: KNOWING Project).

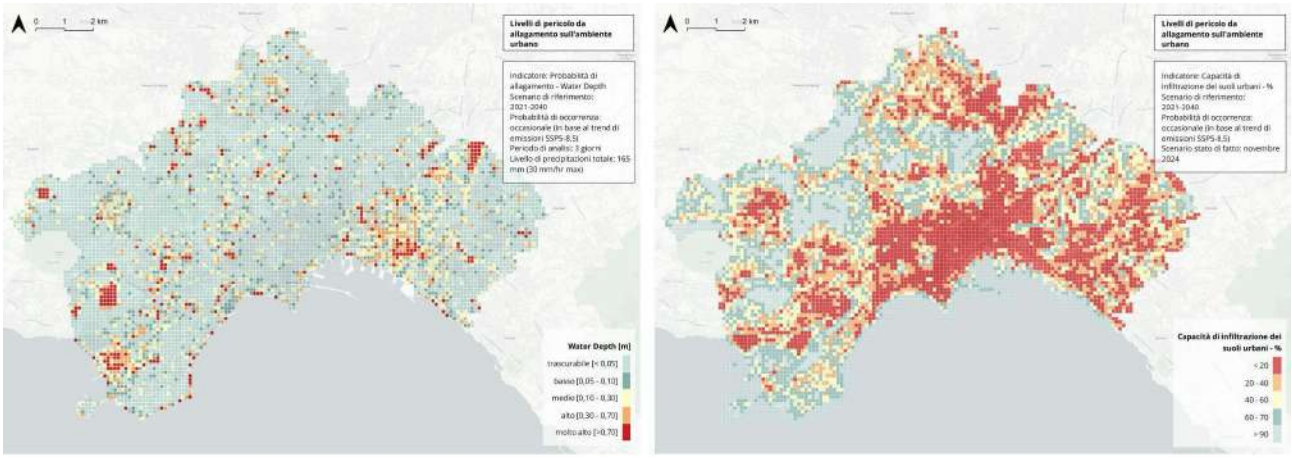

Figure 32: "Probability of flooding" and "Infiltration capacity" refer to a rainfall event of 165 mm in 3 days, with a peak of 30 mm/hr corresponding to an "occasional" scenario in the period 2021-2040 and a "frequent" scenario in the period 2041-2070, based on the SSP5-8.5 emissions trend. The maps represent the scenario referred to the current state as of November 2024 (Source: KNOWING Project).

Exposure and vulnerability are analyzed jointly, following the conceptual framework adopted by international risk assessment methodologies and the local Sustainable Energy and Climate Action Plan (PAESC). Exposure describes the spatial distribution and density of buildings, infrastructure, and population potentially affected by hazardous events. Vulnerability reflects the susceptibility of these elements to damage and is characterized through classes based on physical, environmental, and socio-economic attributes, including building typology, construction period, soil permeability, demographic structure, and access to services. In Naples, the high population density, the significant share of elderly residents, and the limited presence of permeable and vegetated surfaces contribute to elevated levels of exposure and vulnerability, particularly in the central and eastern districts.

Within the adopted framework, impact represents the spatial translation of the expected damage associated with a specific reference event, resulting from the interaction between hazard, exposure, and vulnerability. Unlike risk, which expresses the cumulative probability of losses over time, impact analysis focuses on the effects of individual events of defined intensity. For Naples, impact assessment primarily addresses geophysical hazards, evaluating potential damage to buildings, disruption of urban systems, and risks to the population resulting from seismic activity and volcanic ashfall.

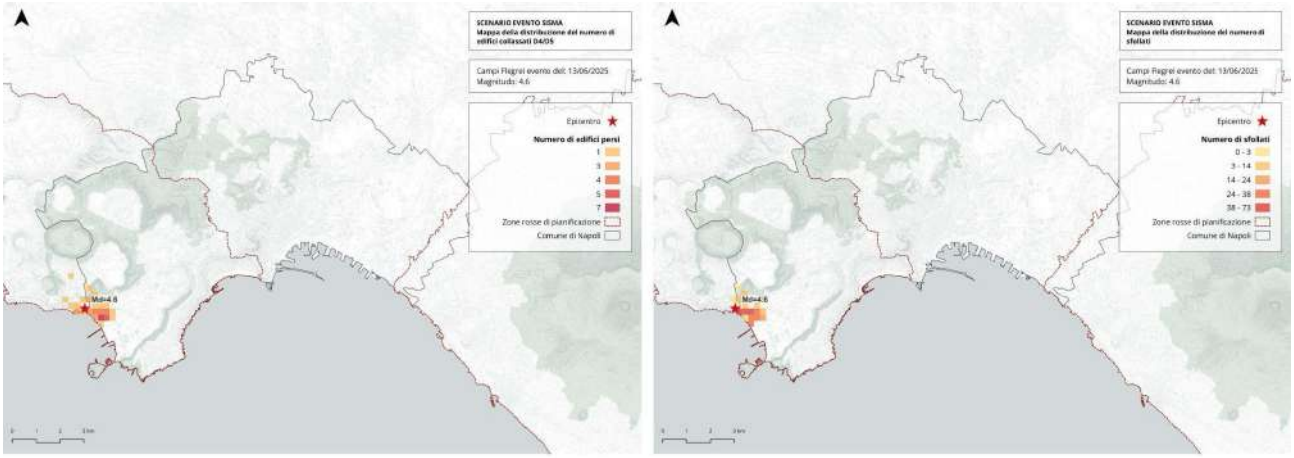

Figure 33: Maps of volcanic seismic impacts for the city of Naples. The maps show (left) the distribution of the estimated number of collapsed or severely damaged buildings and (right) the number of displaced people following a magnitude 4.6 seismic event generated by the Campi Flegrei (2025 scenario). The ground shaking associated with Mount Vesuvius is also

not shown, as it does not have a significant impact on the municipal area (Source: Data processed by Centro Studi P.L.I.N.I.V.S).

Seismic impacts are analyzed considering the potential effects of activity from the Campi Flegrei and Mount Vesuvius, the two main active volcanic systems influencing the metropolitan area. A reference seismic event associated with the Campi Flegrei—similar in magnitude to the one recorded in 2025—indicates higher expected impacts in the western districts of Naples, particularly in Bagnoli, where proximity to the caldera and the presence of vulnerable building stock increase potential damage levels. Conversely, seismic activity associated with Mount Vesuvius produces negligible effects on the city under ordinary conditions. Volcanic impact analysis further evaluates ashfall loads on roofs, estimating the number of buildings potentially affected by critical structural loads during reference eruptive events.

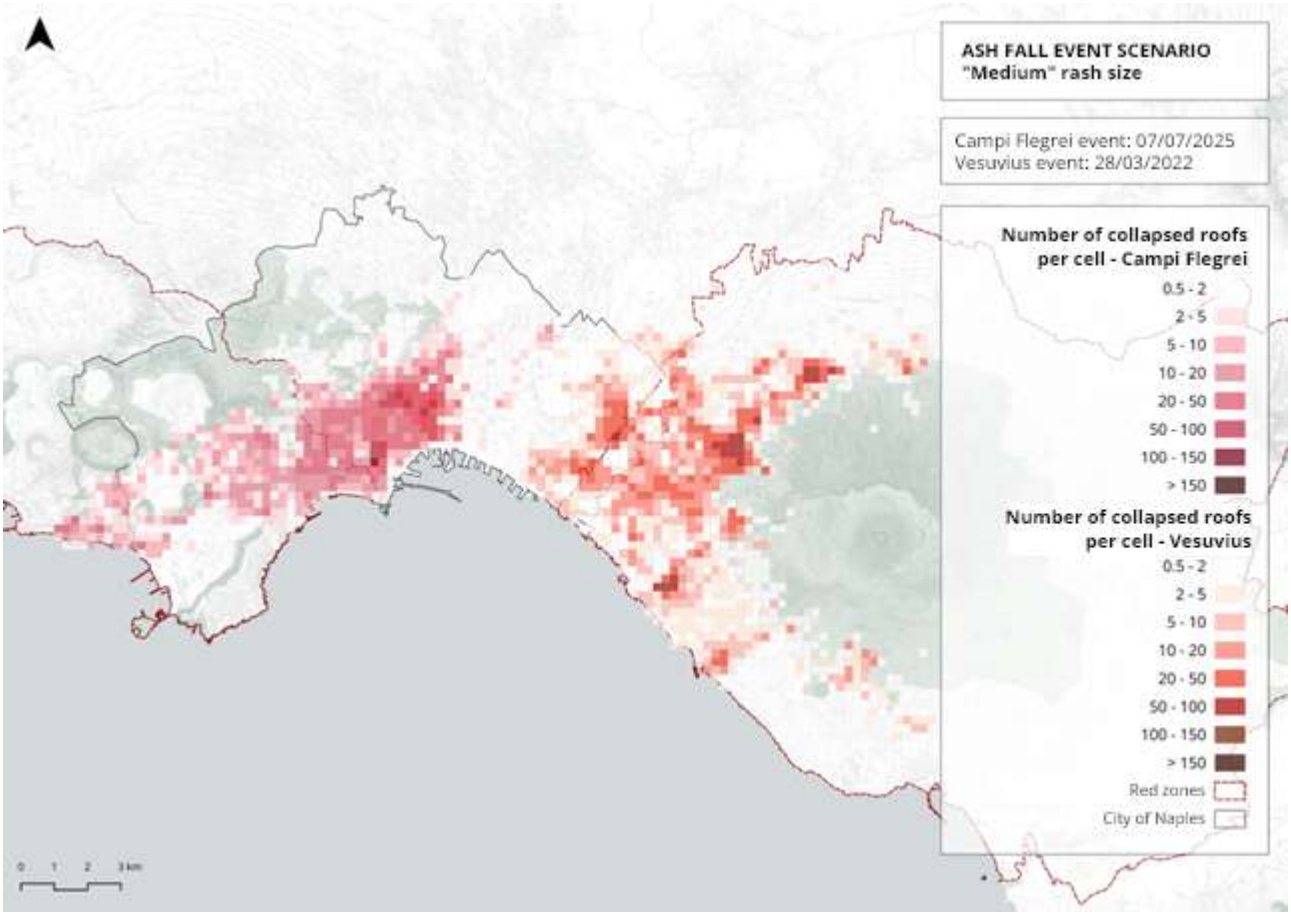

Figure 34: Map of ashfall impacts on building roofs in the municipality of Naples. The maps show the spatial distribution of roofs estimated to have collapsed following the Vesuvius event (2022) and the Campi Flegrei event (2025). The values reported indicate the number of roofs affected per spatial unit; areas with the highest concentration of collapses are highlighted on an increasing scale. (Source: Data processed by Centro Studi P.L.I.N.I.V.S).

Overall, the resulting multi-hazard knowledge framework provides an integrated and spatially detailed understanding of the interactions between natural processes and urban systems in Naples. The analysis highlights how risk conditions emerge from the overlap of physical hazards with socio-spatial vulnerabilities, rather than from hazard intensity alone. The produced maps therefore support the identification of priority intervention areas and provide the analytical foundation for the development of integrated multi-hazard resilience strategies.

Within this perspective, the subsequent in-depth analysis of the Bagnoli district represents a strategic application of the methodology, as the area combines significant environmental vulnerabilities with major

opportunities for urban regeneration, making it a representative case for testing integrated resilience-oriented urban design strategies.

6.3.2 Bagnoli: urban features and environmental systems

The district of Bagnoli, located within the Tenth Municipality of Naples, represents a strategic context for multi-hazard analysis, as environmental, infrastructural, and social components interact directly with both climatic and geophysical pressures. Its proximity to the Campi Flegrei caldera makes it one of the urban areas most exposed to volcanic and seismic phenomena in the metropolitan area, providing a relevant case for investigating urban resilience.

Historically, Bagnoli developed as one of southern Italy's main industrial districts following the construction of the Italsider steel plant along the coastal area during the early twentieth century. Industrialization profoundly transformed the morphology and socio-spatial structure of the district, replacing agricultural and coastal recreational uses with a dense and largely impermeable industrial landscape. The industrial decline that culminated in the closure of the plant in 1992 left a large contaminated area characterized by soil and marine pollution, spatial fragmentation, and restricted coastal access (Giannotti, F. et al., 2019). Former industrial sites and interdicted coastal zones became physically and symbolically disconnected from the urban fabric, reinforcing conditions of environmental and social vulnerability. These conditions are further compounded by the geophysical dynamics associated with the Campi Flegrei volcanic system, particularly the phenomenon of bradyseism, which produces periodic ground uplift and subsidence (Perelli, F.L. et al., 2023). The interaction between geological instability, environmental degradation, and long-standing uncertainties related to land reclamation and redevelopment has produced a layered landscape of environmental, geophysical, and social vulnerabilities. In this sense, Bagnoli represents an emblematic case where natural hazards intersect with long-term urban and infrastructural fragilities.

The analysis therefore focuses on the main systems structuring the district—ecosystems, open spaces, and buildings—in order to understand how they interact with hazard dynamics and with the components of exposure and vulnerability. This perspective enables an integrated reading of the territory that supports the identification of priority intervention areas and informs multi-risk urban design strategies.

From an ecological perspective, Bagnoli includes a diverse set of environmental systems, such as marine, post-industrial wetland, forest, agricultural, dune, and urban ecosystems. These components reflect the coexistence of natural and anthropogenic processes shaping the area. Coastal and marine ecosystems are currently affected by pollution and limited accessibility, while abandoned industrial lands have partially evolved into wetland environments hosting pioneer vegetation and returning fauna. Forested and agricultural areas located along the surrounding slopes contribute to ecological continuity and microclimatic regulation, while dune systems provide natural coastal protection. Within this mosaic, the urban ecosystem functions as the infrastructural matrix in which these environmental components interact, generating both ecological connections and spatial conflicts.

The system of open spaces is characterized by strong discontinuities in accessibility and use. While some parks, squares, and recreational areas remain active and accessible, large portions of the former industrial zone and coastal strip remain abandoned, contaminated, or physically inaccessible. The pedestrian, cycling, and public transport networks are fragmented, limiting direct connections between residential areas and the waterfront. The classification of open spaces—including parks, squares, playgrounds, residual green areas, and beaches—highlights not only the quantity of public space but also its role in mitigating climatic risks. The scarcity of permeable and shaded surfaces increases exposure to thermal stress and reduces stormwater absorption capacity, amplifying the impacts of heat waves and pluvial flooding.

The building system reflects the historical stratification of the district and includes a compact residential core surrounded by large areas of disused industrial structures and transitional spaces, such as the former industrial complex and the ex-NATO base. These areas, often underused or inaccessible, simultaneously represent critical vulnerabilities and strategic opportunities for urban regeneration. Buildings can be categorized into residential structures, critical or degraded buildings—often associated with industrial heritage—strategic facilities identified in emergency planning, and transformative buildings such as schools, museums, universities, and cultural centers. The latter may play an active role in multi-risk strategies, functioning as emergency gathering areas, temporary shelters, or climate refuges.

Spatially, the residential core of Bagnoli is strongly bounded by both natural and infrastructural barriers. A railway line runs along much of its perimeter, limiting permeability, while Monte Spina forms a natural boundary to the north. To the south-east, the residential fabric directly faces the fenced and largely inaccessible former industrial area. This configuration contributes to a sense of urban isolation and restricts connections between housing, open spaces, and the coastal zone, affecting both quality of life and the district's capacity to respond to natural hazards.

Overall, the integrated analysis of environmental and settlement components reveals a fragmented urban system shaped by the overlap of natural processes, industrial development, and post-industrial transformation. The coexistence of ecologically valuable environments, discontinuous open spaces, and heterogeneous building stock generates complex patterns of exposure and vulnerability. At the same time, the presence of transformable spaces and strategic functions offers opportunities for regeneration processes based on a multi-hazard perspective, supporting urban strategies aimed at strengthening resilience while reconnecting ecological, social, and spatial systems within the district.

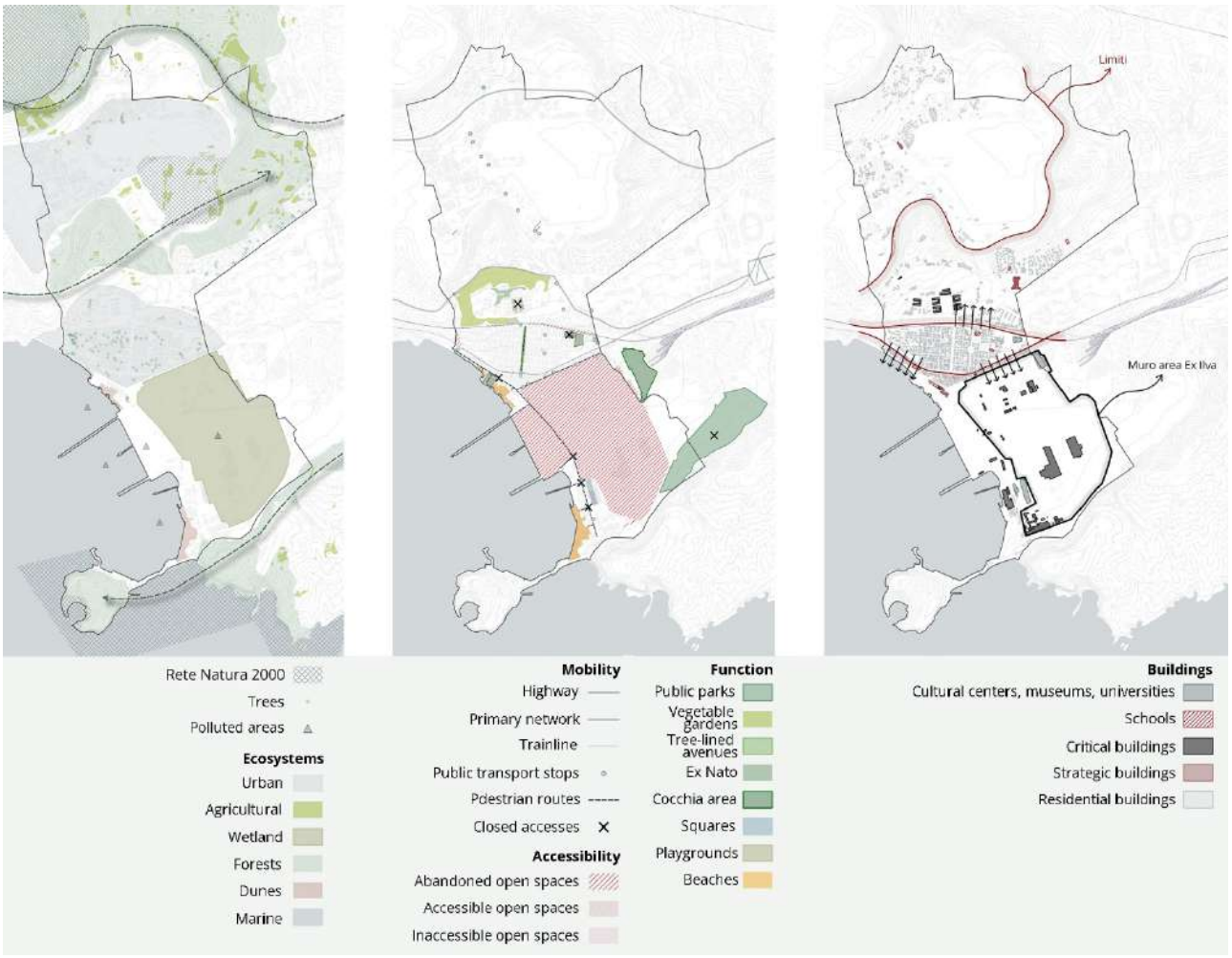

Figure 35: Urban systems analysis of the Bagnoli neighbourhood. The maps document the ecological, spatial, and built dimensions of the study area: the distribution and continuity of ecosystems across natural and anthropized spaces; the classification of open spaces by accessibility and typology — including parks, squares, playgrounds, residual green areas, and beaches — highlighting the fragmentation of the public space network and the limited continuity of cycle-pedestrian paths and coastal access; and the distribution of buildings across residential, critical, strategic, and transformative categories, with attention to the physical and functional isolation of the main residential fabric imposed by the railway line, Monte Spina, and the former industrial complex. Collectively, these maps provide the analytical foundation for evaluating the capacity of existing urban systems to mitigate climate

and geophysical risks and for identifying priority areas for integrated multi-risk intervention (Source: Authors' elaboration).

6.3.3 Natural Hazard Risk Assessment and Emergency Planning Integration in the Bagnoli District

The natural hazard risk assessment for the Bagnoli district builds upon the methodological framework outlined in the preceding chapters, which systematically integrates hazard, exposure, and vulnerability to produce a coherent and dynamic reading of urban risk. Consistent with the city-scale analysis developed for Naples, the assessment distinguishes between climatic hazards and geophysical impacts, acknowledging the fundamentally different ways in which these phenomena interact with the urban fabric, the built environment, and the resident population. To synthesize these outputs into a unified metric, a Synthetic Index was developed combining climate hazard indicators with geophysical impact indicators. This index supports the identification of areas where urban elements are most susceptible to potential losses under multiple risk scenarios. The hybrid nature of this approach — overlapping information from hazard and impact maps — reflects the different relationships that design interventions on buildings and open spaces bear with respect to the H-E-V variables in the case of climatic and geophysical risks. As said before: for climatic risks, adaptation measures primarily target hazard intensity by modifying the environmental and spatial conditions that amplify heat or flooding; for geophysical risks, mitigation focuses on reducing exposure and vulnerability through structural reinforcement and functional upgrades to buildings and infrastructure.

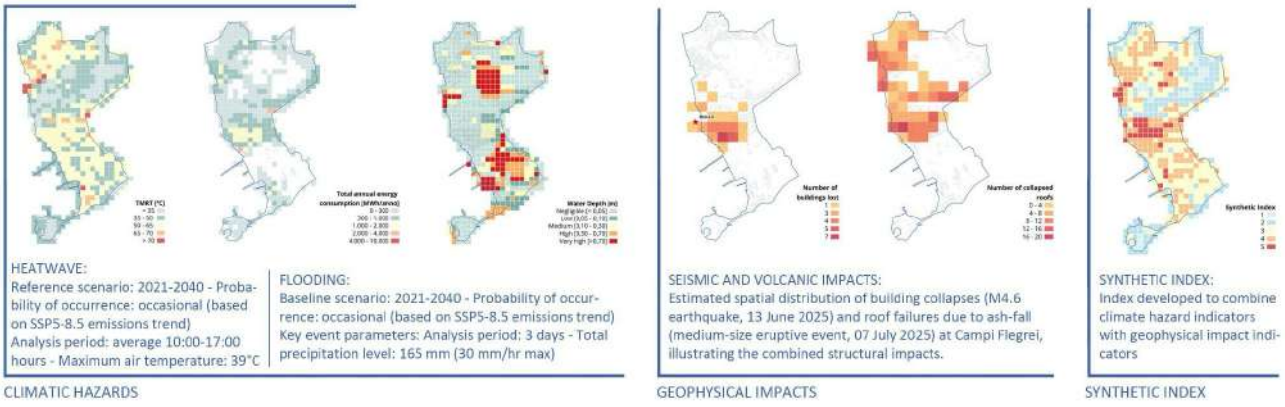

Figure 36: Ex-ante multi-hazard assessment maps for the Bagnoli district. The figure presents the five analytical outputs of the risk assessment framework: the two climatic hazard maps and the two geophysical impact maps together with the Synthetic Index, which integrates all four indicators into a unified metric highlighting the spatial distribution of combined risk conditions and identifying priority areas for integrated multi-hazard intervention (Source: Authors' elaboration).

A further dimension of integration concerns emergency planning, which is closely linked to natural risk management and the definition of design strategies. Bagnoli falls within both the civil protection plan for seismic risk and that for volcanic risk. The seismic plan (Piano comunale per il rischio sismico ed aree di emergenza) identifies three scenarios based on differentiated impacts on urban systems — buildings and infrastructure — while the volcanic plan (Piano rischio vulcanico Campi Flegrei) prescribes the evacuation of 50% of the population using private means and the remaining 50% via public transport within a 48-hour window. The integration of these scenarios with the multi-hazard analysis strengthens the capacity to connect risk management with urban planning, highlighting both constraints and opportunities for design strategies. In particular, knowledge of evacuation routes, assembly areas, and operational priorities allows for an assessment of the compatibility of design measures with population safety and the functional continuity of the neighbourhood. This orients design towards solutions capable of combining risk reduction, urban system resilience, and spatial quality improvement, ensuring that multi-hazard strategies remain coherent with civil protection requirements and defined emergency scenarios. In this way, design measures

become operational instruments for both risk prevention and mitigation and the effective management of emergencies, integrating safety, adaptation, and urban quality within a single systemic vision.

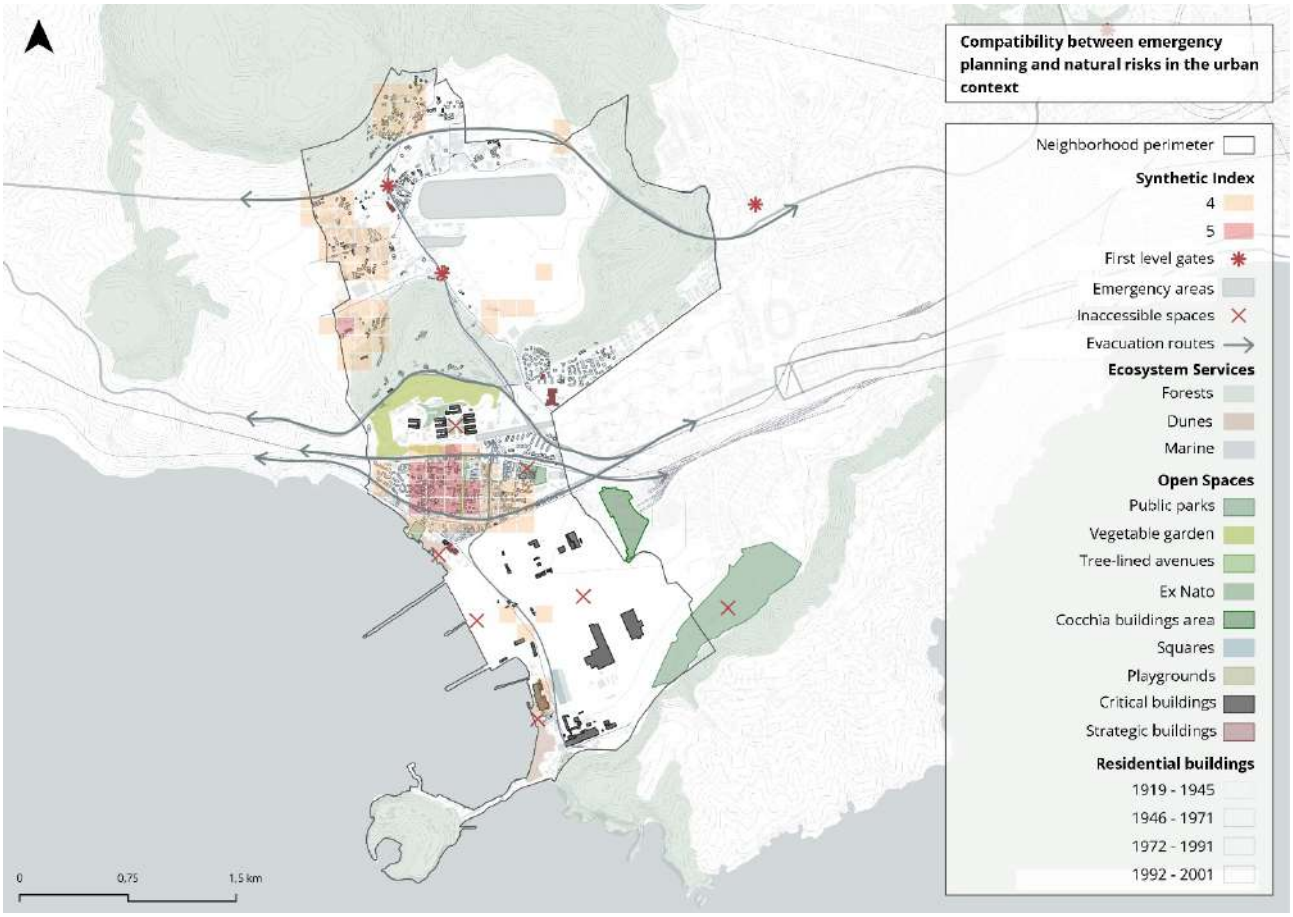

Figure 37: Integration of multi-hazard risk assessment and emergency planning frameworks for the Bagnoli district. The map overlays the spatial distribution of natural risks with the provisions of the two civil protection plans applicable to the area, including evacuation routes, assembly areas, and operational priority zones. This integrated reading reveals the spatial relationships between risk conditions and emergency management infrastructure, highlighting areas of potential conflict or compatibility between multi-hazard exposure and civil protection requirements. The overlay constitutes the analytical basis for ensuring that the proposed design strategies are coherent with existing emergency scenarios and capable of contributing simultaneously to risk reduction, population safety, and the functional continuity of the neighbourhood (Source: Authors' elaboration).

6.3.4 Integrated design strategies

The design strategies developed in this study are situated within the broader planning framework currently shaping Bagnoli's transformation. The district is the subject of the *Programma di Risanamento Ambientale e Rigenerazione Urbana* (PRARU) of the Sito di Interesse Nazionale Bagnoli-Coroglio, a programme encompassing environmental remediation, coastal restoration, and new urban infrastructure. The designation of Naples as host city of the 38th America's Cup in 2027 — with operational bases located within the former industrial site — has further accelerated this trajectory, framing Bagnoli's transformation around tourism, sport, and leisure functions.

This orientation, however, raises substantive questions that the present study takes seriously. The PRARU envisions a significant increase in residential and tourist-receptive uses, implying a considerable growth in population and urban activity — and therefore in exposure to the natural hazards documented in the preceding sections. Moreover, the tension between a neighbourhood-centred vision of regeneration and a

tourism-driven development model remains unresolved, with direct consequences for spatial equity and long-term livability. The design strategies proposed here do not seek to supersede the ongoing institutional planning process, but to complement it critically, insisting on multi-risk resilience, adaptive capacity, and spatial quality as foundational conditions for any future vision of Bagnoli.

Open Spaces

The strategic framework for open spaces is structured around five interconnected lines of action, collectively oriented towards building adaptive urban resilience across multiple risk scenarios.

Ecological reconnection constitutes the foundational layer of the framework, pursued through the restoration of environmental continuity and the regeneration of the most vulnerable areas of the urban territory. Priority actions include the remediation of contaminated sites through phytodepuration techniques, the restoration of the coastline to strengthen natural protection against storm surges, and the re-establishment of ecological corridors and green urban habitats (Kabisch, N. et al., 2017).

Equally central is the structural and climatic upgrading of existing evacuation routes, identified as a priority measure to ensure accessibility, shading, and functionality under conditions of environmental or infrastructural stress, with particular attention to the mobility needs of vulnerable population groups. This is complemented by the design of new pedestrian and cycling connections integrated with the existing road network, which redefines slow and sustainable mobility through the stratification of pedestrian and vehicular flows, the reduction of spatial conflicts, and the implementation of bike-sharing points near interchange nodes and assembly areas to support multimodal connectivity.

Public spaces are further conceived as flexible infrastructures capable of adapting to emergency or seasonal conditions — through the design of equipped waiting areas, the identification of gathering points in high-tourist-flow zones, and the experimentation with mixed-use spaces adaptable to recreational, logistical, or emergency functions throughout the year. Finally, the reactivation of underused urban assets is pursued as a means of transforming disused spaces into new neighbourhood centralities, through maintenance interventions, the integration of new equipment and social functions, and the promotion of temporary and community-driven uses.

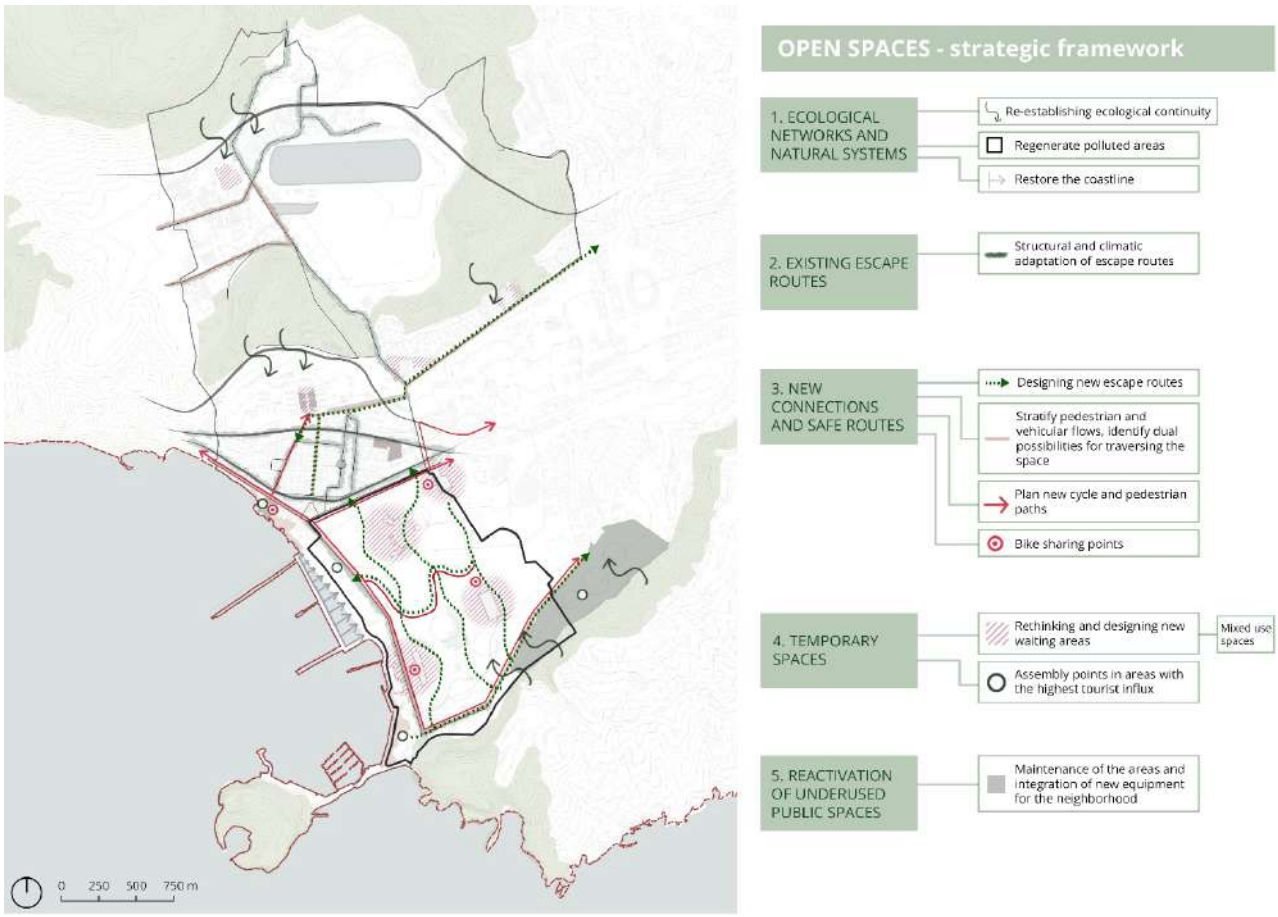

Figure 38: Strategic framework for open spaces in the Bagnoli district. The map illustrates the five interconnected lines of action structuring the open space strategy (Source: Authors' elaboration).

The methodological approach underpinning these strategies is adaptive and integrated, designed to respond in a coordinated manner to three distinct urban conditions: the ordinary scenario, the heat wave emergency scenario, and the seismic evacuation and emergency scenario. These three scenarios are not merely operational categories — they reflect the coexistence of three fundamental and simultaneous natures of the Bagnoli territory: a living urban neighbourhood, a climate-exposed coastal landscape, and a high geophysical risk zone. The design measures identified do not address these dimensions in isolation, but are conceived precisely to respond to and integrate all three, operating across multiple registers at once. Open space is thus conceived as a multifunctional infrastructure whose spatial, ecological, and structural qualities are calibrated to serve everyday sociality and wellbeing, to mitigate thermal stress and flooding under climatic pressure, and to ensure safety and operational continuity under seismic or volcanic emergency conditions — embodying, in a single design logic, the full complexity of the territory it inhabits (Addabbo et al., 2023).

Ordinary Scenario

Under ordinary conditions, the open space network performs an ecological and environmental function, ensuring climatic comfort, accessibility, and urban quality. The regeneration of contaminated areas and the denaturalization of soils re-establish ecological and landscape continuity, promoting biodiversity and depuration processes. Cycling and pedestrian paths form green, shaded corridors connecting different urban districts, while the waterfront is upgraded through reversible interventions compatible with the coastal ecosystem. Multifunctional green areas integrate ecological, social, and productive functions — including green water squares for stormwater management, floating farms, and urban agriculture systems — alongside the integration of renewable energy solutions in public spaces to support a transition towards energetic self-sufficiency.

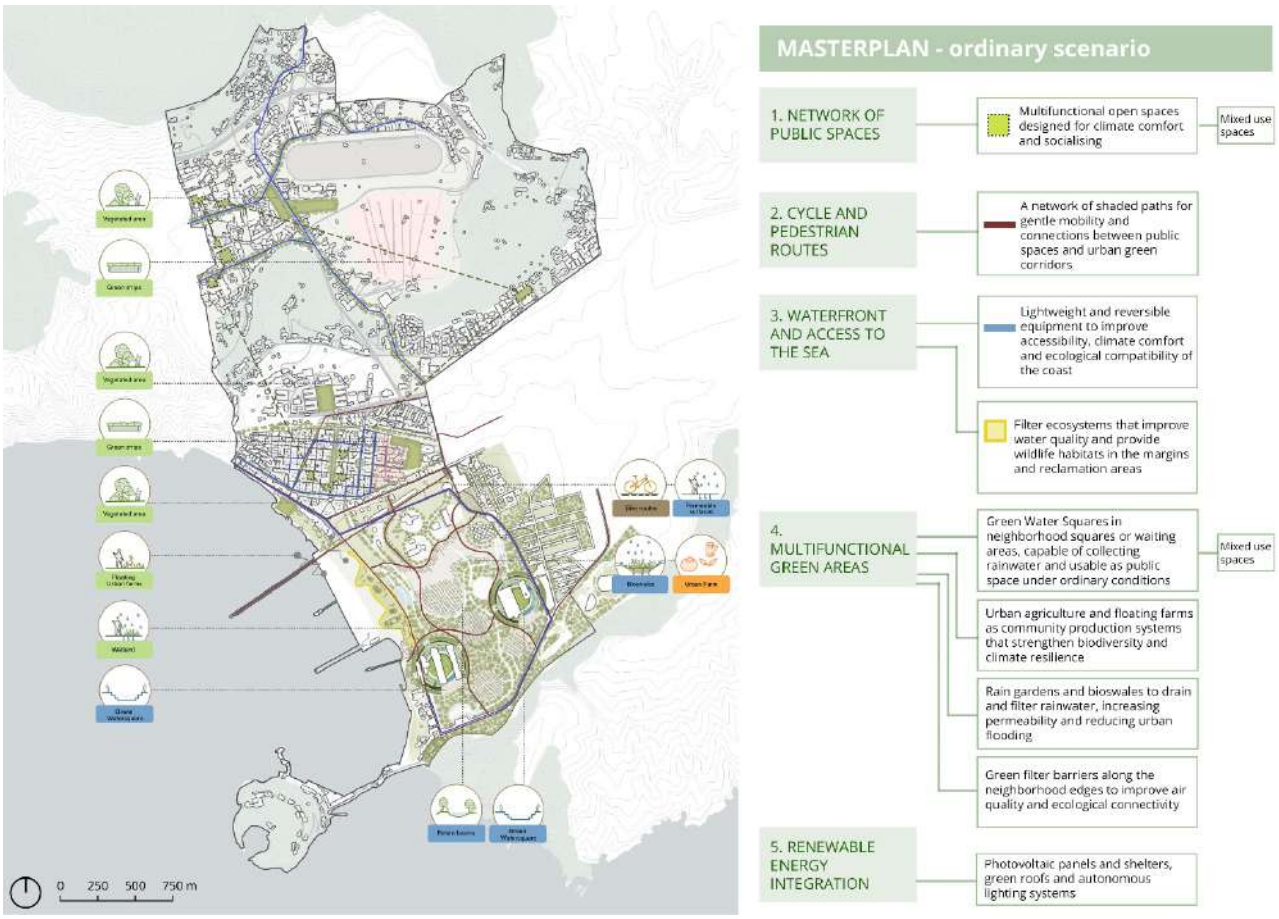

Figure 39: The ordinary scenario masterplan illustrates the configuration of the open space network under ordinary urban conditions, highlighting the spatial distribution of ecological and environmental interventions designed to ensure climatic comfort, accessibility, and urban quality. Together, these elements define a network of open spaces that, under ordinary conditions, functions as an ecological and climatic infrastructure supporting biodiversity, depuration processes, and the transition towards energetic self-sufficiency at the neighbourhood scale (Source: Authors' elaboration).

Emergency Scenario – Evacuation / Seismic Event

Under emergency conditions, open spaces assume an operational and strategic function in the management of population flows, reception, and emergency coordination. Operational waiting spaces, distributed across the main public areas, are temporarily converted to accommodate the population in safety, hosting first-aid, information, and essential goods distribution functions. Evacuation routes are structurally and climatically upgraded to ensure accessibility and functionality even under conditions of environmental or infrastructural stress. Equipped assembly points provide essential services and infrastructure for emergency management — including temporary shelters, medical posts, and logistics coordination — and form part of a network of urban shelters that, under extraordinary conditions, function as civil protection hubs while maintaining community or cultural functions in ordinary times. Finally, the conversion of strategic buildings — schools, civic centers, neighbourhood hubs — into temporary command centers ensures the continuity of vital functions, the coordination of operations, and the distribution of essential goods, fully integrating open space into the overall urban emergency response system.

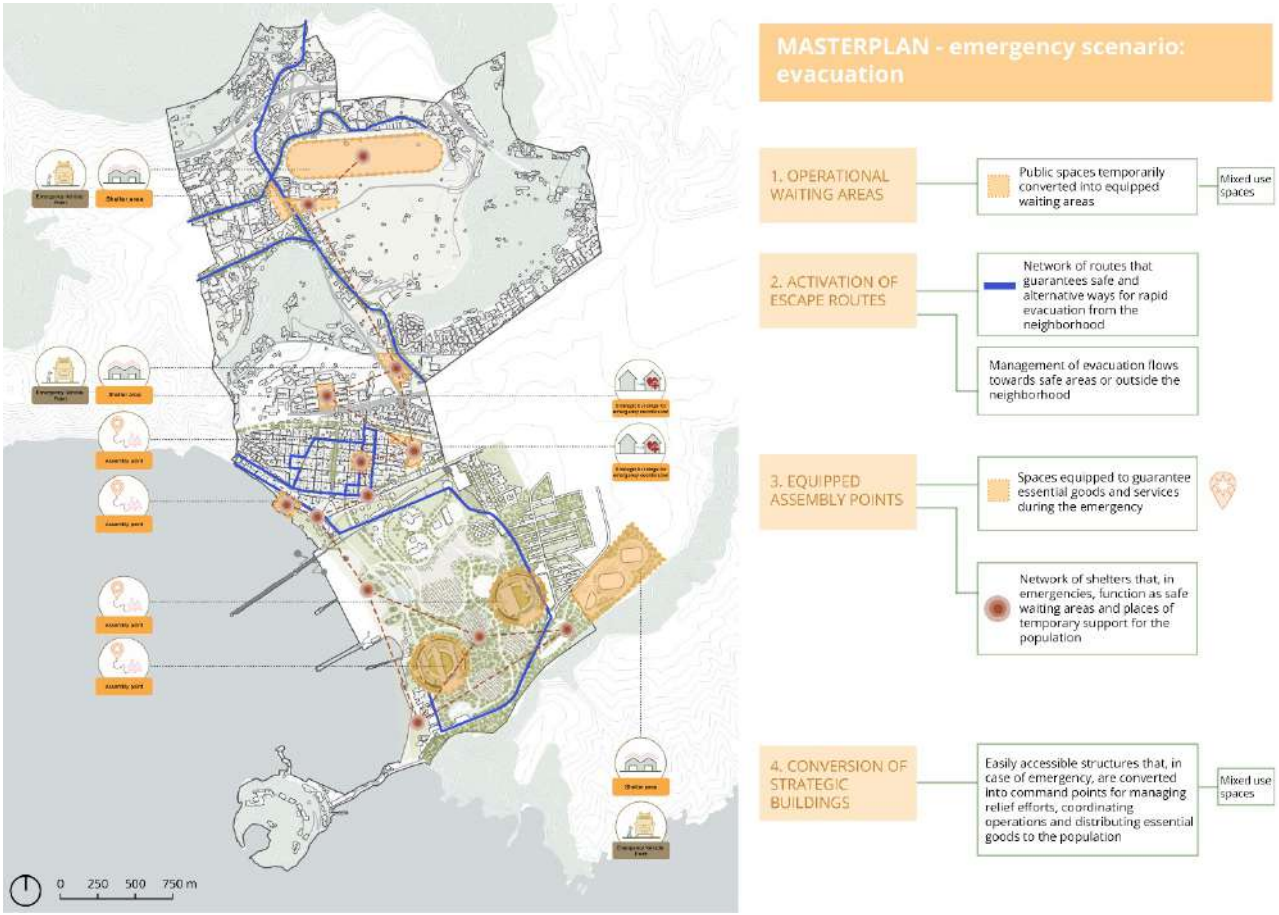

Figure 40: The evacuation scenario masterplan illustrates the operational reconfiguration of the open space network under seismic emergency conditions, highlighting the spatial distribution of elements constituting the urban emergency response system. The map reveals how the spatial organization of open spaces and their relationship with the built environment determine the capacity of the district to manage population flows, ensure safety, and maintain functional continuity during emergency conditions, while simultaneously demonstrating the dual-use potential of spaces and structures conceived to serve both ordinary community functions and extraordinary civil protection requirements (Source: Authors' elaboration).

Emergency Scenario – Heat Wave

During extreme heat events, the open space network is activated as an urban cooling infrastructure and thermal protection system. Shaded, ventilated, and equipped public spaces function as microclimatic relief zones, connected by a network of shaded pathways characterized by tree cover, reflective surfaces, and permeable materials that promote natural ventilation and reduce heat accumulation. Climatically retrofitted refuge buildings serve as thermal safety nodes within the public space network. Circular water management systems — including rainwater collection, storage, and reuse for irrigation and urban cooling devices — reinforce adaptive capacity and contribute to water consumption reduction. A distributed network of climate shelters ensures continuity of services and social protection during heat emergencies.

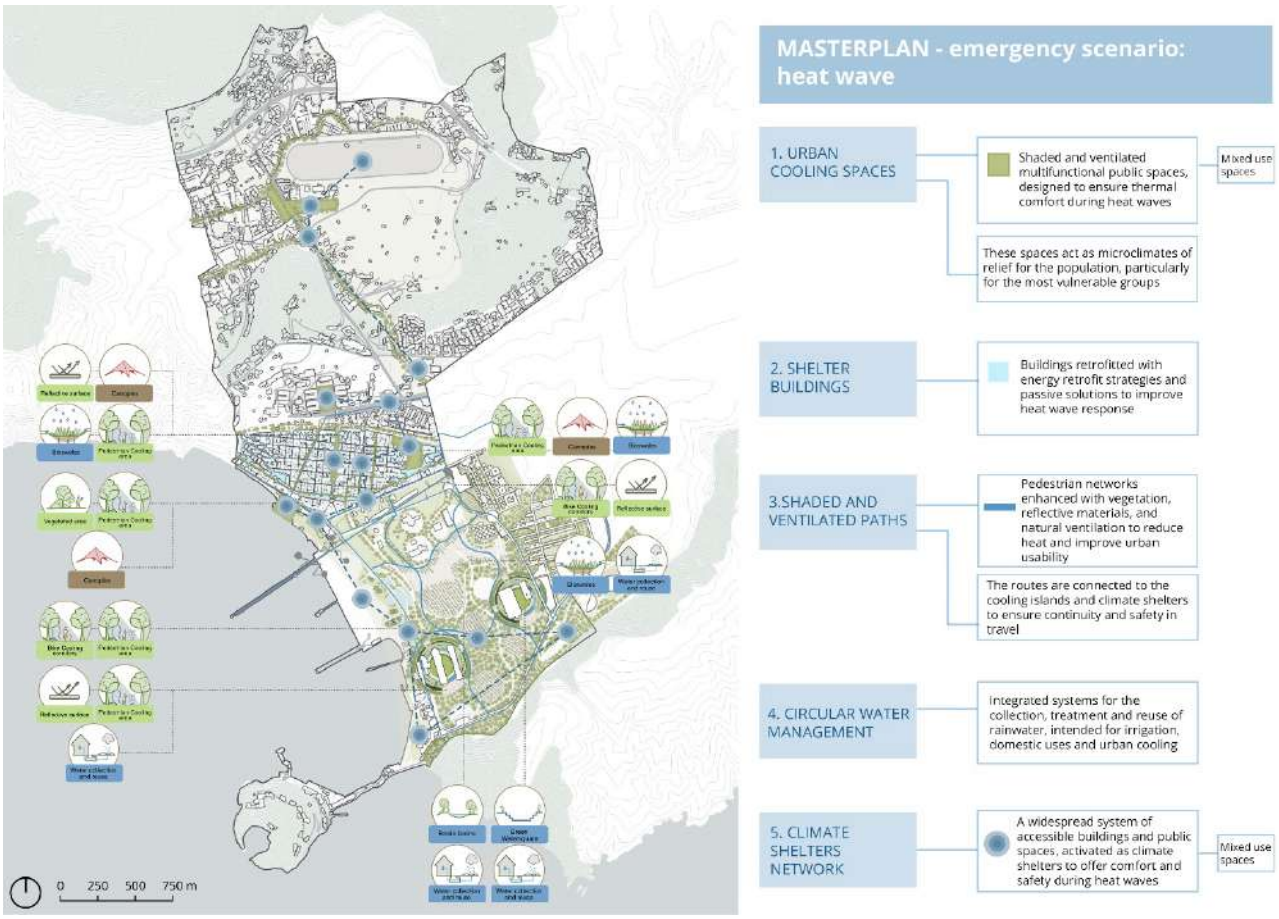

Figure 41: The heatwave scenario masterplan illustrates the activation of the open space network as an urban cooling and thermal protection infrastructure during extreme heat events, highlighting the spatial distribution of elements composing the climate adaptation system. The map reveals the spatial logic underlying the thermal resilience strategy, demonstrating how the coordinated distribution of cooling infrastructure, shaded connectivity, and retrofitted buildings can collectively reduce heat stress across the district and ensure adequate protection for the most vulnerable population groups (Source: Authors' elaboration).

Building Strategies

The strategic framework for buildings is articulated across four interconnected categories, collectively addressing the full spectrum of the existing and future built environment.

The existing building stock is approached through a strategy of preservation, adaptation, and targeted upgrading, combining seismic retrofit and climate adaptation — using technologies compatible with original structures and low-environmental-impact materials — with widespread energy efficiency measures through passive systems and high-performance equipment (Leone & Zuccaro, 2024; Prota, 2024). Where buildings are situated in areas of particularly elevated risk, strategic relocation is considered as a means of contributing to urban rebalancing and exposure reduction.

New residential development is conceived according to multi-risk, sustainability, and livability criteria, ensuring habitability under both climatic and seismic crisis scenarios. The identification of mixed-use areas integrating residential, commercial, and social functions further contributes to reducing forced mobility and strengthening the self-sufficiency of the neighbourhood fabric (Zuccaro & Leone, 2012).

Temporary buildings constitute a distinct and operationally significant category, conceived as a fundamental component of urban resilience. Their role is inherently dual: under extraordinary conditions, they accommodate support structures for ongoing construction, emergency housing, reception centers, and rescue facilities; under ordinary conditions, they host risk information and research centers, community

spaces, and cultural and educational activities. This dual capacity makes them uniquely reconfigurable assets, adaptable to the evolving and unpredictable needs of the territory.

New strategic buildings and urban hubs complete the framework as multifunctional nodes designed to ensure the operational continuity of essential services across both ordinary and emergency conditions. In times of crisis, they function as civil protection coordination centers and equipped assembly points integrated into the territorial emergency network; in ordinary times, they host neighbourhood facilities such as cultural spaces, libraries, coworking centers, and civic hubs, while retaining an inherent conversion capacity. Like temporary buildings, these structures embody the principle of resilient flexibility — spaces designed not for a single predetermined use, but for dynamic adaptation to the full range of urban and social demands they may be called upon to serve.

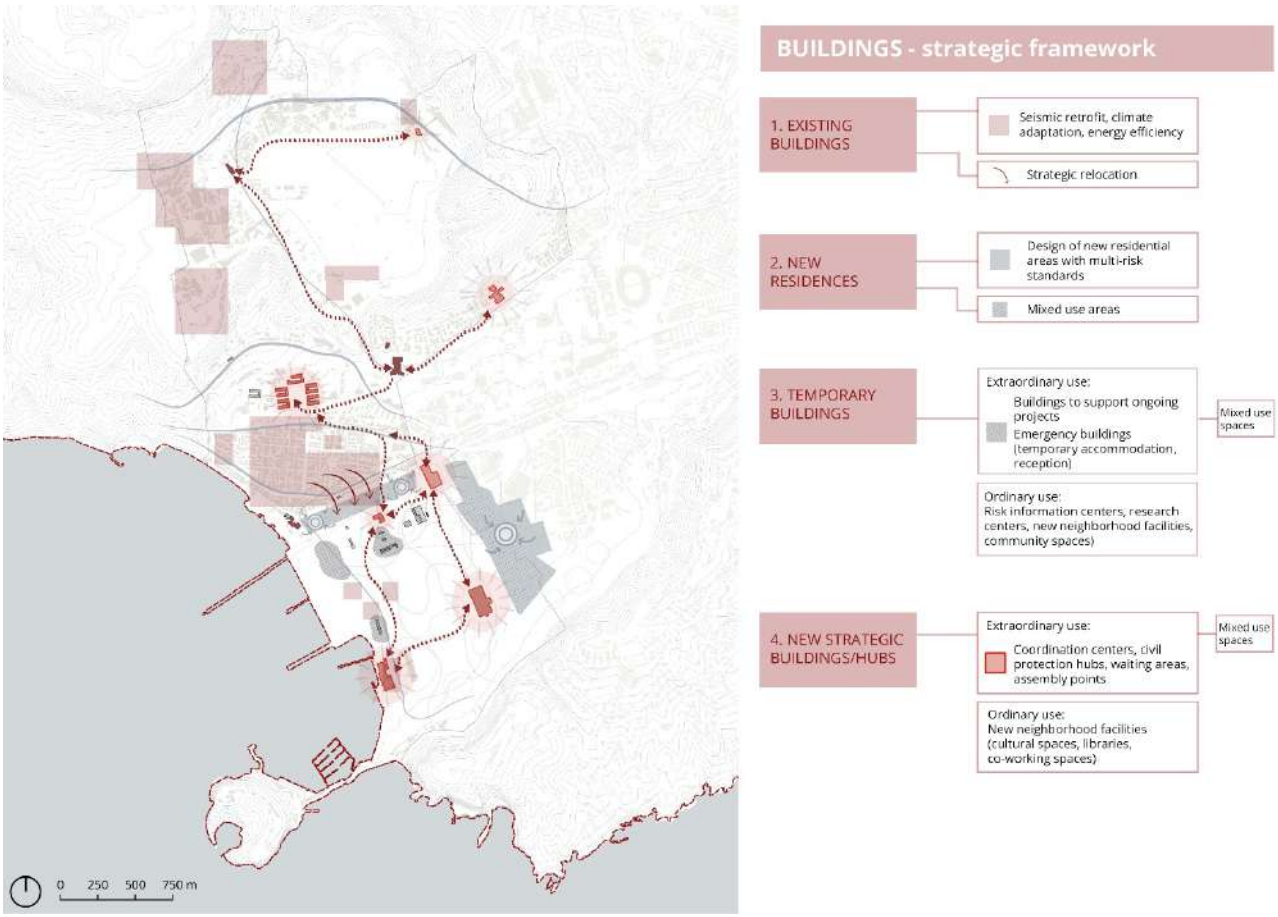

Figure 42: Strategic framework for buildings in the Bagnoli district. The map illustrates the spatial distribution of the four interconnected categories structuring the building strategy. The spatial reading of these four categories in relation to the existing urban fabric and the documented risk conditions reveals the territorial logic of the building strategy, highlighting how the distribution and upgrading of the built environment contributes to reducing exposure and vulnerability while simultaneously strengthening the functional and social resilience of the neighbourhood (Source: Authors' elaboration).

For buildings, the proposed interventions are conceived to operate simultaneously across climatic and geophysical risk dimensions, embodying the same integrated multi-hazard logic applied to open spaces. Each measure is selected not to address a single hazard in isolation, but to generate compounding benefits across the full spectrum of risk conditions that characterize the Bagnoli territory. Energy retrofitting is thus conceived not as an independent layer of improvement, but as an intrinsic component of a broader multi-hazard upgrading strategy, in which climatic and geophysical objectives are pursued in a mutually reinforcing rather than sequential manner (Leone & Zuccaro, 2024; Prota, 2024).

Photovoltaic panels are installed with a calibrated inclination to resist ash deposition while simultaneously contributing to energy autonomy and heat island mitigation. Envelope interventions employ ventilated facades or double-skin systems in Ultra-High Performance Concrete (UHPC), which combine high fire resistance (class A1) and enhanced out-of-plane performance to withstand pyroclastic flows with structural bracing capacity that supports seismic retrofitting — while also improving thermal regulation of the building envelope under extreme heat conditions (Zuccaro & Leone, 2013). For masonry buildings, insulation in rock wool (A1, 1000–1200°C) or hemp fiber (class E, 500°C) ensures thermal efficiency under climatic stress while maintaining full compatibility with geophysical risk interventions.

Structural measures are equally calibrated to serve this dual purpose, differentiated according to building components. Vertical structures are addressed through Fiber Reinforced Cementitious Matrix (FRCM) cladding and confinement, UHPC coatings, and protective barriers — systems that strengthen seismic and volcanic resistance while contributing to the thermal and durability performance of the envelope (Zuccaro & Leone, 2013). Horizontal structures are reinforced through Fiber Reinforced Polymer (FRP) or FRCM slab strengthening, complemented by steel superstructures for inclined roof configurations designed to manage both ash load and seismic forces. At the level of openings, steel panels, anti-explosion protective films, and high-performance shutters and window frames collectively ensure envelope integrity under both seismic loading and volcanic impact scenarios, while high-performance glazing systems contribute to reducing solar heat gain and improving indoor thermal comfort (Zuccaro & Leone, 2012; Leone & Zuccaro, 2024). Taken together, these interventions demonstrate that structural resilience and climatic adaptation are not competing priorities but deeply complementary ones — a design principle that runs through the entire strategic framework developed for Bagnoli.

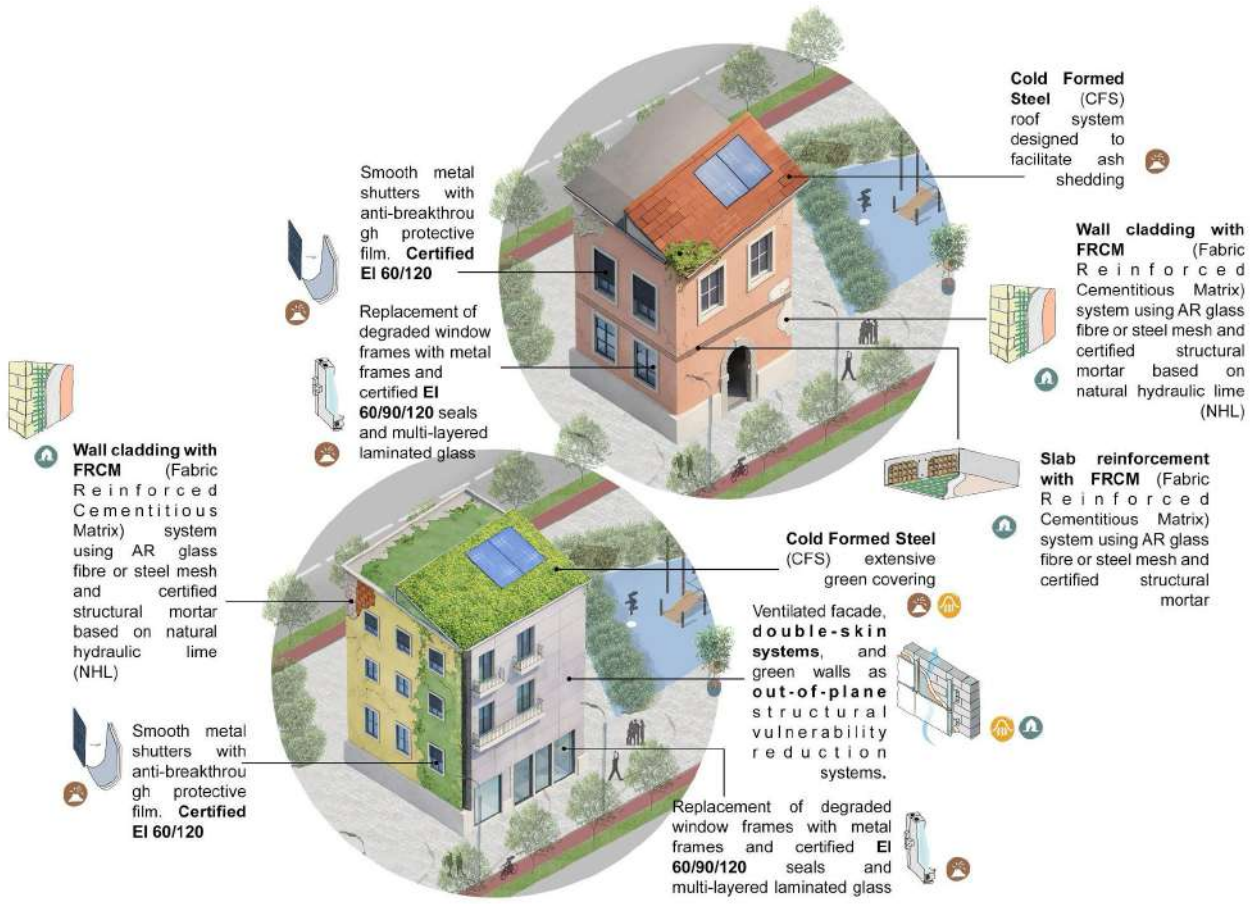

Figure 43: Visualization of integrated multi-hazard building interventions. The views illustrate the spatial and material configuration of the proposed upgrading measures, designed to operate simultaneously across climatic and geophysical risk dimensions. The visualizations demonstrate how each intervention contributes concurrently to seismic resilience, volcanic impact resistance, and climatic adaptation, embodying the principle that structural and

environmental upgrading objectives are not sequential but mutually reinforcing (Source: Authors' elaboration).

6.3.5 Post-intervention evaluation

The ex-post assessment adopts the same analytical structure and indicators applied in the ex-ante analysis, recalculated under the assumption that the integrated multi-risk design strategies have been implemented across both buildings and open spaces. These measures combine climate-oriented adaptation actions with structural and spatial interventions aimed at reducing exposure and vulnerability to seismic and volcanic events, operating simultaneously across climatic and geophysical risk dimensions in accordance with the integrated design logic described in the preceding sections.

Climatic hazard indicators are recalculated to account for the effects of the implemented measures across both heat wave and pluvial flooding conditions. In the case of heat waves, the Mean Radiant Temperature (MRT) reflects the improved outdoor thermal environment resulting from increased vegetation cover, expanded shaded areas, and the introduction of high-albedo and permeable surfaces, while indoor thermal conditions are reassessed through the annual energy consumption per unit of floor area following building-level energy retrofits — including facade optimization, shading devices, and photovoltaic integration — which reduce cooling demand, improve thermal comfort, and contribute to the reduction of associated CO_2 emissions. For pluvial flooding, the probability of inundation is updated by incorporating changes in surface runoff coefficients and soil infiltration capacity resulting from green-blue infrastructure, permeable pavements, and nature-based solutions, which collectively modify the hydrological behaviour of open spaces and reduce the likelihood and spatial extent of urban flooding. Geophysical impacts are consequently recalculated: expected building losses due to seismic events, roof collapses from volcanic ash fall, and the resulting displacement of residents are re-estimated to reflect the enhanced structural performance of the built environment, with reinforcement and envelope upgrading significantly reducing the likelihood of collapse and the scale of associated social impacts. Taken together, these results demonstrate how integrated design actions can effectively alter the way hazard conditions translate into losses, reducing expected impacts without modifying hazard intensity itself — confirming the role of spatial, environmental, and structural interventions as key leverage points for multi-risk mitigation and urban resilience.

The ex-post Synthetic Index integrates updated climate hazard indicators with revised geophysical impact estimates, reflecting the cumulative effects of the implemented interventions and structured according to the same hybrid methodology adopted in the ex-ante analysis. The index provides a unified metric to evaluate the reduction in combined risk levels across the urban territory, to identify areas where exposure or vulnerability persist despite the interventions, and to support the prioritization of ongoing or complementary actions. The comparison between ex-ante and ex-post Synthetic Index values constitutes the primary quantitative instrument for assessing the overall effectiveness of the multi-risk design strategy developed for Bagnoli.

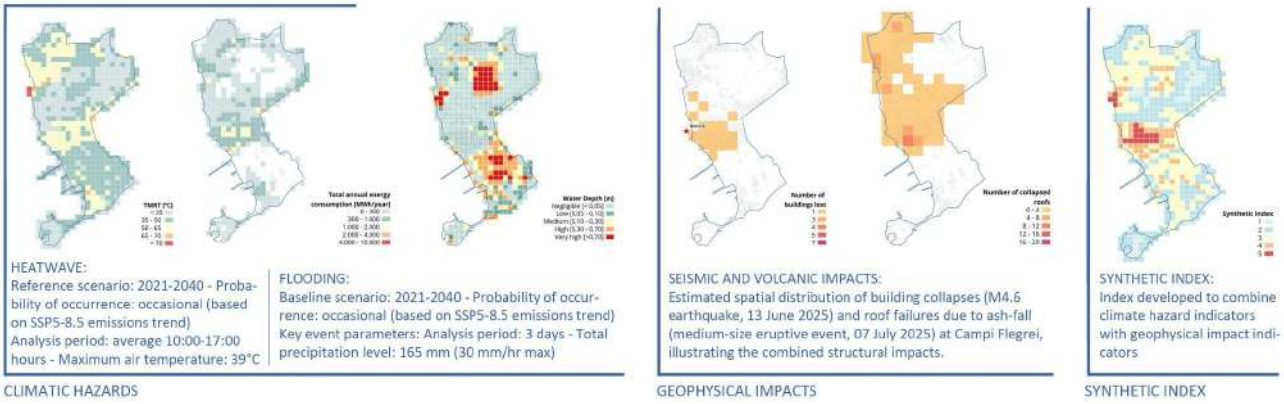

Figure 44: Ex-post multi-hazard assessment maps for the Bagnoli district. The figure presents the five analytical outputs of the risk assessment framework recalculated following the implementation of the integrated multi-hazard design strategies: the two updated climatic

hazard maps and the two revised geophysical impact maps, together with the ex-post Synthetic Index, which integrates all four indicators into a unified metric reflecting the reduction in combined risk conditions achieved through the proposed interventions. The comparison with the ex-ante Synthetic Index constitutes the primary instrument for evaluating the overall effectiveness of the multi-risk design strategy and for identifying areas where exposure or vulnerability persist despite the implemented measures (Source: Authors' elaboration).

6.4. Conclusions

This study has presented an integrated multi-hazard framework for the assessment and mitigation of urban risk, applied to the Bagnoli district of Naples as a representative case of complex socio-environmental and geophysical vulnerability. The methodological approach, grounded in the Multi-Hazard Resilient Urban Development concept and structured around the joint analysis of climatic hazards and geophysical impacts, has demonstrated the feasibility and analytical value of treating heterogeneous risk conditions within a unified and spatially explicit framework.

The methodological distinction between climatic hazards and geophysical impacts has proven to be not only analytically coherent but operationally productive. The framework is grounded in an explicit consideration of what design interventions act upon and what they reduce: in the case of climatic risks, measures predominantly reduce hazard intensity by modifying the environmental and spatial conditions that amplify heat and flooding; in the case of geophysical risks, they primarily reduce exposure and vulnerability through structural reinforcement and functional upgrading of the built environment. This understanding has made it possible to develop design strategies in which climatic and geophysical objectives are pursued in a mutually reinforcing manner, generating compounding benefits across multiple risk dimensions simultaneously.

The application of the framework to Bagnoli has confirmed the potential of integrated multi-risk strategies to generate measurable reductions in combined risk levels, as evidenced by the comparison between ex-ante and ex-post Synthetic Index values. The results show that coordinated interventions on open spaces and buildings — combining ecological reconnection, climatic adaptation, structural retrofitting, and spatial reconfiguration for emergency management — can significantly alter the way hazard conditions translate into urban losses, without modifying the intrinsic intensity of the hazards themselves. This finding reinforces the role of spatial, environmental, and structural design as a primary leverage point for urban resilience.

Beyond its technical contributions, the study has highlighted the importance of situating multi-risk strategies within their planning and governance context. The ongoing transformation of Bagnoli through the PRARU program and the acceleration introduced by the America's Cup 2027 designation represent both an opportunity and a critical challenge: the anticipated increase in population and urban activity implies a corresponding increase in exposure to the natural hazards documented in this study, a dynamic that the design strategies developed here have sought to explicitly address by embedding multi-risk resilience within the broader logic of urban regeneration.

At a broader scale, the framework offers a transferable operational tool for planners and designers working in multi-hazard urban contexts. Its scalability across different hazard configurations, urban morphologies, and governance settings positions it as a replicable methodology for translating multi-risk knowledge into adaptive, performance-driven, and sustainable urban design strategies — contributing to the advancement of integrated approaches to Disaster Risk Reduction and Climate Change Adaptation in complex urban environments.

7 A Markov-chain based model to describe loss and recovery during seismic sequences.

7.1 Introduction

Earthquake clusters are made of the mainshock and its contouring events, foreshocks and aftershocks, respectively. Stochastic modelling of seismic clusters' occurrence, and related shaking at a site of interest, can consist in a hierarchical approach in which mainshocks' occurrence follows a homogeneous Poisson process, whereas the other seismic events in each cluster follow a conditional process (Iervolino et al., 2014). For example, aftershock occurrence can be modelled as a non-homogeneous Poisson process, the intensity of which depends on some mainshock features (Yeo & Cornell, 2009). In the context of seismic risk analysis this can be referred to as hazard modelling.

Any system of interest exposed to seismic risk is virtually vulnerable to each event of a cluster, and seismic loss can accumulate in multiple partially damaging events. This is especially true in the most hazardous part of the cluster, which is around the mainshock, because of the short interarrival time between earthquakes. This issue can be treated as a form of stochastic degradation process, and Markov processes (i.e., Markov chains) have been shown being suitable to describe it (Iervolino et al., 2016; Iervolino et al., 2020). This approach to model seismic vulnerability makes use of the system's state-dependent fragility functions.

Repair is one of the possible strategies to recover from seismic loss. Recovery modelling is necessary for the resilience assessment (Bruneau et al., 2003). Research shows that the starting of the repair process can be delayed by factors such as the availability of resources and administrative issues (Costa et al., 2020). As mentioned above, also the time-space concentration of seismic events can temporarily delay or disrupt the recovery (Iervolino & Giorgio, 2015).

The research question is about developing a holistic Markovian model that enables a holistic modelling of seismic damage (yet neglecting foreshocks) for a system of interest. This was first envisaged in Chioccarelli et al. (2021) and is conceptually formulated herein. Figure 45 sketches the phenomenon which is the subject of the modelling question.

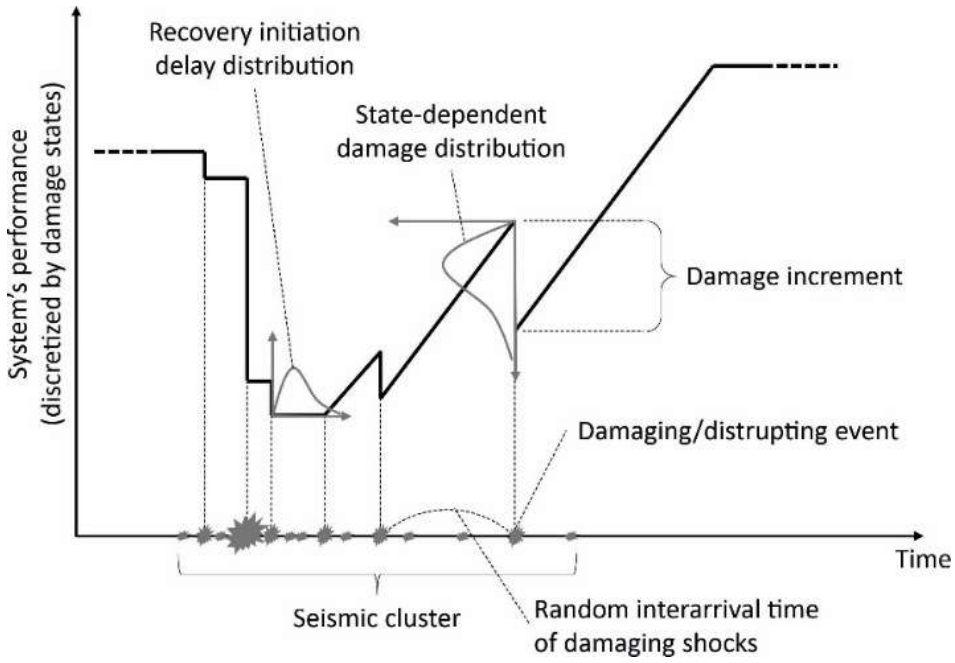

Figure 45: Sketch of the phenomenon which is the target of the question (adopted from Cox & Miller, 1965).

7.2 Methodology

Aftershock probabilistic seismic hazard analysis (APSHA; Yeo & Cornell, 2009) models the occurrence of aftershock according to a non-homogeneous Poisson process; i.e., characterized by a time-variant rate. In this context, the evolution over time of the seismic damage accumulation and recovery in aftershock sequences can be described by using a non-homogeneous Markov chain, where both the damage level and the time elapsed from the mainshock are measured on discrete scales. Given the probability vector of the initial state, the model is fully defined by its transition matrix. This matrix, indicated as $[P(k,k+1)]$, contains the probabilities that in each time unit the system passes from a given damage state to another, as:

$$[P(k,k+1)] = \begin{bmatrix} p_{1,1}(k) & p_{1,2}(k) & p_{1,3}(k) & p_{1,4}(k) \\ p_{2,1}(k) & p_{2,2}(k) & p_{2,3}(k) & p_{2,3}(k) \\ p_{3,1}(k) & p_{3,2}(k) & p_{3,3}(k) & p_{3,4}(k) \\ p_{4,1}(k) & p_{4,2}(k) & p_{4,1}(k) & p_{4,4}(k) \end{bmatrix}. \quad (1)$$

The size of the transition matrix refers to the chosen partition of the system's quality (i.e., performance) function; in the example, four damage states (i.e., $DS_1,\dots,DS_4$), ordered by increasing severity, are considered. The parameter k indicates the number of units of time elapsed from the mainshock. The generic element, $p_{i,j}(k)$, represents the conditional probability that the system, which is in state $D(k) = DS_i$ at time k, is in $D(k+1) = DS_j$ at time $k+1$, that is:

$$p_{i,j}(k) = P\big[D(k+1) = DS_j | D(k) = DS_i\big]. \quad (2)$$

The transition matrix can be formulated as:

$$[P(k,k+1)] = \nu(k)\cdot[D] + [1-\nu(k)]\cdot[R] = \nu(k)\cdot\begin{bmatrix} d_{1,1} & d_{1,2} & d_{1,3} & d_{1,4} \\ 0 & d_{2,2} & d_{2,3} & d_{2,3} \\ 0 & 0 & d_{3,3} & d_{3,4} \\ 0 & 0 & 0 & 1 \end{bmatrix} + [1-\nu(k)]\cdot \begin{bmatrix} 1 & 0 & 0 & 0 \\ r_{2,1} & r_{2,2} & 0 & 0 \\ r_{3,1} & r_{3,2} & r_{3,3} & 0 \\ r_{4,1} & r_{4,2} & r_{4,3} & r_{4,4} \end{bmatrix}, (3)$$

where $\nu(k)$ is the rate of aftershock occurrence evaluated at time k (which is dependent on the magnitude of the mainshock). D is the matrix that contains the (conditional) probabilities of transitions determined by a generic aftershock (of unspecified magnitude and location), that is those of the type $DS_i \to DS_j,\ i \le j$. R is the matrix that contains the (conditional) probabilities of transitions of the type $DS_i \to DS_j,\ i \ge j$, because of the recovery activities. The model assumes that in a unit of time only one of these two types of transitions can occur. For the model to work, it should be $\nu(k) << 1$, that is achieved by assuming a time scale in which units are small enough.

The probability vector of the state of the system at time m, $P(m) = [P_1(m),\dots,P_4(m)]$, where $P_l(m) = P[D(m) = DS_l],\ l = 1,\dots,4$, can be obtained as:

$$P(m) = P(0)\cdot\prod_{k=0}^{m-1}[P(k,k+1)]. \quad (4)$$

The probability vector of the initial state $P(0) = [P_1(0),\dots,P_4(0)]$, refers to the damage state of the system immediately after the mainshock.

Apparently, the model in equation (3) cannot describe the early phase of the recovery process that usually shows a delay in starting the recovery activities (i.e., Figure 45). In fact, a more general Markovian model (i.e., a Markov chain), which can also address this issue, can be formulated by using the device of stages (DOS) technique (e.g., Iervolino et al., 2020). DOS entails modeling a non-exponential sojourn time by a proper arrangement of stages in which sojourn time is exponentially distributed, enabling to deal non-Markovian processes via the Markovian theory.

7.3 Illustrative application

An illustrative example of the described framework is reported here. The structure considered is a six-story, code-conforming reinforced concrete frame building, supposedly located at the site of L'Aquila, Italy. Five damage states are considered to describe the increasing structural damages (i.e., $DS_1, \ldots, DS_5$). The corresponding state-dependent fragility functions are those developed in (Iervolino et al., 2016); they refer to the spectral acceleration (Sa) at vibration period equal to 0.5 s, $Sa(0.5s)$, and provide, via a lognormal model, the probability of exceeding a damage state, DS_j, conditional on the intensity measure and the damage state in which the earthquake finds the structure, DS_i, according to the following equation:

$$P\left[DS \geq DS_j | DS_i, Sa(0.5s) = sa\right] = \Phi\left(\frac{ln(sa) - ln\left(\widetilde{Sa}^{i,j}\right)}{\sigma_{ln\widetilde{Sa}^{i,j}}}\right). \quad (5)$$

In the equation $ln\left(\widetilde{Sa}^{i,j}\right)$ and $\sigma_{ln\widetilde{Sa}^{i,j}}$ are the median and the logarithmic standard deviation of the intensity measure, respectively, and they define the model.

The unit time transition probability matrix is obtained by integrating the state dependent fragility functions with the probability density function derived by the complementary cumulative distribution function, conditional on the occurrence of one generic aftershocks, as reported in Figure 46. It results from an aftershock probabilistic seismic hazard analysis (APSHA, [12]) performed for the site of L'Aquila, assuming that an M6.3 mainshock has occurred.

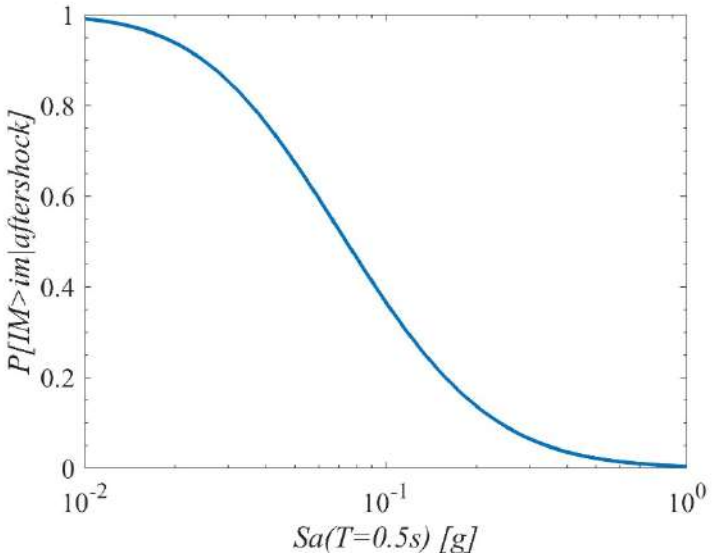

Figure 46: CCDF at the site of L'Aquila assuming that a M6.3 mainshock occurred.

The unit time (i.e., six months) recovery matrix is assumed as reported in Table 2.

The probability of finding the structure in DS_1, given that is was damaged to DS_3 by the mainshock, is reported in Figure 47a, considering or neglecting the recovery component of the model. In the first case, that is, with recovery, the probability monotonically increases with the time since the mainshock. As expected, this probability is constant and equal to zero when no recovery strategy is assumed. Figure 47b shows the probability of DS_5 for the same structure, which is assumed to be in DS_3 after the mainshock. If no recovery is considered, the probability slightly increases after the mainshocks and, because the rate of aftershocks reduces with time, becomes constant. On the other hand, when the recovery matrix is considered, after some time since the mainshock, the rate of aftershocks becomes negligible and the probability of a worsen condition decreases.

Table 2 – Unit-time recovery matrix

	DS_1	DS_2	DS_3	DS_4	DS_5
DS_1	1	0	0	0	0
DS_2	0.4	0.6	0	0	0
DS_3	0.4	0	0.6	0	0
DS_4	0	0	0.2	0.8	0
DS_5	0	0	0	0.2	0.8

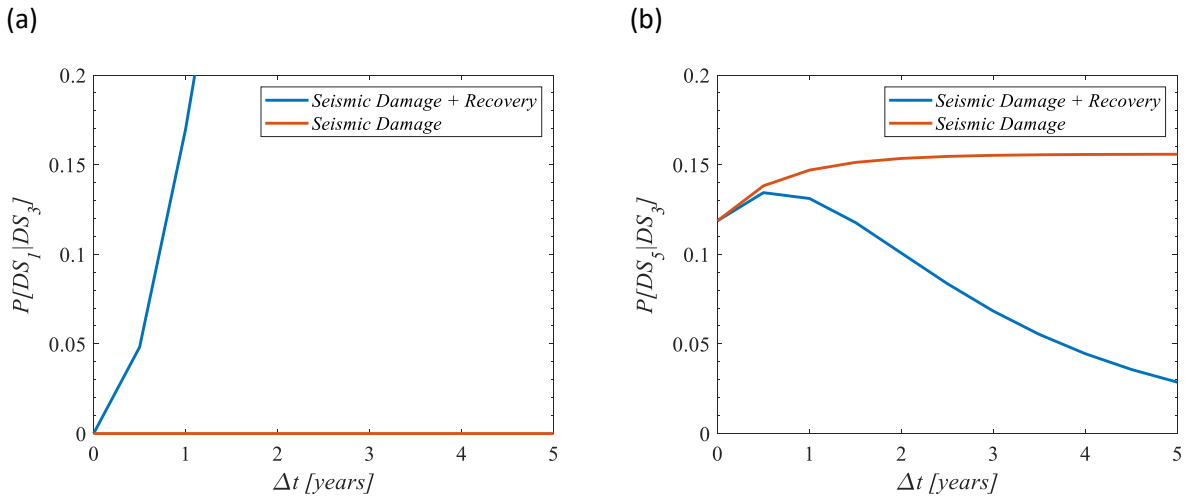

Figure 47: Damage probabilities over time with and without recovery.

7.4 Conclusions

Building on previous works on the topic by the authors, a holistic Markovian model for seismic damage accumulation and recovery during seismic sequences was formulated. The model works in the hypothesis of aftershock probabilistic seismic hazard analysis, that is, following a mainshock of known features. Its main limitations are: (i) that it neglects foreshocks, and (ii) that it does not explicitly model the typical random delay in starting the recovery activities. However, both these issues can be addressed by suitable adjustments of the model. For example, issue (ii) can be readily solved by using the DOS technique.

8 A methodology for mapping hazards and related consequences

8.1 Introduction

A methodology to identify and display areas with potential risks has been developed. The collected data were integrated and processed for the Municipality of Naples in Italy for the year 2011, but the methodology can be replicated.

In this study, large amounts of raw geographic data are transformed into useful knowledge for supporting location-based decisions, mapping hazards and related consequences, to understand, compare, and integrate the environmental, natural, and anthropic risks. The application produced thematic maps using data downloaded from Italian platforms or promoted by the European Union, which provide official data on population and residential buildings in Italian municipalities and a wide range of Earth Observation (EO) data, characterized by free and open access.

8.2 Methodology

The first step was to acquire the type of risks identified by the other WP: natural hazards, earthquake, volcanic, landslides, floods, and anthropic hazards, such as industrial accidents, land consumption, deforestation, and fires. This is central to defining the data that should be collected for the implementation of complete and useful maps.

Subsequently, data about land use and land cover were collected from the CORINE Land Cover (CLC) product, which offers an inventory with thematic classes in the Land Monitoring Service. This is a service of Copernicus, the Earth observation component of the European Union's Space program, looking at our planet and its environment to benefit all European citizens. It offers information services that draw from satellite Earth Observation and in-situ data (www.copernicus.eu). In particular, it was the Urban Atlas suite of product, that gives users access to detailed land cover/land use maps for the main Urban Areas across Europe, in addition to street tree maps, building block height measurements, and population estimates.

The Copernicus data were integrated with Geoportale Nazionale (MASE Ministry of the Environment and Energy Security) data relating to height and type of single building (https://gn.mase.gov.it/portale). The Geoportal contains the available cartography of the Italian territory, useful for obtaining a wide range of information on the main environmental and territorial issues.

Data about the number of inhabitants, number of inhabited and uninhabited buildings, number of floors, intended use, type of buildings (masonry or reinforced concrete or other), period of construction, state of preservation were collected. All data, available by census sections, are open and provided by ISTAT, the Italian National Institute of Statistics. The Institute produces statistical information, analyses, and forecasts in complete independence and in accordance with the most up-to-date scientific standards, in order to develop detailed knowledge of Italy's environmental, economic, and social dimensions at various levels of geographical detail and to assist all members of society (citizens, public administrations, etc.) in decision-making processes (www.istat.it/).

Finally, open data from various sources were collected and processed in a free and open GIS platform (QGis).

GIS (Geographic Information System) is an advanced computer tool that allows you to acquire, store, manage, analyze, and visualize geospatial data—information associated with a specific location on the Earth's surface. Essentially, a GIS connects descriptive data (attributes) to geographic coordinates, allowing for the representation and understanding of spatial phenomena through interactive digital maps.

8.3 Application for Municipality of Naples

The application focused on the entire Municipality of Naples (Figure 48). Some areas are shown to clarify the methodology and, above all, to better visualize the variables considered. The set of collected data allowed for identifying the most vulnerable areas, about the period of construction, type of building, and state of preservation (Figures 3&4), and for assessing the exposure about density of buildings and population (Figure 49).

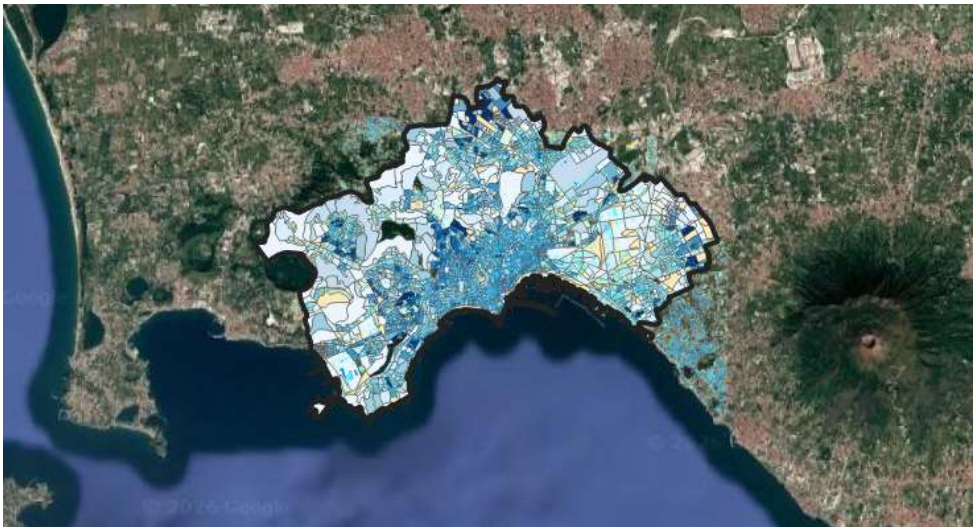

Figure 48: Study area with ISTAT data shown in Figure 2 (Authors' elaboration on Google Maps image).

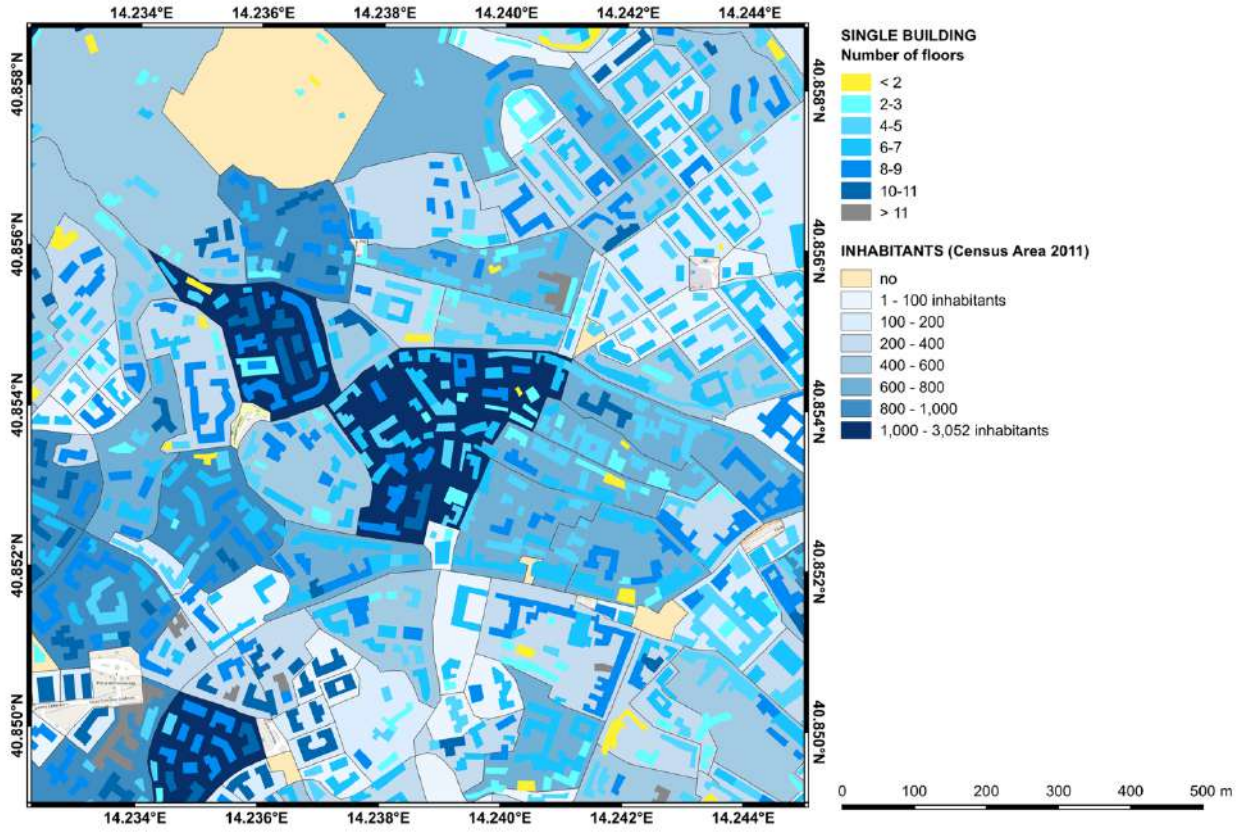

Figure 49: A resized area of the Municipality of Naples. The floors number of single buildings and inhabitants in census areas.

Figure 49 shows the height of individual buildings obtained from data available on Geoportale and the number of inhabitants from ISTAT data. The ISTAT data is divided into census areas, delimited by black lines in the figure. The map allows to immediately identify the most populated areas and correlate them with building heights.

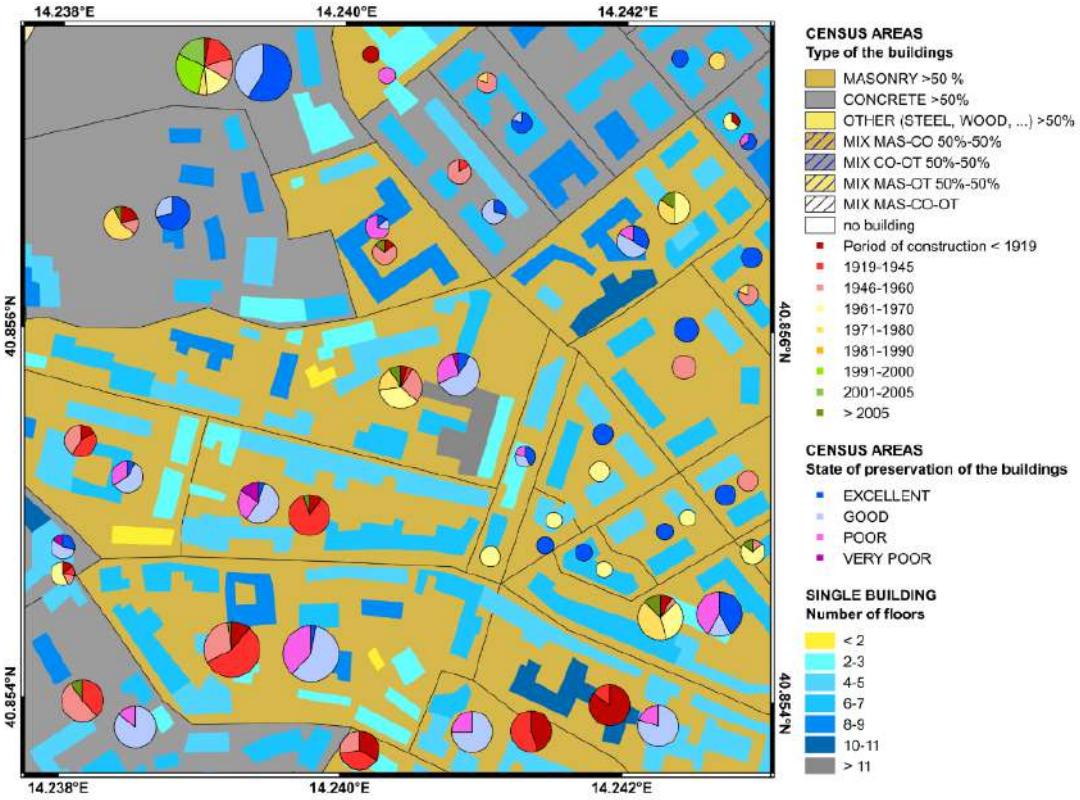

Figure 50: A resized area of the Municipality of Naples. Type of buildings, period of construction, state of preservation and height of buildings are shown.

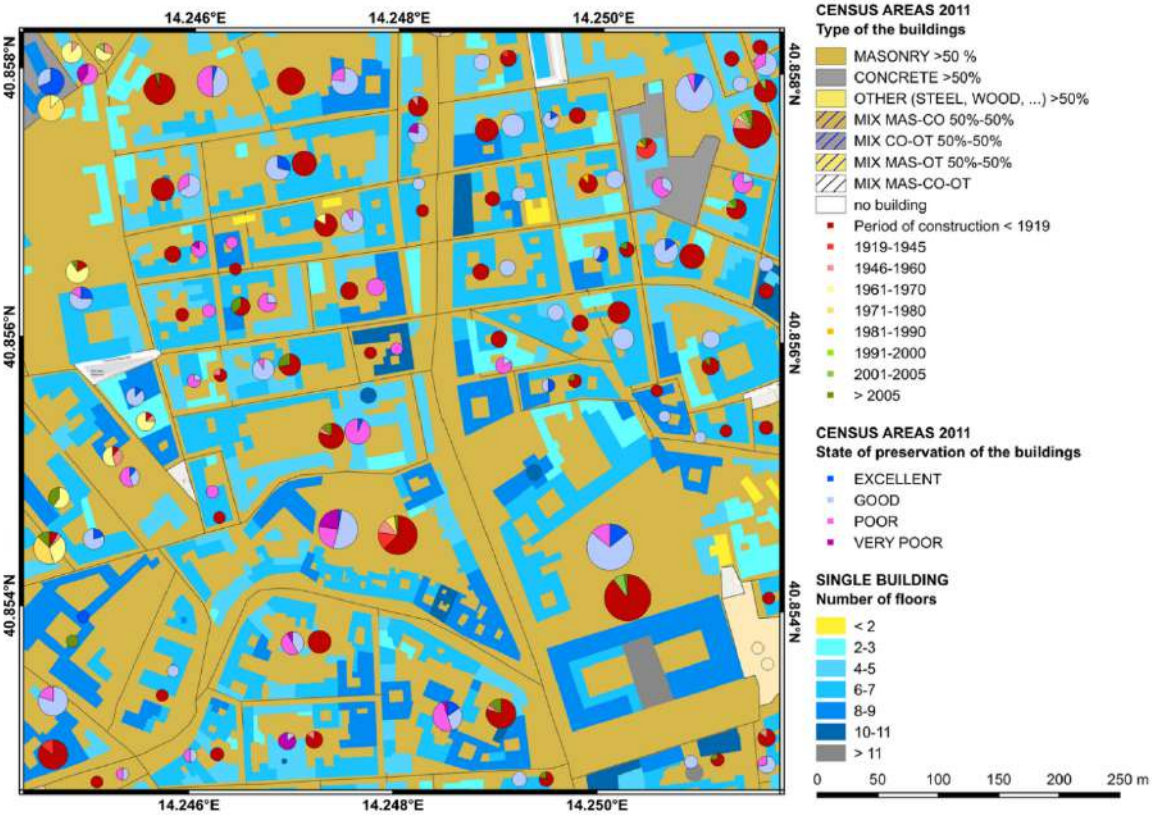

Figure 51: A resized area of the Municipality of Naples. Type of buildings, period of construction, state of preservation and height of buildings are shown.

In Figure 50 and Figure 51, the number of building floors, type of buildings (masonry, reinforced concrete, or other), period of construction, and state of preservation of the buildings were collected. The building types, construction period, and state of preservation are relative to ISTAT census areas. The color of the census area indicates the prevalence of a particular building type within the area, while the two pie charts for each census area highlight the distribution of state of preservation and construction period within the indicated census area.

8.4 Conclusions

Integrating open data is essential for creating detailed, thematic, and up-to-date geographic maps that can be used for risk analysis. These studies enable the construction of integrated risk maps that can combine natural and anthropic elements to provide a more complete view of the overall risk in an area. The goal is to promote safer urban and regional planning, considering all risk factors.

9 General conclusions

This deliverable has presented a comprehensive and multidisciplinary framework for multi-risk assessment and resilience-oriented decision-making, addressing the increasing complexity of natural hazards affecting both urban systems and critical infrastructure. By integrating advanced modelling techniques across seismology, geotechnical engineering, structural analysis, and climate science, the research provides a coherent and scalable approach to understanding and managing cascading and interacting risks.

A key contribution of the work lies in the development of physics-based and probabilistic models capable of capturing the full chain of hazard processes, from seismic source to structural response, as well as their interactions with secondary phenomena such as landslides and long-term deterioration. This approach moves beyond traditional sectoral analyses, enabling a more realistic representation of risk as a dynamic and evolving process.

At the urban scale, the proposed Multi-Hazard Resilient Urban Development framework demonstrates how spatial analysis, environmental modelling, and design strategies can be integrated within a unified decision-support system. The application to the Bagnoli district has shown that coordinated interventions on buildings and open spaces can significantly reduce multi-risk conditions, enhancing both safety and urban quality without altering the intrinsic hazard levels.

The introduction of time-dependent models, such as the Markov-chain-based approach for seismic sequences and the life-cycle assessment of infrastructure, further highlights the importance of considering temporal dynamics in risk evaluation. These aspects are essential for capturing damage accumulation, delayed recovery, and the progressive degradation of systems exposed to repeated or interacting hazards.

Overall, the results emphasize that effective risk mitigation requires a shift from single-hazard and static approaches towards integrated, dynamic, and multi-scale frameworks. The methodologies developed in this deliverable provide a solid basis for future advancements, including the incorporation of uncertainty quantification, probabilistic scenario analysis, and real-time data integration.

10 References

Addabbo, N., Clemente, M. F., Quesada-Ganuza, L., Abdel Khalek, R., Labattaglia, F., Nocerino, G., & Leone, M. F. (2023). A framework for climate resilient urban design: The case of Porte de Montreuil, Paris. Sustainability, 15(18), 13857. https://doi.org/10.3390/su151813857

Bandara, S. (2013). Material Point Method to simulate large deformation problems in fluid saturated granular medium (Doctoral dissertation). University of Cambridge.

Biondini, F., & Vergani, M. (2015). Deteriorating beam finite element for nonlinear analysis of concrete structures under corrosion. *Structure and Infrastructure Engineering*, 11(4), 519–532.

Bruneau, M., Chang, S. E., Eguchi, R. T., Lee, G. C., O'Rourke, T. D., Reinhorn, A. M., et al. (2003). A framework to quantitatively assess and enhance the seismic resilience of communities. Earthquake Spectra, 19(4), 733–752. https://doi.org/10.1193/1.1623497

Casagrande, A. (1976). Liquefaction and cyclic deformation of sands: A critical review. In Proceedings of the 5th Pan American Conference on Soil Mechanics and Foundation Engineering (pp. 80–133).

Castro, G. (1969). Liquefaction of sands (Doctoral dissertation). Harvard University.

Ceccato, F., Redaelli, I., di Prisco, C., & Simonini, P. (2018). Impact forces of granular flows on rigid structures: Comparison between discontinuous (DEM) and continuous (MPM) numerical approaches. Computers and Geotechnics, 103, 201–217.

Chioccarelli, E., Iervolino, I., & Giorgio, M. (2021). Modelling seismic damage accumulation and recovery in aftershock sequences. Proceedings of ESREL 2021.

CLARITY Consortium. (2019). Adaptation measures technical cards (Deliverable D3.3). https://clarity-h2020.eu/content/d33-adaptation-measures-technical-cards

CLARITY Consortium. (2020). Technology support report (Deliverable D4.4). https://clarity-h2020.eu/sites/clarity-h2020.eu/files/public/content-files/deliverables/CLARITY%20D4.4%20Technology%20Support%20Report%20v2_0.pdf

Costa, R., Haukaas, T., & Chang, S. E. (2020). Agent-based model for post-earthquake housing recovery. Earthquake Spectra, 37(1), 46–72. https://doi.org/10.1177/8755293020944175

Cox, D. R., & Miller, H. D. (1965). The theory of stochastic processes. Chapman and Hall. https://doi.org/10.1201/9780203719152

Cuomo, S., Di Perna, A., & Martinelli, M. (2021). MPM hydro-mechanical modelling of flows impacting rigid walls. Canadian Geotechnical Journal, 58(11), 1730–1743.

di Prisco, C., Pastor, M., & Pisanò, F. (2010). Shear wave propagation along infinite slopes: A theoretically based numerical study. International Journal for Numerical and Analytical Methods in Geomechanics, 34(14), 1522–1546.

Fern, J., Rohe, A., Soga, K., & Alonso, E. (2019). The Material Point Method for geotechnical engineering: A practical guide.

Giannotti, F., et al. (2019). The erratic character of the landscape-culture mosaic of the Phlegrean coastline: Regeneration of the Bagnoli former steel area.

Gioffrè, D., Mandaglio, M. C., di Prisco, C., & Moraci, N. (2017). Evaluation of rapid landslide impact forces against sheltering structures. Rivista Italiana di Geotecnica, 3, 79–91.

ICARIA Consortium. (2023). ICARIA strategies platform – Adaptation measures catalogue. https://www.icariastrategies.eu/

Iervolino, I., Giorgio, M., & Polidoro, B. (2014). Sequence-based probabilistic seismic hazard analysis. Bulletin of the Seismological Society of America, 104(2), 1006–1012. https://doi.org/10.1785/0120130207

Iervolino, I., & Giorgio, M. (2015). Stochastic modeling of recovery from seismic shocks. Proceedings of ICASP 2015.

Iervolino, I., Giorgio, M., & Chioccarelli, E. (2016). Markovian modeling of seismic damage accumulation. Earthquake Engineering & Structural Dynamics, 45(3), 441–461. https://doi.org/10.1002/eqe.2668

Iervolino, I., Chioccarelli, E., & Suzuki, A. (2020). Seismic damage accumulation in multiple mainshock–aftershock sequences. Earthquake Engineering & Structural Dynamics, 49(10), 1007–1027. https://doi.org/10.1002/eqe.3275

INGV – Istituto Nazionale di Geofisica e Vulcanologia. (n.d.). SPeeD – Seismic and volcanic prevention through e-database. https://speed.pi.ingv.it/

IPCC. (2022). Climate change 2022: Impacts, adaptation and vulnerability. Cambridge University Press. https://doi.org/10.1017/9781009325844

Ishihara, K. (1993). Liquefaction and flow failure during earthquakes. Géotechnique, 43(3), 351–451.

Jalayer, F., Asprone, D., Prota, A., Manfredi, G., & others. (2011). A decision support system for post-earthquake reliability assessment of structures subjected to aftershocks: An application to L'Aquila earthquake, 2009. *Bulletin of Earthquake Engineering, 9*(4), 997–1014. https://doi.org/10.1007/s10518-010-9230-6

Jefferies, M., & Been, K. (1985). Soil liquefaction: A critical state approach. Taylor & Francis.

Kabisch, N., et al. (2017). Nature-based solutions to climate change adaptation in urban areas. Springer. https://doi.org/10.1007/978-3-319-56091-5

Lagomarsino, S., & Cattari, S. (2013). Seismic vulnerability of existing buildings: Observational and mechanical approaches for application in urban areas. In Seismic vulnerability of structures (pp. 1–62). https://doi.org/10.1002/9781118603925.ch1

Lagomarsino, S., Cattari, S., & Ottonelli, D. (2021). The heuristic vulnerability model: Fragility curves for masonry buildings. Bulletin of Earthquake Engineering, 19, 3129–3163. https://doi.org/10.1007/s10518-021-01063-7

Leone, M. F., et al. (2025). A holistic asset-level modelling framework for a comprehensive multi-hazard risk/impact assessment: Insights from the ICARIA project. International Journal of Disaster Risk Reduction, 119, 105319. https://doi.org/10.1016/j.ijdrr.2024.105319

Leone, M. F., & Zuccaro, G. (n.d.). Seismic and energy retrofitting of residential buildings: A simulation-based approach.

Pastor, M., Quecedo, M., Gonzalez, E., Herreros, M. I., Merodo, J. A., & Mira, P. (2004). Modelling of landslides: (II) Propagation. In Degradation and instability of geomaterials (pp. 319–367). Springer.

Pastor, M., Haddad, B., Sorbino, G., Cuomo, S., & Drempetic, V. (2009). A depth-integrated, coupled SPH model for flow-like landslides and related phenomena. International Journal for Numerical and Analytical Methods in Geomechanics, 33, 143–172.

Pastor, M., Blanc, T., Haddad, B., Petrone, S., Sanchez Morles, M., Drempetic, V., Issler, D., Crosta, G. B., Cascini, L., Sorbino, G., & Cuomo, S. (2014). Application of a SPH depth-integrated model to landslide run-out analysis. Landslides, 11(5), 793–812.

Perelli, F. L., et al. (2023). Impact assessment caused by bradyseism phenomena in the Campi Flegrei area. Frontiers in Built Environment, 9. https://doi.org/10.3389/fbuil.2023.1129175

Prota, A. (n.d.). Criteri e soluzioni per la progettazione di interventi integrati e sostenibili.

Sulsky, D., Zhou, S. J., & Schreyer, H. L. (1995). Application of a particle-in-cell method to solid mechanics. Computer Physics Communications, 87(1-2), 236–252.

Turchi, A., Lumino, R., Gambardella, D., & Leone, M. F. (2023). Coping capacity, adaptive capacity, and transformative capacity in a multi-hazard resilience perspective. Sustainability, 15(14), 10877. https://doi.org/10.3390/su151410877

UNDRR. (2015). Sendai framework for disaster risk reduction 2015–2030.

Yeo, G. L., & Cornell, C. A. (2009). A probabilistic framework for quantification of aftershock ground-motion hazard in California. Earthquake Engineering & Structural Dynamics, 38(1), 45–60. https://doi.org/10.1002/eqe.840

Zuccaro, G., & De Gregorio, D. (2013). Building technologies for the mitigation of volcanic risk. Natural Hazards Review, 14(3).

Zuccaro, G., Dato, F., Papa, F., De Gregorio, D., & Cacace, F. (2014). Seismic vulnerability assessment based on typological characteristics: The SAVE procedure. Soil Dynamics and Earthquake Engineering, 69, 138–152. https://doi.org/10.1016/j.soildyn.2014.09.012

Zuccaro, G., & Leone, M. F. (2021). Climate services to support disaster risk reduction and climate change adaptation in urban areas. Frontiers in Environmental Science, 9, 693319. https://doi.org/10.3389/fenvs.2021.693319

Zuccaro, G., & Leone, M. F. (n.d.). La mitigazione del rischio vulcanico come opportunità per una città ecologica e resiliente.